UNIVERSITY OF CALIFORNIA, SAN DIEGO

Implications of deoxygenation and acidification for deep sea urchins in southern California

A dissertation submitted in partial satisfaction of the requirements for the degree Doctor of Philosophy

in

Oceanography

by

Kirk Nicholas Suda Sato

Committee in charge:

Professor Lisa A. Levin, Chair
Professor Andreas J. Andersson
Professor James M. D. Day
Professor Joanna McKittrick
Professor Jennifer R. A. Taylor
Professor Martin Tresguerres

2017

The Dissertation of Kirk Nicholas Suda Sato is approved, and it is acceptable in quality and form for publication on microfilm and electronically.

Chair

University of California, San Diego

2017

DEDICATION

This doctoral dissertation is dedicated to my family. First and foremost, I dedicate this work to my parents who instilled in me a love for the natural world and its wondrous inhabitants. To my brother for inspiring me to travel and to think outside the proverbial box. And to my grandparents for their unconditional support ever since I was a juvenile competitor exploring the majestic tidepools of the Sonoma County coastline.

EPIGRAPH

You can't study the darkness
by flooding it with light.

- Edward Abbey

TABLE OF CONTENTS

LIST OF TABLES

LIST OF FIGURES

ACKNOWLEDGEMENT

I thank my advisor, Lisa Levin, for providing me with countless opportunities to expand my academic, research, and policy interests. Her tireless effort and support in all aspects of research, education, conservation, policy, and professional development is inspiring. Special thanks to the past and present members of the Levin Lab for providing me with valuable advice, support, and guidance – Christina Frieder, Natasha Gallo, Jen Gonzalez, Ben Grupe, Jen Le, Lilly McCormick, Andrew Mehring, Guillermo Mendoza, Mike Navarro, Carlos Neira, and Eric Sperling. Thanks to Andrew Mehring for being such a generous and easygoing officemate. I am grateful for the opportunity to learn from and work with Phil Zerofski on numerous SIO class cruises. I especially thank those who have volunteered their time to assist me in the lab and in the field including Daniel Jio, Katy Kelsoe, Stephanie Luong, Marissa Mangelli, Milinda Thompson, Ximena Trujillo, and Yuzo Yanagitsuru. I also had the pleasure to work with Jackson Powell and Kieu Tran who participated in the Scripps Undergraduate Research Fellowship summer program.

This dissertation would not have been possible without the collaborative support of multiple research and ocean monitoring programs including those funded by the Los Angeles County Sanitation District (Bill Furlong, Joe Gully, Larry Lovell, Chase McDonald, Bill Power, Shelly Walther), National Oceanic and Atmospheric Administration (Keith Bosley, John Buchanan, Peter Frey, Melissa Head, Aimee Keller, Simon Victor), Long Term Ecological Research – California Current Ecosystem (Cat Nickels, Mark Ohman, Brandon Stephens), Southern California Coastal Water Research Project (Kenneth Schiff, Martha Sutula), and University of California Ship Funds (Bruce

Appelgate). This work was also made possible by extensive volunteer assistance from hundreds of UC San Diego graduate and undergraduate students, employees, and visiting researchers in the field. Special thanks to the SIO Res Techs for their dedication, hard work, and generosity preparing for and during research cruises – Drew Cole, Megan Donohue, Matt Durham, Brett Hembro, Josh Manger, Keith Shadle, and Jay Turnbull.

Each of my committee members has been instrumental in my development as a scientist. They pushed me to consider all possibilities when designing studies, interpreting results, and describing ecological patterns. Their generosity with their time and equipment is something I will always respect, appreciate, and try to emulate. Their individual labs are testaments to their expertise and success, and I am lucky to have had their support.

I owe much of my scientific training to the faculty and former graduate students at the UC Davis Bodega Marine Laboratory. Eric Sanford was initially and continues to be a tremendous source of inspiration and guidance. The mentorship I received from Annaliese Hettinger and Morgan Kelly further inspired me to pursue my doctoral degree, mentor students, and balance my personal life with my research. The sense of community I felt at BML and at SIO helped shape my collaborative experiences throughout grad school.

Thank you to Margaret Leinen, for her leadership and support as SIO Director. “Merci beaucoup” to Margaret and Françoise Gaill for supporting the partnership between SIO and the Ocean and Climate Platform. Thank you to Lisa, Kathryn Mengerink, Penny Dockry, and Jane Weinzierl at the Center for Marine Biodiversity and Conservation for presenting me with new opportunities to advocate for ocean science and conservation. Dave Rudie, Catalina Offshore Products, continues to be an invaluable resource to me and other scientists at SIO interested in working with the seafood industry.

Moving forward, I am grateful to Satoshi Mitarai at the Okinawa Institute of Science and Technology for providing me with a new opportunity to advance my research and teaching endeavors internationally.

Chapter 2, in full, is a reprint of the material as it appears in Deep Sea Research Part II: Topical Studies in Oceanography. Sato, Kirk N.; Levin, Lisa A.; Schiff, Kenneth, 2017. The dissertation author was the primary investigator and author of this material.

Chapter 3, in full, has been submitted for publication of the material as it may appear in ICES Journal of Marine Science, 2017, Sato, Kirk N.; Powell, Jackson; Rudie, David; Levin, Lisa A. The dissertation author was the primary investigator and author of this material.

Chapter 4, in part, is currently being prepared for submission for publication of the material. Sato, Kirk N.; Andersson, A.J.; Day, James M. D.; Taylor, Jennifer R. A.; Frank, Michael; Jung, Jae-Young; McKittrick, Joanna; Levin, Lisa A. The dissertation author was the primary investigator and author of this material.

VITA

2008	Bachelor of Science, University of California, Davis
2008 - 2010	Junior Specialist, Bodega Marine Laboratory, University of California, Davis
2014	Master of Science, University of California, San Diego
2017	Doctor of Philosophy, University of California, San Diego

PUBLICATIONS

Sato, KN, LA Levin, and K Schiff. 2017. Habitat compression and expansion of sea urchins in response to changing climate conditions on the California continental shelf and slope (1994-2013). *Deep Sea Research Part II: Topical Studies in Oceanography* 137: 377–389.

Levin, LA, K Mengerink, KM Gjerde, AA Rowden, CL Van Dover, MR Clark, E Ramirez-Llodra, B Currie, CR Smith, KN Sato, N Gallo, AK Sweetman, H Lily, CW Armstrong, and J Brider. 2016. Defining "serious harm" to the marine environment in the context of deep-seabed mining. *Marine Policy* 74: 245–259.

Frank, MB, SE Naleway, TS Wirth, J-Y Jung, CL Cheung, FB Loera, S Medina, KN Sato, JRA Taylor, and J McKittrick. 2016. A Protocol for Bioinspired Design: A Ground Sampler Based on Sea Urchin Jaws. *Journal of Visualized Experiments* 110: e53554.

Hettinger, A, E Sanford, TM Hill, AD Russell, KN Sato, J Huey, M Forsch, H Page, and B Gaylord. 2012. Persistent carry-over effects of planktonic exposure to ocean acidification in the Olympia oyster. *Ecology* 93: 2758–2768.

Bagulayan, A, JN Bartlett, AC Carter, B Inman, E Keen, EC Orenstein, N Patin, KNS Sato, EC Sibert, AE Simonis, AM Van Cise, and PJS Franks. 2012. Journey to the Center of the Gyre: A Lagrangian perspective on the fate of the Tohoku tsunami debris field. *Oceanography* 25: 200–207.

Gaylord, B, TM Hill, E Sanford, EA Lenz, LA Jacobs, KN Sato, AD Russell, and A Hettinger. 2011. Functional impacts of ocean acidification in an ecologically critical foundation species. *Journal of Experimental Biology* 214: 2586–2594.

ABSTRACT OF THE DISSERTATION

Implications of deoxygenation and acidification for deep sea urchins in southern California

by

Kirk Nicholas Suda Sato

Doctor of Philosophy in Oceanography

University of California, San Diego, 2017

Professor Lisa A. Levin, Chair

Implications of multiple climate drivers for sea urchins were investigated across a spectrum of biological organization ranging from the urchin guild scale, to individual life history traits, to the geochemistry, material properties and porosity of sea urchin calcium carbonate skeletal tests. Using pink fragile sea urchins (*Strongylocentrotus fragilis*) on the southern California upwelling margin as a model species, links between

biological traits and environmental parameters in nature across multiple spatial and temporal scales revealed correlations with dissolved oxygen (DO), pH, and temperature. Temporal trends in sea urchin populations assessed from trawl surveys conducted in southern California over the last 20 years (1994-2013) revealed changes in deep-sea urchin densities and depth distributions that coincide with trends in DO and pH on multidecadal and interdecadal (El Niño Southern Oscillation) time scales. The shallower urchin species (*Lytechinus pictus*) decreased in density in the upper 200 m by 80%, and the deeper *S. fragilis* increased in density by ~300%, providing the first evidence of habitat compression and expansion in sea urchin populations associated with secular and interdecadal variability in DO and pH. In this context, marketable food quality properties of the roe were compared between *S. fragilis* and the currently fished California red urchin, *Mesocentrotus franciscanus*, to assess the feasibility of developing a climate change-tolerant future *S. fragilis* trap fishery. Although roe color, texture, and resilience were similar between the two species, smaller and softer *S. fragilis* roe suggest it may only supplement, but not replace *M. franciscanus* in future fisheries. In comparisons across natural margin depth and climate gradients from 100-1100 m, *S. fragilis* exhibited reduced gonad production, smaller, weaker and more porous calcified tests in the Oxygen Minimum Zone (DO < 22 μmol kg^{-1}) and pH Minimum Zone (*in situ* pH_{Total} < 7.57) than those collected from less acidic and more oxygenated shelf and oxygen limiting zones above and the lower OMZ below. Thus *S. fragilis* may be more vulnerable to crushing predators if low oxygen, low pH OMZs continue to shoal and intensify in the future. This research highlights the utility of quantifying natural variability in species' traits along natural gradients on upwelling margins to improve understanding about potential impacts of changing climate drivers.

CHAPTER 1

Introduction

Anthropogenic ocean warming and ocean acidification (*i.e.*, decreased seawater pH due to increased absorption of anthropogenic carbon emissions) are widely acknowledged as upper water column phenomena (Caldeira and Wickett 2003, Sabine *et al.* 2004). The deep ocean (>200 m water depth) is the largest reservoir of carbon on Earth and mitigates over 35% of the excess heat content trapped by anthropogenic greenhouse gas emissions (IPCC 2014, Gleckler *et al.* 2016). Deoxygenation, the observed and future loss of dissolved oxygen from coastal and open ocean waters, is another climate driver in the deep ocean that results from a combination of eutrophication and ocean warming effects (Keeling *et al.* 2010, Bopp *et al.* 2013, Rabalais *et al.* 2014). Increased water temperature decreases the solubility of dissolved oxygen in seawater and increases stratification, which reduces ventilation of deep, oxygen-deprived waters (Keeling and Garcia 2002). These cumulative global phenomena, also known as a "triple whammy" of climate drivers (Gruber 2011), may directly affect benthic species, communities, and ecosystems and indirectly *via* poorly understood changes in allochthonous food flux to the deep ocean seafloor (Levin and Le Bris 2015, Levin *et al.* 2015, Sweetman *et al.* 2017).

True sea urchins (Subclass: Euechinoidea; Class: Echinoidea; Phylum: Echinodermata) have been extensively studied because of their position in metazoan evolution (Sodergren *et al.* 2006), representation in the fossil record (Moffitt *et al.* 2015), central role in benthic ecosystem structure (Pearse 2006), and economic value as food in

various countries (Lawrence 2006). As slow-moving calcifying animals with free-swimming planktonic larvae (Moore 1959a, 1959b), sea urchins have been identified as vulnerable to future ocean acidification (Dupont *et al.* 2010, Kroeker *et al.* 2010, Dubois 2014); however, recent evidence suggests strong biological control by urchin species to calcify and persist in unfavorable environments (Dupont *et al.* 2013, Collard *et al.* 2014, Lebrato *et al.* 2016). As studies on the effects of future ocean acidification and other climate-driven stressors accrue, it is clear that different sea urchin species will emerge as either vulnerable or tolerant taxa.

Regional Setting for the Dissertation

The Southern California Bight (SCB) stretches ~1,000 km from Point Conception in Santa Barbara County south to the US-Mexico border and is characterized by dynamic, heterogeneous ecosystems, geomorphology, and hydrography (reviewed in Dailey *et al.*, 1993). Continental margin ecosystems provide important ecological functions such as nutrient regeneration and food web linkages (Levin and Dayton 2009), and humans benefit from various ecosystem services such as carbon sequestration, fisheries production, tourism, and inspiration (Levin and Sibuet 2012, Thurber *et al.* 2014, Frank *et al.* 2015).

The overlying water adjacent to the SCB continental shelf and slope benthos is characterized by multiple depth-related gradients of physicochemical variables (*e.g.*, carbonate chemistry, oxygen, temperature, salinity, and pressure). Relatively low pH waters occur naturally beneath the mixed layer associated with cold, nutrient-rich, and oxygen-limited waters (Paulmier *et al.* 2011, Gilly *et al.* 2013, Nam *et al.* 2015). These

waters, characterized by co-varying climate change variables, are periodically upwelled onto the continental shelf throughout the SCB (Feely *et al.* 2008, Frieder *et al.* 2012, Reum *et al.* 2016). Even though seawater pH levels at outer shelf and slope depths (100-1,000 m) are naturally lower than what is predicted for open ocean surface water under ocean acidification (OA) scenarios, calcifying organisms (*i.e.*, benthic echinoderms) often dominate the SCB megafauna community (McCauley and Carey 1967, Thompson *et al.* 1993, Lebrato *et al.* 2016). Thus, some species are already adapted to persistent hypoxic (oxygen stressed) and hypercapnic (carbon dioxide stressed) environments (Pörtner *et al.* 2005, Byrne and Przeslawski 2013, Somero *et al.* 2016). In a region where secular shoaling of oxygen-limited, reduced pH water has been observed (Bograd *et al.* 2008, 2015), an improved understanding of community and species responses to natural environmental gradients across space and time will inform predictions about the future state of marine ecosystems.

The objective of this dissertation is to investigate the spatiotemporal variability of population sizes and distributions of multiple sea urchin species, and for one species, *Strongylocentrotus fragilis*, compare fitness-related and microstructural properties along natural gradients of multiple climate change co-variables. By examining the variability of traits in populations of soft-bottom echinoids throughout the SCB, the aim of this dissertation is to elucidate species-specific phenotypic variability along a deep margin to better understand how urchins may be affected by multiple climate change drivers. These studies also provide a platform of *in situ* biological links to the environment upon which further study of biological mechanisms involved in species response to future climate change can be investigated.

The Thesis: Introductory Remarks

Around the beginning of the 21st century, the field of climate change and ocean acidification research had emerged as a prominent focus of interest among marine scientists, particularly among biologists and ecologists. Until recently however, appreciation for the complexity of species' interactions and ecological responses to anthropogenic climate change was lacking (Andersson *et al.* 2015, Kroeker *et al.* 2017). As our understanding of model systems and organisms improve, the potential devastating direct and synergistic impacts of multiple climate change drivers on ecosystem functioning and services will become more likely to drive decisions in science, policy, industry, and society.

This dissertation focuses on how organismal and population attributes of deep, continental margin sea urchins change along gradients of and spatiotemporal changes in temperature, dissolved oxygen, and carbonate chemistry. In Chapter 2, I examined interannual trends in sea urchin species depth distributions and densities from environmental monitoring surveys conducted over the last 20 years (1994-2003) throughout the continental shelf and slope of the SCB (Figure 1.1). These were related to secular trends and interannual variability in oxygen and pH, and possibly food supply observed over this time period.

In Chapter 3, further in-depth analyses determined changes in density, growth, and gonad index by the pink fragile sea urchin, *Strongylocentrotus* (previously *Allocentrotus*) *fragilis*, along natural gradients of dissolved oxygen, pH, and temperature within its current depth range. Spatial and seasonal patterns of *S. fragilis* gonad production were determined for the first time in the SCB. The food qualities (color,

texture, firmness) of sea urchin gonads were compared between *S. fragilis* and the currently fished California red urchin (*Mesocentrotus* (previously *Strongylocentrotus*) *franciscanus*) to consider the potential feasibility of developing *S. fragilis* as a future, climate change tolerant fishery.

Finally, in Chapter 4, also considering environmental changes along depth gradients linked to climate change variables, I investigated various changes among phenotypes of *S. fragilis* including morphology and reproduction, as well as geochemical elemental composition and microscale differences in skeletal structure and material properties. Higher concentrations of trace metal elements in *S. fragilis* calcite relative to seawater suggested *S. fragilis* may either actively control the incorporation of these trace metals into the test or actively remove these elements from the organic matrix. However, kinetic effects of elemental incorporation may also explain these results, and further investigation of calcification mechanisms is required. More porous and softer skeletal tests, slower growth, and lower reproductive potential in low oxygen and calcium carbonate undersaturated waters suggest possible increased vulnerability of *S. fragilis* to crushing by predators as *S. fragilis* may expand upslope.

The final chapter summarizes and integrates the findings of this dissertation and their implications. Together, these dissertation chapters present a holistic approach to better understand the ecology of deep-sea echinoids on a rapidly changing upwelling margin, as well as potential species-specific responses to multiple climate change drivers.

References

Andersson, A. J., D. I. Kline, P. J. Edmunds, S. D. Archer, N. Bednaršek, R. C. Carpenter, M. Chadsey, P. Goldstein, A. G. Grottoli, T. P. Hurst, A. L. King, J. E. Kübler, I. B. Kuffner, K. R. M. Mackey, B. A. Menge, A. Paytan, U. Riebesell, A. Schnetzer, M. E. Warner, and R. C. Zimmerman. 2015. Understanding ocean acidification impacts on organismal to ecological scales. Oceanography 28:16–27.

Bograd, S. J., M. P. Buil, E. Di Lorenzo, C. G. Castro, I. D. Schroeder, C. R. Anderson, C. Benitez-Nelson, and F. A. Whitney. 2015. Changes in source waters to the Southern California Bight. Deep Sea Research Part II: Topical Studies in Oceanography 112:42–52.

Bograd, S. J., C. G. Castro, E. Di Lorenzo, D. M. Palacios, H. Bailey, W. Gilly, and F. P. Chavez. 2008. Oxygen declines and the shoaling of the hypoxic boundary in the California Current. Geophysical Research Letters 35:L12607.

Bopp, L., L. Resplandy, J. C. Orr, S. C. Doney, J. P. Dunne, M. Gehlen, P. Halloran, C. Heinze, T. Ilyina, R. Séférian, J. Tjiputra, and M. Vichi. 2013. Multiple stressors of ocean ecosystems in the 21st century: projections with CMIP5 models. Biogeosciences 10:6225–6245.

Byrne, M., and R. Przeslawski. 2013. Multistressor impacts of warming and acidification of the ocean on marine invertebrates' life histories. Integrative and Comparative Biology 53:582–596.

Caldeira, K., and M. E. Wickett. 2003. Anthropogenic carbon and ocean pH. Nature 425:365–365.

Collard, M., A. Dery, F. Dehairs, and P. Dubois. 2014. Euechinoidea and Cidaroidea respond differently to ocean acidification. Comparative Biochemistry and Physiology Part A: Molecular & Integrative Physiology 174:45–55.

Dailey, M., D. Reish, and J. Anderson, editors. 1993. Ecology of the Southern California Bight: A synthesis and interpretation. University of California Press, Berkeley, CA, USA.

Dubois, P. 2014. The Skeleton of Postmetamorphic Echinoderms in a Changing World. Biological Bulletin 226:223–236.

Dupont, S., N. Dorey, M. Stumpp, F. Melzner, and M. Thorndyke. 2013. Long-term and trans-life-cycle effects of exposure to ocean acidification in the green sea urchin *Strongylocentrotus droebachiensis*. Marine Biology 160:1835–1843.

Dupont, S., O. Ortega-Martínez, and M. Thorndyke. 2010. Impact of near-future ocean acidification on echinoderms. Ecotoxicology 19:449–462.

Feely, R. A., C. L. Sabine, J. M. Hernandez-Ayon, D. Ianson, and B. Hales. 2008. Evidence for upwelling of corrosive “acidified” water onto the continental shelf. Science 320:1490–1492.

Frank, M., S. Naleway, J.-Y. Jung, T. Wirth, C. Cheung, F. Loera, S. Medina, K. Sato, J. Taylor, and J. McKittrick. 2015. A Protocol for Bioinspired Design: A Ground Sampler Based on Sea Urchin Jaws. Journal of Visualized Experiments 110:e53554.

Frieder, C. A., S. H. Nam, T. R. Martz, and L. A. Levin. 2012. High temporal and spatial variability of dissolved oxygen and pH in a nearshore California kelp forest. Biogeosciences 9:3917–3930.

Gilly, W. F., J. M. Beman, S. Y. Litvin, and B. H. Robison. 2013. Oceanographic and Biological Effects of Shoaling of the Oxygen Minimum Zone. Annual Review of Marine Science 5:393–420.

Gleckler, P. J., P. J. Durack, R. J. Stouffer, G. C. Johnson, and C. E. Forest. 2016. Industrial-era global ocean heat uptake doubles in recent decades. Nature Climate Change 6:394–398.

Gruber, N. 2011. Warming up, turning sour, losing breath: ocean biogeochemistry under global change. Philosophical Transactions of the Royal Society of London A: Mathematical, Physical and Engineering Sciences 369:1980–1996.

IPCC. 2014. Climate Change 2014: Synthesis Report. Contribution of Working Groups I, II and III to the Fifth Assessment Report of the Intergovernmental Panel on Climate Change. R. K. Pachauri and L. A. Meyer, Eds. Geneva, Switzerland.

Keeling, R. F., and H. E. Garcia. 2002. The change in oceanic O_2 inventory associated with recent global warming. Proceedings of the National Academy of Sciences of the United States of America 99:7848–53.

Keeling, R. F., A. Körtzinger, and N. Gruber. 2010. Ocean Deoxygenation in a Warming World. Annual Review of Marine Science 2:199–229.

Kroeker, K. J., R. L. Kordas, R. N. Crim, and G. G. Singh. 2010. Meta-analysis reveals negative yet variable effects of ocean acidification on marine organisms. Ecology Letters 13:1419–1434.

Kroeker, K. J., R. L. Kordas, and C. D. G. Harley. 2017. Embracing interactions in ocean acidification research: confronting multiple stressor scenarios and context dependence. Biology Letters 13.

Lawrence, J., editor. 2006. Edible sea urchins: Biology and ecology. Second edition. Elsevier Science.

Lebrato, M., A. J. Andersson, J. B. Ries, R. B. Aronson, M. D. Lamare, W. Koeve, A. Oschlies, M. D. Iglesias-Rodriguez, S. Thatje, M. Amsler, S. C. Vos, D. O. B. Jones,

H. A. Ruhl, A. R. Gates, and J. B. McClintock. 2016. Benthic marine calcifiers coexist with $CaCO_3$-undersaturated seawater worldwide. Global Biogeochemical Cycles 30:1038–1053.

Levin, L. A., and N. Le Bris. 2015. The deep ocean under climate change. Science 350:766–768.

Levin, L. A., and P. K. Dayton. 2009. Ecological theory and continental margins: Where shallow meets deep. Trends in Ecology & Evolution 24:606–617.

Levin, L. A., and M. Sibuet. 2012. Understanding Continental Margin Biodiversity: A New Imperative. Annual Review of Marine Science 4:79–112.

Levin, L., K.-K. Liu, K.-C. Emeis, D. L. Breitburg, J. Cloern, C. Deutsch, M. Giani, A. Goffart, E. E. Hofmann, Z. Lachkar, K. Limburg, S.-M. Liu, E. Montes, O. Ragueneau, C. Rabouille, S. K. Sarkar, D. P. Swaney, P. Wassman, and K. F. Wishner. 2015. Comparative biogeochemistry–ecosystem–human interactions on dynamic continental margins. Journal of Marine Systems 141:3–17.

McCauley, J., and A. Carey. 1967. Echinoidea of Oregon. Journal of the Fisheries Research Board of Canada 24:1385–1401.

Moffitt, S. E., T. M. Hill, P. D. Roopnarine, and J. P. Kennett. 2015. Response of seafloor ecosystems to abrupt global climate change. Proceedings of the National Academy of Sciences of the United States of America 112:4684–4689.

Moore, A. R. 1959a. On the embryonic development of the sea urchin Allocentrotus fragilis. Biological Bulletin 117:492–496.

Moore, A. R. 1959b. Some effects of temperature on development in the sea urchin Allocentrotus fragilis. Biological Bulletin 117:150–153.

Nam, S., Y. Takeshita, C. A. Frieder, T. Martz, and J. Ballard. 2015. Seasonal advection of Pacific Equatorial Water alters oxygen and pH in the Southern California Bight. Journal of Geophysical Research: Oceans 120:5387–5399.

Paulmier, A., D. Ruiz-Pino, and V. Garçon. 2011. CO_2 maximum in the oxygen minimum zone (OMZ). Biogeosciences 8:239–252.

Pearse, J. S. 2006. Ecological role of purple sea urchins. Science 314:940–941.

Pörtner, H. O., M. Langenbuch, and B. Michaelidis. 2005. Synergistic effects of temperature extremes, hypoxia, and increases in CO_2 on marine animals: From Earth history to global change. Journal of Geophysical Research 110:C09S10.

Rabalais, N., W.-J. Cai, J. Carstensen, D. Conley, B. Fry, X. Hu, Z. Quiñones-Rivera, R. Rosenberg, C. Slomp, E. Turner, M. Voss, B. Wissel, and J. Zhang. 2014. Eutrophication-Driven Deoxygenation in the Coastal Ocean. Oceanography 27:172–

183.

Reum, J. C. P., S. R. Alin, C. J. Harvey, N. Bednaršek, W. Evans, R. A. Feely, B. Hales, N. Lucey, J. T. Mathis, P. McElhany, J. Newton, and C. L. Sabine. 2016. Interpretation and design of ocean acidification experiments in upwelling systems in the context of carbonate chemistry co-variation with temperature and oxygen. ICES Journal of Marine Science 73:582–595.

Sabine, C. L., R. A. Feely, N. Gruber, R. M. Key, K. Lee, J. L. Bullister, R. Wanninkhof, C. S. Wong, D. W. R. Wallace, B. Tilbrook, F. J. Millero, T.-H. Peng, A. Kozyr, T. Ono, and A. F. Rios. 2004. The Oceanic Sink for Anthropogenic CO_2. Science 305:367–371.

Sodergren, E., G. M. Weinstock, E. H. Davidson, R. A. Cameron, R. A. Gibbs, R. C. Angerer, L. M. Angerer, M. I. Arnone, D. R. Burgess, R. D. Burke, J. A. Coffman, M. Dean, M. R. Elphick, C. A. Ettensohn, K. R. Foltz, A. Hamdoun, R. O. Hynes, W. H. Klein, W. Marzluff, *et al.* 2006. The Genome of the Sea Urchin *Strongylocentrotus purpuratus*. Science 314:941–952.

Somero, G. N., J. M. Beers, F. Chan, T. M. Hill, T. Klinger, and S. Y. Litvin. 2016. What Changes in the Carbonate System, Oxygen, and Temperature Portend for the Northeastern Pacific Ocean: A Physiological Perspective. BioScience 66:14–26.

Sweetman, A. K., A. R. Thurber, C. R. Smith, L. A. Levin, C. Mora, C.-L. Wei, A. J. Gooday, D. O. B. Jones, M. Rex, M. Yasuhara, J. Ingels, H. A. Ruhl, C. A. Frieder, R. Danovaro, L. Würzberg, A. Baco, B. M. Grupe, A. Pasulka, K. S. Meyer, K. M. Dunlop, L.-A. Henry, and J. M. Roberts. 2017. Major impacts of climate change on deep-sea benthic ecosystems. Elementa 5:4.

Thompson, B., D. Tsukada, and J. Laughlin. 1993. Megabenthic assemblages of coastal shelves, slopes, and basins off southern California. Bulletin of the Southern California Academy of Sciences 92:25–42.

Thurber, A. R., A. K. Sweetman, B. E. Narayanaswamy, D. O. B. Jones, J. Ingels, and R. L. Hansman. 2014. Ecosystem function and services provided by the deep sea. Biogeosciences 11:3941–3963.

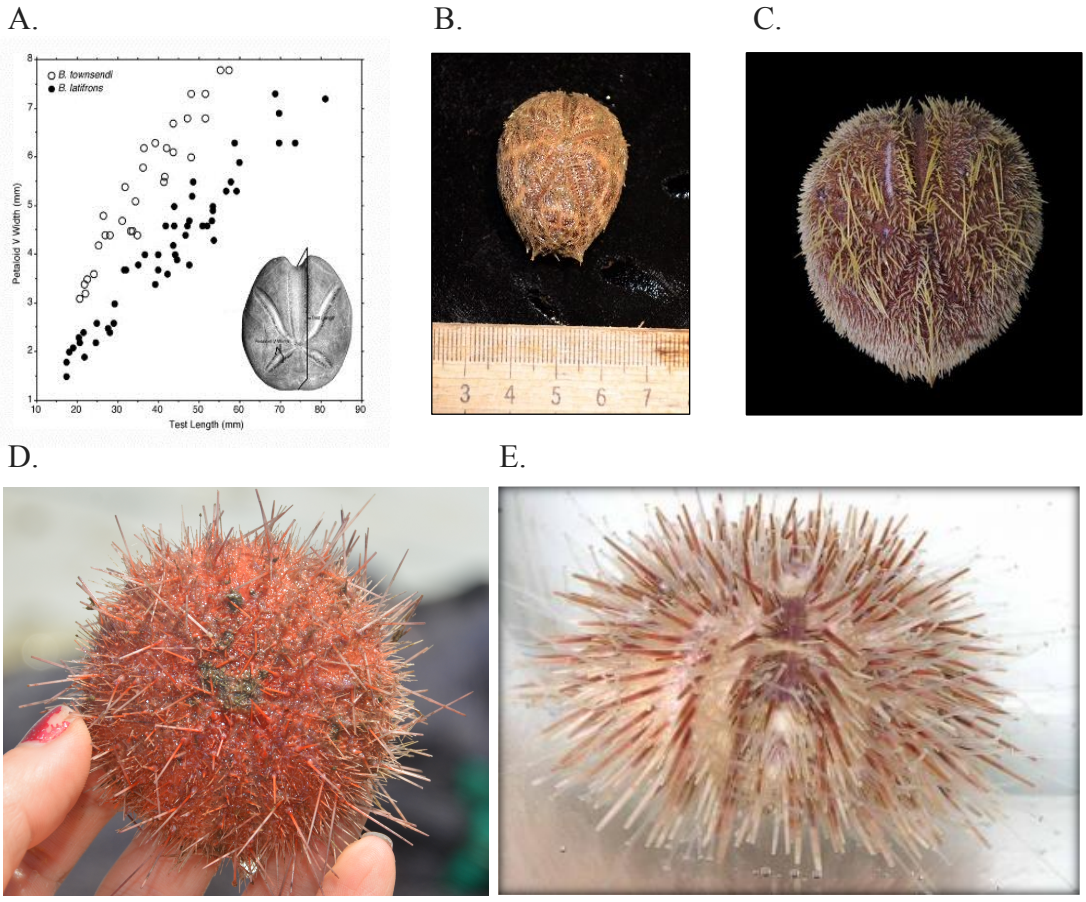

Figure 1.1. **A.** *Brisaster latifrons* and *B. townsendi*. Common name: Northern heart urchin. Subsurface feeders; Size: 5-80 mm. Photo credit: Southern California Association of Marine Invertebrate Taxonomists. **B.** *Brissopsis pacifica*. Common name: Pacific heart urchin. Subsurface feeders; Size: 5-80 mm. **C.** *Spatangus californica*. Common name: California heart urchin. Subsurface feeder; Size: up to 50 cm. **D.** *Strongylocentrotus fragilis*. Common name: Pink fragile urchin. Surface feeder; Size: up to 90 mm diameter; **E.** *Lytechinus pictus*. Common name: white urchin. Surface feeder; Size: up to 50 mm diameter. Photo credit: http://www.Biosciweb.net.

CHAPTER 2

Habitat compression and expansion of sea urchins in response to changing climate conditions on the California continental shelf and slope (1994-2013)

Synopsis

This chapter examines historical changes in depth distributions and densities of multiple southern California sea urchin species and their relationships with variations in dissolved oxygen and pH related to the El Niño Southern Oscillation and secular trends.

This chapter is presented as a paper published in Deep Sea Research Part II: Topical Studies in Oceanography in 2017. "Habitat compression and expansion of sea urchins in response to changing climate conditions on the California continental shelf and slope (1994-2013)," also appears as an Appendix in the Southern California Bight 2013 Regional Monitoring Program (Bight '13) survey report by the Southern California Coastal Water Research Project (see Walther *et al.*, 2017).

Contents lists available at ScienceDirect

Deep-Sea Research II

journal homepage: www.elsevier.com/locate/dsr2

Habitat compression and expansion of sea urchins in response to changing climate conditions on the California continental shelf and slope (1994–2013)

Kirk N. Sato [a,*], Lisa A. Levin [a], Kenneth Schiff [b]

[a] Center for Marine Biodiversity and Conservation, Scripps Institution of Oceanography, University of California, San Diego, 9500 Gilman Dr., La Jolla, CA 92093-0218, United States
[b] Southern California Coastal Water Research Project, 3535 Harbor Blvd., Costa Mesa, CA 92626, United States

ARTICLE INFO

Keywords:
Deoxygenation
Acidification
Continental slope
El Niño phenomena
Echinoid
Southern California Bight
Habitat compression
Depth distribution

ABSTRACT

Echinoid sea urchins with distributions along the continental shelf and slope of the eastern Pacific often dominate the megafauna community. This occurs despite their exposure to naturally low dissolved oxygen (DO) waters (<60 μmol kg^{-1}) associated with the Oxygen Limited Zone and low-pH waters undersaturated with respect to calcium carbonate ($\Omega_{CaCO3} < 1$). Here we present vertical depth distribution and density analyses of historical otter trawl data collected in the Southern California Bight (SCB) from 1994 to 2013 to address the question: Do changes in echinoid density and species' depth distributions along the continental margin in the SCB reflect observed secular or interannual changes in climate? Deep-dwelling burrowing urchins (*Brissopsis pacifica*, *Brisaster* spp. and *Spatangus californicus*), which are adapted to low-DO, low-pH conditions appeared to have expanded their vertical distributions and populations upslope over the past decade (2003–2013), and densities of the deep pink urchin, *Strongylocentrotus fragilis*, increased significantly in the upper 500 m of the SCB. Conversely, the shallower urchin, *Lytechinus pictus*, exhibited depth shoaling and density decreases within the upper 200 m of the SCB from 1994 to 2013. Oxygen and pH in the SCB also vary inter-annually due to varying strengths of the El Niño Southern Oscillation (ENSO). Changes in depth distributions and densities were correlated with bi-monthly ENSO climate indices in the region. Our results suggest that both a secular trend in ocean deoxygenation and acidification and varying strength of ENSO may be linked to echinoid species distributions and densities, creating habitat compression in some and habitat expansion in others. Potential life-history mechanisms underlying depth and density changes observed over these time periods include migration, mortality, and recruitment. These types of analyses are needed for a broad suite of benthic species in order to identify and manage climate-sensitive species on the margin.

1. Introduction

Continental margin ecosystems in eastern boundary upwelling regions such as the west coast of North America experience dynamic natural variations in biogeochemical cycles on various spatiotemporal scales. Oscillations in ocean-atmosphere coupled processes occur naturally on millennial (Moffitt et al., 2015), decadal (Mantua et al., 1997), and interannual (Bjerknes, 1966) timescales; these can have basin-wide effects on population dynamics and global climate change variables such as seawater pH, dissolved oxygen (DO), and temperature (reviewed in Levin et al., 2015). The Southern California Bight (SCB) is a 700-km long region influenced by the upwelling of cold, nutrient-rich, deep water characterized by relatively low DO, low pH, and high carbon dioxide (CO_2). Benthic and epibenthic organisms may already be functioning at their physiological limits at the seawater-seafloor interface where the continental slope intersects with a permanent dissolved Oxygen Minimum Zone (OMZ) and Carbon Maximum Zone (Paulmier et al., 2011), therefore making these regions particular 'hotspots' of future climate change (Gruber, 2011).

Oxygen Limited Zones (OLZs) are the regions above and beneath the OMZ where DO concentrations of <60 μmol kg^{-1} are often considered hypoxic habitat for marine organisms (Gilly et al., 2013), although this threshold may not be relevant for organisms with very low metabolic oxygen demands (Seibel, 2011; Somero et al., 2016). Time-series analysis from 1984 to 2006 of quarterly cruise data in the SCB collected by the

* Corresponding author.
E-mail addresses: knsato@ucsd.edu (K.N. Sato), llevin@ucsd.edu (L.A. Levin), kens@sccwrp.org (K. Schiff).

http://dx.doi.org/10.1016/j.dsr2.2016.08.012
0967-0645/

California Cooperative Ocean Fisheries Investigations (CalCOFI) reveal oxygen declines, with an average decrease in DO of $\sim$1 μmol kg^{-1} yr^{-1} at 200-m stations and a shoaling of the OLZ boundary of >80 m at some inshore stations (Bograd et al., 2008). An updated analysis of these data (1984–2010) showed a decrease of 0.76 μmol kg^{-1} yr^{-1} at the 25.8 kg m^{-3} isopycnal (Bograd et al., 2015). Due to microbially-mediated remineralization processes, similar reductions in pH and increases in pCO_2 are expected to have accompanied the expansion of low oxygen zones in the SCB (Gilly et al., 2013; Gruber, 2011; Paulmier et al., 2011; Reum et al., 2016). Seawater pH and DO are strongly cor-related in nearshore kelp forests (Frieder et al., 2012) and in the deep sea (Alin et al., 2012; Nam et al., 2015). In addition, secular increases in nutrient concentrations and chlorophyll *a* have been observed from the same CalCOFI dataset (Bograd et al., 2015). One potential mechanism for shoaling hypoxia and changes in nutri-ents in the SCB include a strengthening of the CA Undercurrent, which originates from subtropical equatorial water from the south and is characterized by relatively warm, high saline, low DO, and low pH water (Bograd et al., 2015).

Koslow et al. (2011) reported striking shifts in mesopelagic and demersal larval fish community structure accompanying these decadal changes in midwater DO. Twenty four of 27 larval fish taxa collected by seasonal CalCOFI cruises demonstrated a strong relationship with midwater DO and multiple climate indices such as the Pacific Decadal Oscillation (PDO), El Niño Southern Oscillation (ENSO), and the North Pacific Gyre Oscillation (NPGO) (Koslow et al., 2011, 2015). Although the CalCOFI biological time-series provides extensive spatial and temporal coverage of pelagic species, the interactions of benthic faunal populations with climate variability along the SCB continental margin have been understudied. The phenomenon of vertical habitat compression in the ocean due to shoaling hypoxia was hypothesized to negatively affect aerobic groundfish (McClatchie et al., 2010) and mesopelagic fish (Netburn and Koslow, 2015) in southern CA and billfish in the Eastern Tropical Pacific (Prince and Goodyear, 2006; Stramma et al., 2012). However, few datasets exist to assess trends in megafauna species populations that dominant the benthos such as echinoids in the SCB (Keller et al., 2012).

Beyond the longer-term changes in oxygenation and likely pH and pCO_2, the SCB is highly dynamic on interannual, seasonal, and even diurnal and semidiurnal time scales (Nam et al., 2015; Booth et al., 2012; Send and Nam, 2012). For example, during El Niño events, elevated temperatures and reduced upwelling lead to low productivity, less respiration and biogeochemical drawdown, thus higher oxygen levels (Ito and Deutsch, 2013), while the opposite occurs during La Niña events (Nam et al., 2011). Over the last 25 years, the Multivariate ENSO Index (MEI), a composite of six key ocean-atmospheric variables: sea-level pressure, zonal and meridional components of the surface wind, sea surface temperature, surface air temperature, and total cloudiness (Wolter and Timlin, 2011), indicates a range of El Niño and La Niña strengths occurring in the Pacific Ocean, including one exceedingly strong El Niño in 1997–1998 (Fig. 1). Nam et al. (2011) advise caution when extrapolating their correlation results from a single El Niño-La Niña cycle to other ENSO indices, and few studies examined the direct relationship between ENSO and dissolved oxygen (see Arntz et al., 2006) despite the abundance of historical cruise data and the potentially important ecological implications (McClatchie, 2014).

Echinoderms are important benthic fauna ecologically; they are often identified as ecosystem engineers and in some cases, keystone predators or grazers (Paine, 1966). Biocalcification by echinoderms (*e.g.* sea urchins, sea stars, cucumbers, brittle stars, crinoids) contributes to globally significant carbon production rates that may rival production rates of coral reefs (Lebrato et al., 2010), and are surprisingly tolerant to low carbonate saturation states (Lebrato et al., 2016).

In the SCB, multiple deep-dwelling sea urchin species are abundant over broad depth ranges (Thompson et al., 1993) characterized by sharp gradients in oxygen, pH, and Ω (saturation state) levels that are comparable to or much lower than future ocean acidification and deoxygenation scenarios predicted for the surface ocean (Alin et al., 2012; Levin and Dayton, 2009; Nam et al., 2015). Experiments suggest that multiple life-history stages of calcifying benthic organisms, including echinoid urchins, will respond negatively to ocean acidification and hypoxia conditions (Dupont et al., 2010; Frieder, 2014; Kroeker et al., 2013). The vast majority of these studies have been conducted on shallow-water species however, and the response of deep-margin species to deoxygenation, ocean acidification, and calcium carbonate saturation ($\Omega_{CaCO_3}=1$) reduction is poorly understood (Barry et al., 2014; Hofmann et al., 2010; Taylor et al., 2014).

Detecting faunal response to long-term environmental change requires time-series sampling (Glover et al., 2010). The Southern California Coastal Water Research Project (SCCWRP) is a collaborative inter-agency environmental monitoring program that makes publicly available a time-series dataset of georeferenced benthic and epibenthic megafauna community data in southern California along the continental shelf and slope. The SCCWRP otter trawl surveys of the SCB shelf and slope benthos have occurred every 4–5 years since 1994 to water depths of 200 m, providing 5 time points in order to assess population trends in benthic fauna. In 2003 the SCCWRP *Bight* program extended their sampling depths down to 500 m, providing only 3 survey time points to the present, but extending spatial coverage into deep waters. These fishery-independent data provide a unique suite of multi-decadal samples that can be used to address questions about benthic community changes over time in the SCB.

The objective of this study was to investigate temporal changes in (1) depth distributions and (2) density estimates of five continental margin sea urchin species throughout the SCB from 1994 to 2013 to better understand echinoid response to environmental change. We hypothesized that various depth distribution parameters of deeper-occurring urchin species, which are tolerant to low oxygen, high CO_2 conditions in the upper OMZ (Helly and Levin, 2004) and OLZ (Gilly et al., 2013) would exhibit evidence of habitat expansion consistent with observed shoaling oxyclines in the region (Bograd et al., 2015; Bograd et al., 2008). This secular trend would suggest that these species have expanded their distribution into shallower waters enabled by a combination of environmental adaptation and ecological interactions. Urchin species with shallower distributions were hypothesized to be more vulnerable to expanding OMZ conditions and to have experienced habitat compression over this time period. In addition, we hypothesized that the density of shallower-occurring urchins would decrease in the upper 200 m from 1994 to 2013 due to the shoaling and intensification of hypoxic waters, and the density of deeper-occurring urchins in the upper 500 m would increase from 2003 to 2013 due to migration from deeper depths as habitat compression excludes shallower competitors. Alternatively, these trends could also be driven by environmental factors other than oxygen that may co-vary with time, such as changes in dissolved CO_2, food, temperature, and ecological interactions. Chlorophyll *a* concentration in the SCB has increased over recent decades (Bograd et al., 2015) and could lead to more food and higher densities in all species over time. In contrast, El Niño conditions, which occurred in 1997–1998 and 2002–2003 are associated with higher oxygenation and lower phytoplankton and kelp production (Ito and Deutsch, 2013), and should produce an opposite response to that expected from expanding OMZs. We

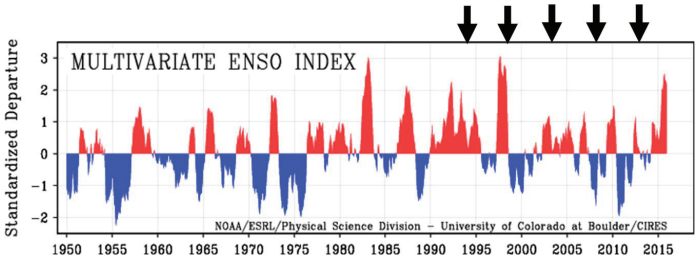

Fig. 1. Figure modified from http://www.esrl.noaa.gov/psd/enso/mei/. Time-series of MEI with black arrows indicating years when trawl surveys occurred throughout the Southern California Bight. Negative values of the MEI (blue) represent the cold ENSO phase (La Niña). Positive MEI values (red) represent the warm ENSO phase (El Niño).(For interpretation of the references to color in this figure legend, the reader is referred to the web version of this article.)

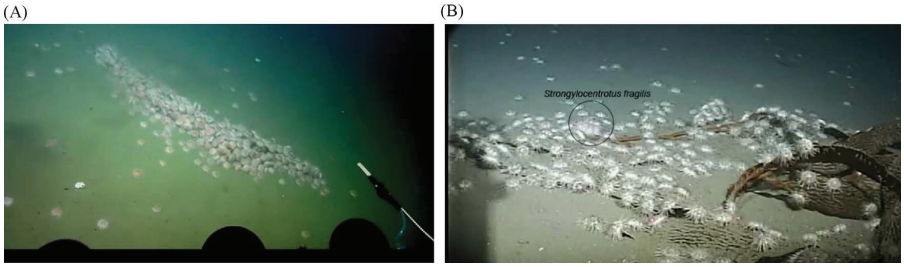

Fig. 2. A. Aggregation of pink urchins (*Strongylocentrotus fragilis*) in the OLZ (~400 m) off of San Diego, CA. Remotely operated vehicle (ROV) footage courtesy: R/V *Nautilus*, NOAA, cruise ID NA066. B. Feeding aggregation of white urchins (*Lytechinus pictus*) on giant kelp (*Macrocystis pyrifera*) a t ~100 m depth off the coast of La Jolla, CA. Presence of individual *S. fragilis* (circled) suggests these species compete for kelp resources at this depth. ROV footage courtesy: Scripps Institution of Oceanography, cruise ID MV1217.

hypothesized a deepening of hypoxia-intolerant species and pos-sibly lower densities of all species in response to El Niño.

2. Materials and methods

We analyzed biological benthic survey data collected along continental shelf and slope in the SCB. Depth distributions of shelf and slope sea urchins in the upper 200 and upper 500 m were determined for each survey year for five species of echinoderm echinoids: the white urchin (*Lytechinus pictus*), the pink urchin (*Strongylocentrotus fragilis*), and three burrowing urchins (*Brissopsis pacifica*, *Brisaster* spp. and *Spatangus californicus*). *Brisaster townsendi* and *B. latifrons* were grouped together as their ranges overlap in the SCB (Hood and Mooi, 1998) and they were often reported as *Brisaster* spp. in the field. Site-specific counts were standardized to obtain population density (count m^{-2}) for each sea urchin species and were compared among survey years and depth bins.

2.1. Data collection: trawl program and counts

The megafauna community was sampled at randomized stations by otter trawl across the SCB by trained taxonomists during the summer months (July–September) of years in which the Bight program was conducted (1994, 1998, 2003, 2008 and 2013) with 7.6 m head-rope semiballoon otter trawl nets fitted with 1.25-cm cod-end mesh. Trawls were towed along open-coast isobaths for ~10 min at 1.5–2.0 nautical miles per hour during daylight hours. Trawl distance was calculated from the start and stop fishing GPS coordinates, which acted as a proxy for the net's relative position. It was assumed the net remained on the bottom and was fishing the entire time. *S. fragilis* and *L. pictus* often form feeding aggregations on kelp falls (Sato and Levin, *personal observation*; Fig. 2A, B), which may bias density estimates, but the high number of trawls conducted each survey year is likely to capture this variability. One exception where kelp falls have been found to be more abundant is in submarine canyons (Harrold et al., 1998), but sites were surveyed for flat, trawlable ground prior to net deployment and sites in canyons were avoided. Upon retrieval, catches were sorted, identi-fied to species, and enumerated. Each station was sampled once per survey (Fig. 3). Bay sites and sites at water depths <10 m were removed from this analysis in order to minimize zero inflated data (Thompson et al., 1993). Only echinoid data representing 5 species are reported here.

2.2. Evaluation of area sampled and density estimates

The area swept by each trawl was calculated as the distance trawled (m) x 4.9 m (the width of the trawl) (*sensu* Miller and Schiff, 2012). Densities obtained per trawl were determined for each of the 5 urchin species for each survey year by dividing the species count by the area swept. Density means were also calculated for 50-m and 100-m depth bins in addition to 10–200 m (1994–2013 survey time period) and 10–500 m (2003–2013 sur-veys) depth bins.

2.3. Species distribution in the SCB

The start depths of each trawl station were recorded to the nearest meter on board survey vessels; trawls were made along depth contours so the start depth reflected the actual depth of the trawl. All individuals of each species were assigned the start depth of the trawl from which they were collected. Depth distributions of trawls containing one or more individuals were determined for each species for each survey year. For each species, trawls that contained one or more individuals were separated, and the upper and lower depth limits, the mean depth, and the first and third

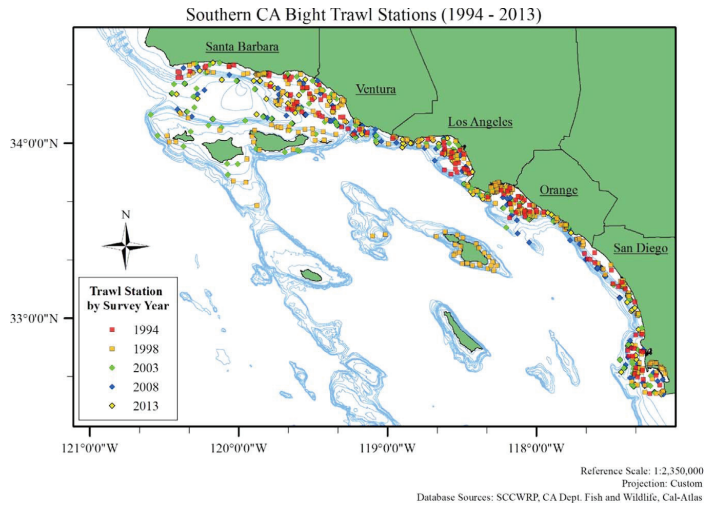

Fig. 3. Map of otter trawl survey stations from 1994 to 2013 in the Southern California Bight (SCCWRP). Black lines indicate boundaries between California counties (green) (Cal-Atlas, http://atlas.ca.gov/download.html#/). Ocean depth contours (light blue lines) are marked every 50-m starting at 50 m and extending to 500 m (CA Department of Fish and Wildlife, ftp://ftp.dfg.ca.gov/R7_MR/BATHYMETRY/). Diamond symbols indicate stations between 10 m and 500 m used for every urchin species during 2003 (light green), 2008 (blue), and 2013 (yellow) surveys. Square symbols indicate stations between 10 m and 200 m used in *L. pictus* analyses for 1994 (red) and 1998 (orange) surveys. Map created using ArcMap™ v.10.1. (For interpretation of the references to color in this figure legend, the reader is referred to the web version of this article.)

quartile depths were determined using R. In addition, for each species in each sampling year, the median urchin depth was identified (with 50% of urchins shallower and 50% deeper).

2.4. Temporal changes in depth

The assumptions of normality and homogeneous variances were tested using the Shapiro–Wilk normality test and the studentized Breusch–Pagan test in R. If the data met these assumptions, parametric analyses were used to determine temporal changes in depth. When the data violated these assumptions, we used the Box–Cox power transformation to transform the data. If the transformation did not improve normality or homoscedasticity of the data then non-parametric tests were used. Two-way Komolgorov–Smirnov tests were carried out for each species to compare depth distributions of trawl depths containing one or more individual among paired survey years. Linear regressions between various depth distribution parameters and survey years indicated how closely the changes in depth characteristics matched the secular changes in oceanographic variables observed over recent decades in this region (Bograd et al., 2015). The depth parameters analyzed were upper and lower limits, first and third quartiles, and mean and median depths of inhabited trawls, as well as the median depth of urchins for each species.

2.5. Temporal changes in density

Mean density for each species was calculated for each sampling date from all trawls including those where zero individuals were present. Due to the zero-inflated dataset, the implementation of data transformation had no effect on the normality nor the homogeneity of variance for any species. Thus, a Kruskal–Wallis test was used for each species to compare species density across years for the entire survey area and for each depth bin. If a significant difference was detected, a *post hoc* Dunn's test treated with a Bonferroni correction was conducted using the Pairwise Multiple Comparison of Mean Ranks Package in R.

2.6. Multivariate El Niño Southern Oscillation (ENSO) Index (MEI) relationships with depth distributions and density

Depth distribution and density data from trawl samples that contained urchins were examined for a relationship to the MEI obtained from the following NOAA website: http://www.esrl.noaa.gov/psd/enso/mei. Linear regressions for each depth parameter (see Section 2.4) and mean density (see Section 2.5) were conducted for each species' dataset with bi-monthly MEI values taken between Dec–Jan of the year before the trawl survey and Sept–Oct of the year that the SCCWRP trawl survey occurred. If the data were found to be normally distributed and have homogenous variances, then linear regression was carried out between the following metrics with bi-monthly MEI indices: various depth parameters, mean density, and depth-binned densities. Regression R^2 values indicated how closely the changes in depth characteristics and densities matched the strength of the El Niño conditions. If the t-statistic was negative, the distribution parameter was determined to shoal or density was determined to decrease during stronger El Niño conditions. In contrast, if the *t*-statistic was positive, the distribution parameter was determined to deepen or density was determined to increase during stronger El Niño conditions. If a significant regression was found with one or more bi-monthly MEI, relationships were reported with seasons rather than monthly pairs.

2.7. Dissolved oxygen and pH relationships with MEI in the SCB

To examine the relationship between ENSO cycles and DO and pH, seasonal DO data collected at 100 m, 200 m, and 300 m depth between 1994 and 2013 from 4 nearshore CalCOFI stations (line 81.8, station 46.9; line 86.7, station 35.0; line 90.0, station 30.0; line 93.3, station 30.0) were obtained from the CalCOFI website (http://calcofi.org/data.html). These stations provide a spatial overlap with the 1994–2013 trawl surveys used in this study. Estimates of pH (seawater scale) were calculated using empirical relationships with temperature and DO (Alin et al., 2012). Regression analysis of DO and pH were carried out to determine

their respective relationships with respect to time and MEI. Bimonthly MEI indices were assigned to DO and pH values based on the date of sample collection according to the CalCOFI database. To determine the magnitudes of DO and pH changes between strong El Niño years where MEI was greater than 1 and strong La Niña years where MEI was less than 1, DO and pH in those years were compared using a *t*-test.

2.8. DO and pH relationships with species depth distributions and densities

Mean DO and mean pH were calculated among 4 CalCOFI stations for each survey year (4 cruises per year) and were matched with species distributions and densities depending on the approximate depth of peak density for that species (e.g., mean DO and pH at 100 m during 1994, 1998, 2003, 2008, and 2013 were matched with *L. pictus*). Collinearity between DO and pH in the study region prevented the use of multiple regression, and therefore, linear regressions of depth distributions and densities were carried out with DO and pH independently.

3. Results

3.1. Lytechinus pictus

3.1.1. Temporal changes in depth

L. pictus was found deeper in 1998 than in 2003 and 2008 (KS test: $D>0.25$, $p<0.05$) (Fig. 4A) (Table 1). The upper part of its range (first quartile) appeared to shoal by 1.34 m yr^{-1} from 54 m in 1994 to 34 m in 2013 ($t_3=-3.931$, $p=0.03$, $R^2=0.78$), as did the median depth of trawls with *L. pictus* by 0.94 m yr^{-1} ($t_3=-2.515$, $R^2=0.57$) from 74.5 m in 1994 to 59.5 m in 2013, but this latter relationship was not significant ($p=0.09$). The median urchin depth shoaled by 1.44 m yr^{-1} from 86 m in 1994 and 1998 to 58 m in 2013 ($t_3=-5.143$, $p=0.01$, $R^2=0.86$). The lower depth limit appeared to shoal from 191 m in 1993 to 137 m in 2003, but was found deeper in 2013 at 189 m (Table 1).

3.1.2. Temporal changes in density

The mean density of *L. pictus* throughout the upper 200 m varied significantly among survey years (Kruskal–Wallis Test: $\chi^2=11.98$, $p=0.02$) (Fig. 5A) (Table 1). *L. pictus* mean density in 2008 (0.028 indiv. m^{-2}) and 2013 (0.023 indiv. m^{-2}) was 76% and 80% lower than in 1994 (0.117 indiv. m^{-2}), respectively (post hoc Dunn's test: $p<0.05$), while densities in 1998 (0.087 indiv. m^{-2}) and 2003 (0.038 indiv. m^{-2}) were not significantly different from any other year. When evaluated by finer 50-m depth bins, *L. pictus* density varied significantly among survey years within 51–100 m (Kruskal–Wallis Test: $\chi^2=12.68$, $p=0.01$) and 101–150 m depth bins ($\chi^2=14.15$, $p<0.01$) (Fig. 6A). Density within the 51–100 m depth bin declined by 74% from 0.252 indiv. m^{-2} in 1998 to 0.065 indiv. m^{-2} in 2003 (post hoc Dunn's test: $p=0.02$). During the 2003 survey, *L. pictus* density was reduced to zero in the 151–200 m depth bin and increased in 2008, but this increase is indistinguishable from the sampling error (Fig. 6A). Survey year significantly predicted density within the 101–150 m depth bin from 1994 to 2013, with density decreasing by 0.02 indiv. m^{-2} yr^{-1} ($t_{56}=-2.956$, $p=0.02$, $R^2=0.12$).

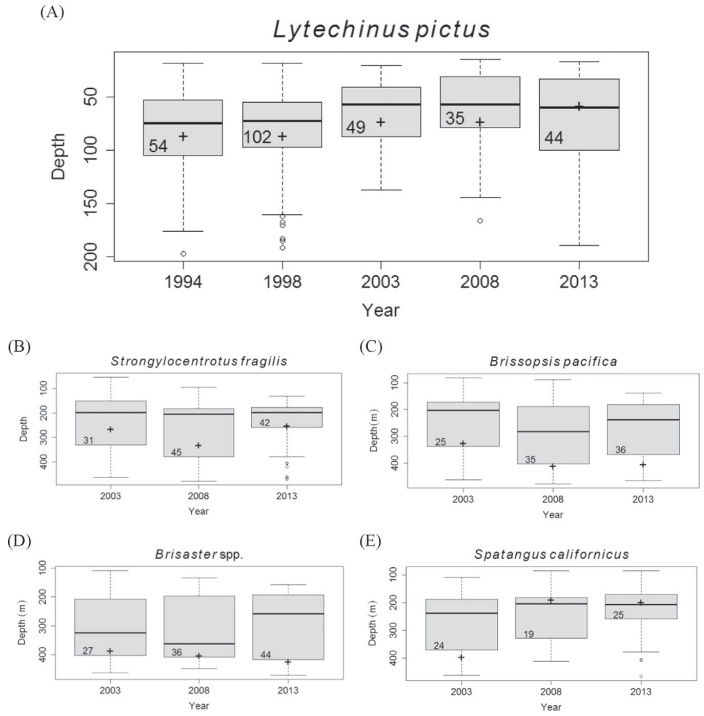

Fig. 4. Sea urchin depth distribution boxplots for the Southern California Bight based on trawls with one or more individual of each species. Box plots represent upper and lower depth limits, first and third quartile depths, and median depth. Plus signs indicate the median depth of urchins. Numbers within each boxplot indicate number of independent trawls used for the calculation. (A) *Lytechinus pictus*. (B) *Strongylocentrotus fragilis*. (C) *Brissopsis pacifica*. (D) *Brisaster* spp. (E) *Spatangus californicus*.

Table 1
Sea urchin depth distribution metrics and density changes over time in the Southern California Bight. No Change represents a non-significant change in depth distribution metrics or density over time. Negative results indicate a consistent shallowing of depth distribution metrics or a decrease in mean density over time (p-values < 0.05 indicate a significant relationship between depth distribution metric and time or a significant difference in density among years). Positive results indicate a consistent deepening of depth distribution metrics or an increase in density over time.

Species	Time period	Depth range	Two-way K–S test	Linear regression							Kruskal–Wallis
			Depth distribution	Upper depth limit	Median trawl depth	Mean trawl depth	First quartile trawl depth	Third quartile trawl depth	Lower depth limit	Median urchin depth	Mean urchin density
L. pictus	1994–2013	10–200 m	Significant	Negative $p=0.03$	Negative $p=0.09$	No Change	Negative $p=0.03$	No Change	No Change	Negative $p=0.01$	Negative $p=0.02$
S. fragilis	1994–2013	10–200 m	NA								No Change
S. fragilis	2003–2013	10–500 m	Not Significant	Positive $p=0.01$	No Change	No Change	No Change	No Change	No Change	No Change	Positive $p=0.02$
B. pacifica	2003–2013	10–500 m	Not Significant	No Change	No Change	No Change	No Change	No Change	No Change	No Change	No Change
Brisaster spp.	2003–2013	10–500 m	Not Significant	Positive $p=0.07$	No Change	No Change	No Change	No Change	No Change	Positive $p=0.04$	Positive $p=0.02$
S. californicus	2003–2013	10–500 m	Not Significant	No Change	No Change	No Change	Negative $p=0.06$	Negative $p=0.10$	No Change	No Change	No Change

3.1.3. Urchin relationship with MEI

L. pictus median and first and third quartile depths were positively related to summer MEI ($F_{1,3} > 3.32$, $p < 0.05$, $R^2 > 0.70$)(Table 2), suggesting that the species occupied deeper depths during stronger El Niño conditions. In addition, the strength of El Niño conditions in the summer months significantly predicted *L. pictus* density (t_3=3.978, p=0.03, R^2=0.78).

3.1.4. Depth distribution and density relationship with DO and pH

Between 1994 and 2013, *L. pictus* density in the upper 200 m was positively related to both mean DO (t_3=6.121, $p < 0.01$, R^2=0.90) and mean pH at 100 m (t_3=4.535, p=0.02, R^2=0.83)(Table 3). pH significantly predicted the depths of the first quartile (t_3=5.432, p=0.01, R^2=0.88), the median depth of trawls with *L. pictus* (t_3=3.432, p=0.04, R^2=0.73), and the median urchin depth (t_3=6.280, $p < 0.01$, R^2=0.91) (Table 3).

3.2. Strongylocentrotus fragilis

3.2.1. Temporal changes in depth

The depth distribution of *S. fragilis* did not change in the upper 500 m from 2003 to 2013 (KS tests: $p > 0.05$) (Fig. 4B) (Table 1). The upper depth limit of *S. fragilis* was found to deepen by 7.7 m yr^{-1} on average from 53.1 m in 2003 to 130.1 m in 2013 (t_1=44.46, p=0.01, R^2=0.99), but no trend was found for any other depth metric over this time period (Fig. 4B) (Table 1).

3.2.2. Temporal changes in density

The mean density of *S. fragilis* throughout the upper 200 m varied significantly among survey years from 1994–2013 (Kruskal–Wallis Test: χ^2=11.84, p=0.02) (Fig. 5B) (Table 1). There was a significant positive relationship between density in the upper 200 m and year (1994–2013), with density increasing at 0.001 indiv. m^{-2} yr^{-1} (t_3=14.61, p=0.03, R^2=0.77). Post hoc Dunn's test revealed significant differences in *S. fragilis* density among years, but when treated with a Bonferroni correction, these differences became insignificant (Fig. 5B). Compared to the 2003 mean density within the upper 500 m (0.028 indiv. m^{-2}), *S. fragilis* density was 35% higher in 2008 (0.039 indiv. m^{-2}) and 133% higher in 2013 (0.067 indiv. m^{-2}) (Kruskal–Wallis Test: χ^2=7.40, p=0.02) (Fig. 5C). This resulted in an annual density increase from 2003 to 2013 by 0.003 indiv. m^{-2} yr^{-1} (t_{440}=1.99, $p < 0.05$, $R^2 < 0.01$)(Table 1). At finer depth bins, *S. fragilis* density varied significantly among survey years; between 101 and 200 m, density increased from 0.038 indiv. m^{-2} in 2003 to 0.090 indiv. m^{-2} in 2008 (138%increase) and from 2008 to 0.105 indiv. m^{-2} in 2013 (17% increase)(Kruskal–Wallis Test: χ^2=6.62, p=0.04) (Fig. 5C). Although *S. fra-gilis* density appears to decrease in the upper 100 m between 2003 and 2013, these values correspond to very small densities ($\sim 10^{-5}$ indiv. m^{-2}), thus they are indistinguishable from sampling error.

3.2.3. Urchin relationship with MEI

S. fragilis median depths were negatively correlated with spring MEI ($t_1 = -134.5$, $p < 0.05$, R^2=0.99), and mean depths were negatively correlated with summer MEI ($t_1 = -43.2$, $p < 0.05$, R^2=0.99) (Table 2), suggesting that the species occupied shallower depths during stronger El Niño conditions. In addition, the strength of El Niño conditions in the summer months was negatively related to *S. fragilis* density (R^2=0.98), but this relationship was not significant (p=0.06).

3.2.4. Depth distribution and density relationship with DO and pH

Between 2003 and 2013, *S. fragilis* density in the upper 500 m was significantly predicted by mean DO at 200 m ($t_1 = -13.9$, $p < 0.05$, R^2=0.99), but not pH at 200 m. However, *S. fragilis* density in the upper 200 m between 1994 and 2013 was

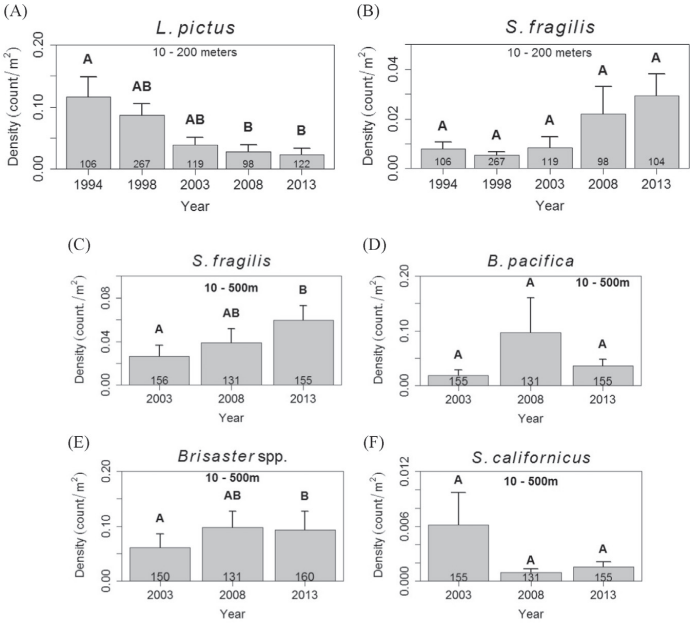

Fig. 5. Mean density (+1 SE) of sea urchins throughout the entire Southern California Bight survey region. For *Lytechinus pictus*, surveys dating back to 1994 covered depths from 10 to 200 m. For deeper species, surveys were extended to 500 m in 2003. Letter indicates significant difference resulting from a Kruskal–Wallis and *post hoc* Dunn's tests. Numbers within each barplot indicate the number of independent trawls used for the calculation. (A) *Lytechinus pictus*. (B) *Strongylocentrotus fragilis* (upper 200 m from 1994 to 2013). (C) *Strongylocentrotus fragilis* (upper 500 m from 2003 to 2013). (D) *Brissopsis pacifica*. (E) *Brisaster* spp. (F) *Spatangus californicus*.

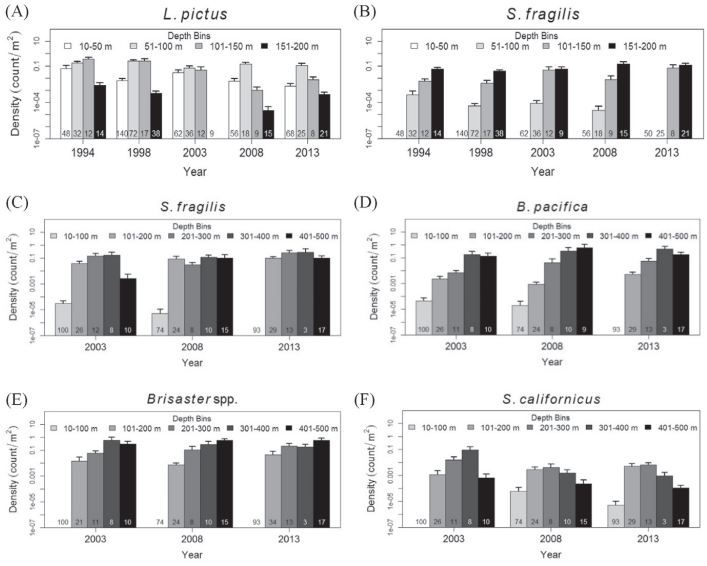

Fig. 6. Mean log-scale density (+1 SE) of (A) *Lytechinus pictus*. (B) and (C) *Strongylocentrotus fragilis*. (D) *Brissopsis pacifica*. (E) *Brisaster* spp. (F) *Spatangus californicus* in the Southern California Bight from 1994 to 2013. Urchins were separated into 50-m depth bins (*L. pictus and S. fragilis*) and 100-m depth bins (other species). Numbers within each barplot indicate number of independent trawls used for calculation.

Table 2
Linear regression results showing relationships of sea urchin depth distribution metrics to ENSO conditions based on bi-monthly MEI values. Negative relationships indicate shoaling of depth distribution metrics and decreasing density in response to stronger El Niño-like conditions (e.g., higher oxygen, higher pH). Positive relationships indicate deepening of depth distribution metrics and increasing density in response to stronger El Nino-like conditions (e.g., higher oxygen, higher pH). *p*-Values < 0.05 indicate a significant relationship between depth distribution metrics and density with MEI values. NS indicates a non-significant relationship, and NA results indicate Not Available because these analyses were not ecologically relevant.

Response to increasing strength of El Niño conditions	Upper depth limit	First quantile depth	Median trawl depth	Third quantile depth	Mean trawl depth	Lower limit depth	Mean urchin density	Median urchin depth
L. pictus	NS	Positive $p < 0.05$	Positive $p < 0.05$	Positive $p < 0.05$	NS	NS	Positive $p < 0.05$	Positive $p = 0.07$
S. fragilis 10–200 m	NA						NS	NA
S. fragilis 10–500 m	Negative $p = 0.09$	Negative $p = 0.06$	Negative $p < 0.05$	NS	Negative $p < 0.05$	Negative $p < 0.05$	Negative $p = 0.06$	Negative $p = 0.07$
B. pacifica	Negative $p < 0.05$	Negative $p = 0.07$	Negative $p < 0.05$	Negative $p < 0.01$	Negative $p < 0.01$	Negative $p < 0.05$	Negative $p < 0.05$	Negative $p = 0.12$
Brisaster spp.	Positive $p < 0.05$	NS	Positive $p = 0.06$	Positive $p < 0.01$	NS	Positive $p < 0.01$	Negative $p = 0.10$	Negative $p = 0.07$
S. californicus	NS	NS	NS	NS	NS	Positive $p < 0.05$	NS	NS

Table 3
Linear regression results of sea urchin depth distribution metrics and density with mean dissolved oxygen (DO) and pH in the Southern California Bight. Significant relationships with DO or pH at 100 m, 200 m, or 300 m are listed as response variable (+ or − sign of relationships). Negative relationships (−) indicate deepening of depth distribution metrics and increasing density in response to decreasing DO or decreasing pH ($p < 0.05$). Positive relationships (+) indicate shallowing of depth distribution metrics and decreasing density in response to decreasing DO or decreasing pH ($p < 0.05$). NS indicates a non-significant relationship, and NA results indicate Not Available because these analyses were not ecologically relevant.

		100 m		200 m		300 m	
Species	Years analyzed	DO	pH	DO	pH	DO	pH
L. pictus 10–200 m	1994–2013	Density (+)	Density; 1st Quartile Depth; Median Trawl Depth; Median Urchin Depth (+)	Density; 1st Quartile Depth; Median Trawl Depth; Median Urchin Depth (+)		NA	NA
S. fragilis 10–200 m	1994–2013	NS	Density (−)	NS	NS	NA	NA
S. fragilis 10–500 m	2003–2013	NS	NS	Density (−)	NS	NS	NS
B. pacifica 10–500 m	2003–2013	NS	NS	NS	NS	NS	NS
Brisaster spp. 10–500 m	2003–2013	Upper Depth Limit (−)	Upper Depth Limit; Median Urchin Depth (-)	NS	Upper Depth Limit; Median Urchin Depth (−)	NS	NS
S. californicus 10–500 m	2003–2013	1st Quartile Depth (+)	1st Quartile Depth; 3rd Quartile Depth (+)	3rd Quartile Depth (+)	1st Quartile Depth; 3rd Quartile Depth (+)	NS	NS

significantly predicted by pH at 100 m ($t_3 = -3.24$ $p < 0.05$, $R^2 = 0.99$) (Table 3).

3.3. Burrowing urchins

3.3.1. Temporal changes in depth

The depth distributions of each burrowing urchin species (*Brissopsis pacifica*, *Brisaster* spp. and *Spatangus californicus*) did not vary significantly in the upper 500 m from 2003 to 2013 (KS tests: $p > 0.05$) (Fig. 4C–E) (Table 1). The first and third quartile depths of *B. pacifica* appeared to shoal, but these relationships were not significant (Fig. 4C). The median depth of *Brisaster* spp. deepened by 3.85 m yr^{-1} ($t_1 = 14.82$, $p = 0.04$, $R^2 = 0.99$) (Fig. 4D). From 2003 to 2013, the upper limit, first and third quartiles, mean and median depths of *S. californicus* appeared to shoal by 2–11 m yr^{-1} (Fig. 4E) but again, these relationships were not significant.

3.3.2. Temporal changes in density

Neither *B. pacifica* nor *S. californicus* density within the upper 500 m significantly varied across years (Kruskal–Wallis Test: *B. pacifica*: $\chi^2 = 4.85$, $p = 0.08$; *S. californicus*: $\chi^2 = 0.13$, $p = 0.94$)(Fig. 5D, F). *Brisaster* spp. density did vary significantly within the upper 500 m from 2003 to 2013 (Kruskal–Wallis Test: $\chi^2 = 7.66$, $p = 0.02$), but density did not show a consistent change with time ($p = 0.24$) (Fig. 5E) (Table 1). Compared to 2003 mean *Brisaster* spp. density (0.06 indiv. m^{-2}), density was 61% higher in 2008 and 54% higher in 2013 (post hoc Dunn's test: $p < 0.05$).

B. pacifica and *S. californicus* density within each 100-m depth bin did not significantly vary among survey years (Fig. 6D, F). The mean *B. pacifica* density increased at a rate of 0.03 indiv. m^{-2} yr^{-1} within the 301–400 m depth bin from 2003 to 2013 ($t_1 = 166.6$, $p < 0.01$, $R^2 > 0.99$) and at a rate of 0.005 indiv. m^{-2} yr^{-1} within the 201–300 m depth bin from 2003 to 2013, although this latter relationship was not significant ($p = 0.13$) (Fig. 6D). From 2003 to 2013, the mean density of *S. californicus* increased within the 101–200 m depth bin and decreased within the 201–300 m, 301–400 m, and 401–500 m depth bins, but these relationships were not significant ($p > 0.05$) (Fig. 6F). *Brisaster* spp. density varied significantly among survey years within the 101–200 m depth bin (Kruskal–Wallis Test: $\chi^2 = 8.14$, $p = 0.02$), but mean density did not change consistently with time ($p = 0.36$) (Fig. 6E).

3.3.3. Depth and density relationship with MEI

B. pacifica mean, median, third quartile, and lower limit depths were negatively related to fall and winter MEI ($t_1 < -10$, $p < 0.05$, $R^2 = 0.99$), and upper limit depth was negatively related to summer MEI ($t_1 < -14$, $p < 0.05$, $R^2 = 0.99$) (Table 2), suggesting that the species occupied shallower depths during stronger El Niño

conditions. In addition, the strength of El Niño conditions in the spring and summer months predicted *B. pacifica* density ($F_{1,1} < -16$, $p < 0.05$, $R^2 = 0.99$). *Brisaster* spp. upper and lower limit depths were positively related to summer MEI ($F_{1,1} > 23$, $p < 0.05$, $R^2 = 0.99$) (Table 2), suggesting that this species occupied deeper depths (or was more likely to be on the surface in deeper waters) during stronger El Niño conditions. *Brisaster* spp. third quartile depth was positively related to spring MEI ($t_1 = 10.4$, $p < 0.05$, $R^2 = 0.99$), and while spring MEI was also positively related to *Brisaster* spp. density, this latter relationship was not significant ($p = 0.10$) (Table 2). *S. californicus* lower depth limit was positively related to spring MEI ($t_1 = 13.4$, $p < 0.05$, $R^2 = 0.99$), but no other depth distribution metric or density were related to any bi-monthly MEI (Table 2).

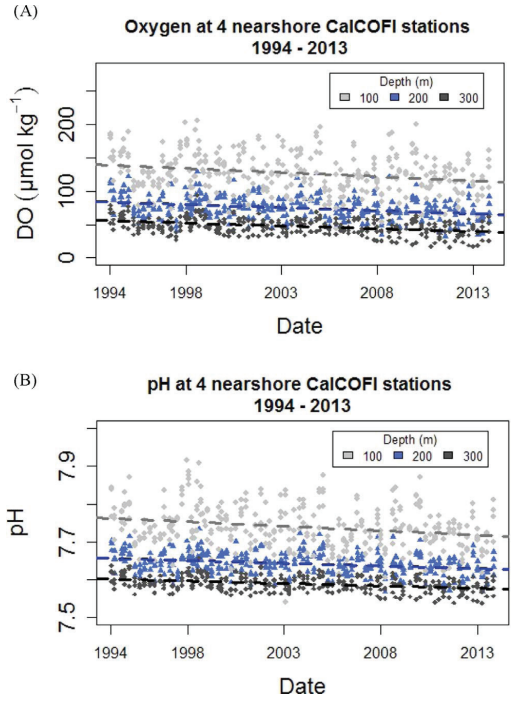

Fig. 7. Changes in (A) dissolved oxygen (DO) concentration and (B) pH for CalCOFI stations (line 81.8, station 46.9; line 86.7, station 35.0; line 90.0, station 30.0; line 93.3, station 30.0) at 100 m (gray), 200 m (blue), and 300 m (black) between 1994 and 2013 in the Southern California Bight. Depth-specific regression lines for DO and pH were all significantly related to time. (For interpretation of the references to color in this figure legend, the reader is referred to the web version of this article.)

3.3.4. Depth distribution and density relationship with DO and pH

The upper depth limit of *Brisaster* spp. was negatively related to mean DO at 100 m ($t_1 = -15.35$, $p = 0.04$, $R^2 = 0.99$), pH at 100 m ($t_1 = -32.56$, $p = 0.02$, $R^2 = 0.99$), and pH at 200 m ($t_1 = -54.13$, $p = 0.01$, $R^2 = 0.99$). The median depth of *Brisaster* spp. was also negatively related to pH at 100 m ($t_1 = -34.34$, $p = 0.02$, $R^2 = 0.99$), and pH at 200 m ($t_1 = -12.75$, $p < 0.05$, $R^2 = 0.99$). The 75% quartile of *S. californicus* was positively related to both DO and pH at 100 m and 200 m, while the 25% quartile was only positively related to pH (Table 3). No significant relationships between *B. pacifica* depth metrics or density and mean DO or pH were found (Table 3).

3.4. Dissolved oxygen and pH relationships with time and MEI in the SCB

Between 1994 and 2013, DO was negatively related to survey year at 100 m ($t_{329} = -4.551$, $p < 0.001$, $R^2 = 0.06$), 200 m ($t_{329} = -5.551$, $p < 0.001$, $R^2 = 0.08$), and 300 m ($t_{328} = -7.982$, $p < 0.001$, $R^2 = 0.16$) (Fig. 7A), as was pH at 100 m ($t_{329} = -4.6$, $p < 0.001$, $R^2 = 0.05$), 200 m ($t_{329} = -5.434$, $p < 0.001$, $R^2 = 0.08$), and 300 m ($t_{328} = -7.347$, $p < 0.001$, $R^2 = 0.14$) (Fig. 7B). DO and pH values at 100 m were positively related to MEI values from 1994 to 2013 (DO: $t_{336} = 4.306$, $p < 0.001$, $R^2 = 0.05$; pH: $t_{336} = 5.26$, $p < 0.001$, $R^2 = 0.07$), with DO increasing at a rate of 3.166 µmol DO kg^{-1} MEI unit^{-1} (Fig. 8A), and pH increasing at a rate of 0.015 pH units MEI unit^{-1} (Fig. 8C). At 100 m in the SCB, mean DO during strong El Niño years (MEI > 1) between 1994 and 2013 (145.5 ± 29.8 µmol kg^{-1} [mean ± 1 SD]) was found to be 25%

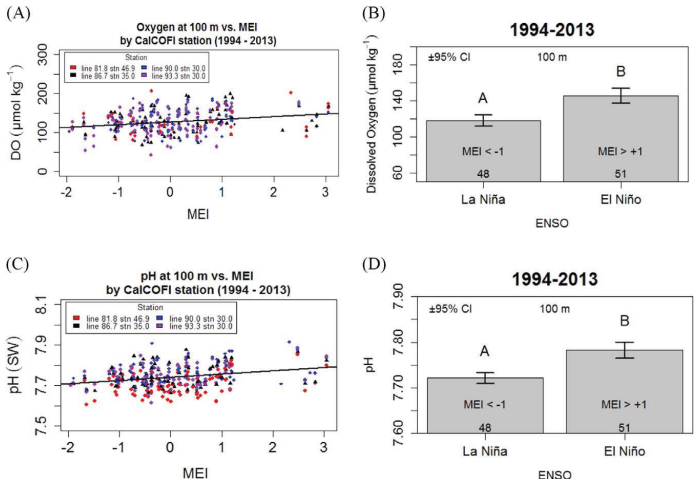

Fig. 8. (A) Dissolved oxygen (DO) concentration and (C) pH as a function of MEI (1994–2013) for CalCOFI stations (line 81.8, station 46.9; line 86.7, station 35.0; line 90.0, station 30.0; line 93.3, station 30.0) at 100 m in the Southern California Bight. (B) Mean DO concentration and (D) mean pH ± 95% confidence intervals for MEI < −1.0 (La Niña conditions) and MEI > 1.0 (El Niño conditions).

higher than during strong La Niña years (118.0 ± 22.3 μmol kg^{-1}; *t*-Test: $t_{94} = -5.19$, $p < 0.001$) (Fig. 8B), while mean pH during strong El Niño years (7.78 ± 0.06) was a significant 0.06 pH units higher than during strong La Niña years (7.72 ± 0.04; *t*-Test: $t_{87} = -5.78$, $p < 0.001$; Fig. 8D).

4. Discussion

Observed temporal trends in echinoid species depth distributions and densities (Table 1, Figs. 4–6) suggest that deep-dwelling urchin species may have experienced habitat expansion upslope in the upper 500 m and shallower-dwelling urchin species may have experienced habitat compression in the upper 200 m over the past 21 years due to multiple climate stressors in the SCB such as DO, temperature, pH, Ω, and pCO_2 (Alin et al. 2012; Frieder et al., 2012; Nam et al. 2015). Trawl survey data reflect (1) shoaling of depth distributions and possible habitat compression in *L. pictus*, and (2) habitat expansion or upslope shifts in *Brisaster* spp. and *S. californicus* (Table 1). Examination of DO and pH data in the upper 200 m at single nearshore CalCOFI stations within the study region between 1994 and 2013 indicates that a change in habitation depth of 20–30 m can yield a 15–63 μmol kg^{-1} change in DO exposure and a 0.03–0.15 unit change in pH exposure (Appendix 1). Although our data did not allow us to assess the potential intensification of the OMZ at depths greater than 500 m, these deep species may have responded to secular deoxygenation and acidification in the SCB, but may have also been influenced by variability in environmental conditions such as oxygen and pH associated with ENSO (Fig. 8). ENSO-related variations in the system can affect major population drivers such as food availability, food quality, and competition. However, other secular changes in the SCB over this time period such as increasing primary productivity and frontal frequency (Bograd et al., 2015; Kahru et al., 2012), intensifying upwelling winds (Sydeman et al., 2014), and warming in the upper 200 m (Di Lorenzo et al., 2005) are potential covariates that could contribute to interannual variability in suitability of urchin habitat. In addition, the positive and negative relationships of population size and distributions with MEI (Table 2), indicate that other factors may have driven temporal change in population densities and distributions in this system.

While changes in benthic fish and invertebrate populations in response to climate events are expected, our results indicate that these effects are species-specific (Arntz et al., 2006). A significant positive relationship between MEI and *L. pictus* density suggest stronger El Niño conditions favor this species, while negative relationships of *S. fragilis* and *B. pacifica* density with MEI suggest they are negatively affected by El Niño conditions. Significant relationships of *L. pictus* and *S. fragilis* density with annual means of DO and pH suggest that these species are affected by these environmental factors (Table 3), and opposite density trends suggest competition in the upper 200 m may also limit *L. pictus* and favor *S. fragilis* (Fig. 5A, B). Interpreting these differences requires a deeper understanding of life history, food sources, and spatio-temporal dynamics.

The urchin species discussed are grossly understudied despite the potentially high impact they may have on the deep-sea community, and specific mechanisms of population structure change cannot be revealed with the current sampling design. Possible lags in species response (i.e. changes in depth distribution or density) to environmental variables likely exist depending on the species' life history (Glover et al., 2010). For example, although the lifespan of *L. pictus* is unknown, the estimated lifespan of the congener, *L. variegatus*, is <5 yr (Watts et al., 2007; Bodnar and Coffman, 2016). Five years after the strong El Niño of 1998, the mean density of *L. pictus* declined by 56%; this decline persisted until 2013 (Fig. 5A). Thus, it is possible that *L. pictus* populations responded to kelp food availability at shorter time scales than the longer-lived *S. fragilis* (Taylor et al., 2014), and trawl surveys at 5-yr intervals could not reveal the influence of ENSO events on *L. pictus* populations.

To determine the feasibility of urchin migration as a possible mechanism for the observed depth changes, we estimated the average slope of the continental shelf and slope in the SCB using Google Earth. We found that a 10 m reduction in depth for the shallower, *L. pictus* on the shelf might occur over a 1 km horizontal distance. Although the average travel speed of adult *L. pictus* is unknown, Pisut (2004) found the average speed of *L. variegatus* to be ~0.7 m h^{-1}, and Barry et al. (2014) found the average speed of *S. fragilis* to be ~0.25 m h^{-1}. Therefore, it is feasible for individuals to migrate 1 km in 5 years, so depth changes may reflect migration rather than mortality and recruitment. The significant decrease in density of *L. pictus* in the SCB over the time period of this study however, would suggest that mortality and lowered recruitment did occur. Potential mechanisms for increased mortality and lower recruitment for *L. pictus* over time include physiological intolerance to low pH or low DO, increased predation, increased competition and/or reduced larval supply.

L. pictus and *S. fragilis* are epibenthic omnivores that primarily feed on allochthonous kelp detritus (Barry et al., 2014; Thompson et al., 1983; Fig. 2A, B) that originates from the inshore zone of the coastal SCB (Dayton, 1985; Krumhansl and Scheibling, 2012; Parnell et al., 2010). During and following El Niño years, anomalously higher nearshore sea surface temperatures off the southern California coast can persist for at least 2 years (McGowan et al., 1998). Results of warmer surface waters include intensified stratification, reduced upwelling, and reduced primary production by phytoplankton (Barber and Chavez, 1983; Contreras et al., 2007) and kelp (Tegner and Dayton, 1987). This could negatively affect the availability of autochthonous food in the form of sinking organic matter (phytodetritus) for deep-sea benthic communities including epibenthic and burrowing urchins (Lange et al., 2000Gutierrez et al., 2000; Levin et al., 2002; Sellanes and Neira, 2006), and may also explain the negative relationships between MEI and *S. fragilis* and *B. pacifica* densities (Table 2). Alternatively, burrowing spatangoid urchins may benefit from increased input of terrestrial organic matter during stronger El Niño years as a result of increased runoff from winter storms (Lange et al., 2000, and others). However, sinking organic matter of terrestrial origin has been found to have lower protein content, higher C: N ratios and lower nutritional quality than marine sources (Cowie et al., 2009). Stable isotope analysis of deposit-feeding urchins combined with gonad analyses may help to better understand the differential effects of food source quality and origin on reproduction and fitness during El Niño and non-El Niño years.

Winter storms during El Niño years can also dislodge and export significant kelp forest biomass (Dayton and Tegner, 1984; Parnell et al., 2010), which may temporarily increase supply of allochthonous food to deep-sea habitats in the form of kelp detritus (Harrold et al., 1998; Vetter and Dayton, 1998). However, low overall production of *Macrocystis pyrifera* kelp canopy during summer El Niño years should limit food and reduce urchin populations (Edwards 2004 and references therein). While this understanding could explain the negative relationship between MEI and *S. fragilis*, it cannot explain the opposite response of *L. pictus* at depths less than 200 m. Instead the higher DO and pH associated with El Niño conditions may favor *L. pictus* (Fig. 8). However, the lower depth bins of *L. pictus* (101–200 m) overlap with *S. fragilis*, so it is possible that during strong El Niño years when there is limited food, a competitive interaction between the two urchins occurs. Density data support the hypothesis that these two species interact in the upper 200 m (Fig. 5A, B), and possibly within smaller depth bins where they coexist (Fig. 6A, B), but

further analysis is required to test this. It is also possible that decadal oscillations in climate may affect trends in density. For example, changes in the NPGO and PDO in the last decade can affect bottom-up processes that likely influence entire marine communities (Bell et al., 2015; Di Lorenzo et al., 2008; Miller et al., 2015). A better understanding of how food source dynamics interact with stressors to influence margin urchin populations is required, particularly regarding the origin and fate of autochthonous and allochthonous food sources in response to physical oceanographic processes affected by ENSO cycles.

In addition to food availability, climate-related perturbations in the physical, chemical and biological structure of the environment can result in shifts in the vertical zonation of entire land- and seascapes (Cheung et al., 2011; Parmesan, 2006; Wishner et al., 2013). For example, La Niña years often follow El Niño years (Table 1) and are characterized by enhanced upwelling and pro-longed exposure to hypoxic and acidic conditions (Booth et al., 2014; Nam et al., 2011). This pattern of low food years (El Niño), followed by low-oxygen, low-pH periods (La Niña) can represent a one-two punch and be detrimental to population growth (Ramajo et al., 2016). As OMZs expand and OLZs shoal, waters low in pH and high in CO_2 are also expected to creep upslope (Gruber et al., 2012) and onto the shelf (Feely et al., 2008). This may exacerbate negative consequences for vulnerable larval stages of calcifying urchin species adapted to shallower conditions by increasing metabolic energy demand (Pan et al., 2015), but it is unclear if larvae of deep-sea species have greater tolerance to future climate change than those of shallower species (Jager et al., 2016; Stumpp et al., 2012). These secular trends of deoxygenation and ocean acidification may induce a competitive advantage for deeper urchins (e.g. *S. fragilis*, *B. pacifica* and *Brisaster* spp.) equipped with the adaptive machinery to persist in hypoxic and hypercapnic environments over those restricted by such conditions (Byrne and Przeslawski, 2013; Portner et al., 2005; Taylor et al., 2014). Deep-sea, *in situ* manipulation experiments simulated future deep-ocean acidification and revealed longer foraging time and no difference in speed of adult *S. fragilis* under acidic conditions, which implied tolerance to acidification (Barry et al., 2014). Behavioral responses coupled with adaptive capacities for *S. fragilis* to regulate acid-base balance under acidic conditions (Taylor et al., 2014) and low oxygen-consumption rates under hypoxic conditions (Thompson et al., 1983) may induce a competitive advantage over *L. pictus*, which could explain the increase in *S. fragilis* density by 174% in the 101–200 m depth bin zone from 2003 to 2013 (Fig. 6A, B). Higher oxygen or pH limits in *L. pictus* may also explain the 56%decrease from 10 to 200 m from 2003 to 2013 given the positive relationship with oxygen and pH (Fig. 7A, B; Table 3).

Despite statistically insignificant density differences among years, *B. pacifica* and *Brisaster* spp. may be better competitors than *S. californicus* echinoids in a deoxygenated, acidic future. A shoaling of median depth of 50% and a density decrease of 75% from 2003 to 2013 suggests habitat compression in *S. californicus* (Figs. 4F, 5F). As infaunal burrowers, heart urchins are exposed to even more reduced conditions than that of overlying OMZ and OLZ waters (Reimers et al., 1990). Despite the function of fascioles, which direct currents over respiratory tube feet, burrowing urchins are still exposed to surrounding pore water that is reduced in pH and oxygen relative to near-bottom waters; this has been found in both *in situ* observations of sediment pore-water chemistry (Reimers et al., 1990) and laboratory experiments focused on burrowing urchins (Vopel et al., 2007). Accordingly, their distributions and peak densities indicate that they are tolerant of extremely low-oxygen, high-CO_2 environments (Moffitt et al., 2015).

Burrowing urchins in the eastern Pacific OMZ occur in dense patches (Thompson et al., 1993; Thompson and Jones, 1987) and contribute to significant nutrient recycling processes through bioturbation of sediments (Lohrer et al., 2004; Lohrer et al., 2005). Our density estimates likely underestimated the subsurface density of spatangoid heart urchins in the SCB since otter trawls cannot accurately sample all the urchins, which may dwell as deep as 20 cm and are best sampled by boxcorers (Kanazawa, 1992; Thompson and Jones, 1987). As such, trends of shoaling depth distributions and increasing density of *Brisaster* spp. associated with deoxygenation could simply reflect movement of heart urchins to the surface to access more oxygenated waters (i.e. higher catchability). It is interesting to note the varying responses to El Niño among the three burrowing spatangoid urchin species in the upper 500 m (Table 2). Further evidence for oxygen limitation in *Brisaster* spp. and *S. californicus* may be inferred from their deepening distributions during stronger El Niño years (Table 2). While density decreases during stronger El Niño years may be explained by the overall decrease in food availability in the SCB (Nichols et al., 1989), it is likely that competitive interactions occur among *B. pacifica*, *Brisaster* spp. and *S. californicus* during years when food is limited (Dayton and Hessler, 1972).

Future studies focusing on adaptations to combined hypoxia, hypercapnia, and food limitation in different deep-sea urchin species are needed. Phenomena such as the presence and activity of sulfide-oxidizing gut microbes (Thorsen, 1998) and resource partitioning (Thompson et al., 1983) among competitors could provide further insight into how deep-margin echinoids respond to future climate change.

Acknowledgments

The authors would like to thank the water quality monitoring agencies in southern California associated with the SCCWRP Bight program for their permission to publish these data. We would also like to thank Kieu Tran, Andrew Mehring, Carlos Neira, and two anonymous reviewers for their assistance with improving this manuscript. This work was funded by National Oceanic and Atmospheric Administration (NOAA) Grant no. NA14OAR4170075, California Sea Grant College Program Project no. R/SSFS-02 through NOAA's National Sea Grant College Program, U.S. Department of Commerce. Additional stipend and tuition support for KNS was provided by the Center for Marine Biodiversity and Conservation and the Scripps Education Office and for LAL from NSF.EAR1324095. The statements, findings, conclusions and recommendations are those of the authors and do not necessarily reflect the views of California Sea Grant, NOAA or NSF.

Appendix A. Supplementary material

Supplementary data associated with this article can be found in the online version at http://dx.doi.org/10.1016/j.dsr2.2016.08.012.

References

Alin, S.R., Feely, R.A., Dickson, A.G., Hernandez-Ayon, J.M., Juranek, L.W., Ohman, M.D., Goericke, R., 2012. Robust empirical relationships for estimating the carbonate system in the southern California Current System and application to CalCOFI hydrographic cruise data (2005–2011). J. Geophys. Res. 117.

Arntz, W.E., Gallardo, V.A., Gutiérrez, D., Isla, E., Levin, L.A., Mendo, J., Neira, C., Rowe, G.T., Tarazona, J., Wolff, M., 2006. El Niño and similar perturbation effects on the benthos of the Humboldt, California, and Benguela Current upwelling ecosystems. Adv. Geosci. 6, 243–265.

Barber, R.T., Chavez, F.P., 1983. Biological consequences of El Niño. Science 222, 1203–1210.

Barry, J.P., Lovera, C., Buck, K.R., Peltzer, E.T., Taylor, J.R., Walz, P., Whaling, P.J., Brewer, P.G., 2014. Use of a free ocean CO_2 enrichment (FOCE) system to

evaluate the effects of ocean acidification on the foraging behavior of a deep-sea urchin. Environ. Sci. Technol. 48, 9890–9897.
Bell, T.W., Cavanaugh, K.C., Reed, D.C., Siegel, D.A., 2015. Geographical variability in the controls of giant kelp biomass dynamics. J. Biogeogr. 42, 2010–2021.
Bjerknes, J., 1966. A possible response of atmospheric Hadley circulation to equatorial anomalies of ocean temperature. Tellus 18, 820–829.
Bodnar, A.G., Coffman, J.A., 2016. Maintenance of somatic tissue regeneration with age in short- and long-lived species of sea urchins. Aging Cell. http://dx.doi.org/10.1111/acel.12487.
Bograd, S.J., Buil, M.P., Di Lorenzo, E., Castro, C.G., Schroeder, I.D., Goericke, R., Anderson, C.R., Benitez-Nelson, C., Whitney, F.A., 2015. Changes in source waters to the Southern California Bight. Deep-Sea Res. 112 (Pt. II), 42–52.
Bograd, S.J., Castro, C.G., Di Lorenzo, E., Palacios, D.M., Bailey, H., Gilly, W., Chavez, F.P., 2008. Oxygen declines and the shoaling of the hypoxic boundary in the California Current. Geophys. Res. Lett. 35.
Booth, J.A.T., McPhee-Shaw, E.E., Chua, P., Kingsley, E., Denny, M., Phillips, R., Bograd, S.J., Zeidberg, L.D., Gilly, W.F., 2012. Natural intrusions of hypoxic, low pH water into nearshore marine environments on the California coast. Cont. Shelf Res. 45, 108–115.
Booth, J.A.T., Woodson, C.B., Sutula, M., Micheli, F., Weisberg, S.B., Bograd, S.J., Steele, A., Schoen, J., Crowder, L.B., 2014. Patterns and potential drivers of declining oxygen content along the southern California coast. Limnol. Oceanogr. 59, 1127–1138.
Byrne, M., Przeslawski, R., 2013. Multistressor impacts of warming and acidification of the ocean on marine invertebrates' life histories. Integr. Comp. Biol. 53, 582–596.
Cheung, W.W.L., Meeuwig, J.J., Lam, V.W.Y., 2011. Ecosystem-based fisheries management in the face of climate change. In: Christensen, V., Maclean, J. (Eds.), Ecosystem Approaches to Fisheries. A Global Perspective Cambridge University Press, New York, pp. 171–188.
Contreras, S., Pantoja, S., Neira, C., Lange, C.B., 2007. Biogeochemistry of surface sediments off Concepción (~36°S), 75. El Niño vs. non-El Niño conditions. Progr. Oceanogr, Chile, pp. 576–585.
Cowie, G.L., Mowbray, S., Lewis, M., Matheson, H., McKenzie, R., 2009. Carbon and nitrogen elemental and stable isotopic compositions of surficial sediments from the Pakistan margin of the Arabian Sea. Deep-Sea Res. II (56), 271–282.
Dayton, P.K., 1985. The structure and regulation of some South American kelp communities. Ecol. Monogr., 447–468.
Dayton, P.K., Hessler, R.R., 1972. Role of biological disturbance in maintaining diversity in the Deep Sea. Deep-Sea Res 19, 199–208.
Dayton, P.K., Tegner, M.J., 1984. Catastrophic storms, El Niño, and patch stability in a southern California kelp community. Science 224, 283–285.
Di Lorenzo, E., Miller, A.J., Schneider, N., McWilliams, J.C., 2005. The warming of the California current system: dynamics and ecosystem implications. J. Phys. Oceanogr. 35, 336–362.
Di Lorenzo, E., Schneider, N., Cobb, K.M., Franks, P.J.S., Chhak, K., Miller, A.J., McWilliams, J.C., Bograd, S.J., Arango, H., Curchitser, E., Powell, T.M., Riviere, P., 2008. North Pacific Gyre Oscillation links ocean climate and ecosystem change. Geophys. Res. Lett. 35.
Dupont, S., Ortega-Martinez, O., Thorndyke, M., 2010. Impact of near-future ocean acidification on echinoderms. Ecotoxicology 19, 449–462.
Edwards, M.S., 2004. Estimating scale-dependency in disturbance impacts: El Niños and giant kelp forests in the northeast Pacific. Oecologia 138, 436–447. Feely, R.A.,
Sabine, C.L., Hernandez-Ayon, J.M., Ianson, D., Hales, B., 2008. Evidence for upwelling of corrosive "acidified" water onto the continental shelf. Science 320, 1490–1492.
Frieder, C.A., 2014. Present-day nearshore pH differentially depresses fertilization in congeneric sea urchins. Biol. Bull. 226, 1–7.
Frieder, C.A., Nam, S.H., Martz, T.R., Levin, L.A., 2012. High temporal and spatial variability of dissolved oxygen and pH in a nearshore California kelp forest. Biogeosciences 9, 3917–3930.
Gilly, W.F., Beman, J.M., Litvin, S.Y., Robison, B.H., 2013. Oceanographic and biological effects of shoaling of the oxygen minimum zone. Annu. Rev. Mar. Sci. 5, 393–420.
Glover, A.G., Gooday, A.J., Bailey, D.M., Billett, D.S.M., Chevaldonné, P., Colaco, A., Copley, J., Cuvelier, D., Desbruyeres, D., Kalogeropoulou, V., Klages, M., 2010. Temporal change in deep-sea benthic ecosystems: a review of the evidence from recent time-series studies. Adv. Mar. Biol. 58, 1–95.
Gruber, N., 2011. Warming up, turning sour, losing breath: ocean biogeochemistry under global change. Philos. Trans. R. Soc. A 369, 1980–1996.
Gruber, N., Hauri, C., Lachkar, Z., Loher, D., Frolicher, T.L., Plattner, G.K., 2012. Rapid progression of ocean acidification in the California current system. Science 337, 220–223.
Gutierréz, D., Gallardo, V.A., Mayor, S., Neira, C., Vásquez, C., Sellanes, J., Rivas, M., Soto, A., Carrasco, F., Baltazar, M., 2000. Effects of dissolved oxygen and fresh organic matter on the bioturbation potential of macrofauna in sublittoral sediments off Central Chile during the 1997/1998 El Niño. Mar. Ecol. Prog. Ser 202, 81–99.
Harrold, C., Light, K., Lisin, S., 1998. Organic enrichment of submarine-canyon and continental-shelf benthic communities by macroalgal drift imported from nearshore kelp forests. Limnol. Oceanogr. 43, 669–678.
Helly, J.J., Levin, L.A., 2004. Global distribution of naturally occurring marine hypoxia on continental margins. Deep-Sea Res. Pt. I 51, 1159–1168.
Hofmann, G.E., Barry, J.P., Edmunds, P.J., Gates, R.D., Hutchins, D.A., Klinger, T., Sewell, M.A., 2010. The effect of ocean acidification on calcifying organisms in marine ecosystems: an organism-to-ecosystem perspective. Annu. Rev. Ecol. Evol. S 41, 127–147.
Hood, S., Mooi, R., 1998. Taxonomy and phylogenetics of extant *Brisaster* (Echinoidea: Spatangoida). In: Balkema, A.A. (Ed.), Echinoderms. International Publishers, San Francisco, pp. 681–686.
Ito, T., Deutsch, C., 2013. Variability of the oxygen minimum zone in the tropical North Pacific during the late twentieth century. Glob. Biogeochem. Cy 27, 1119–1128.
Jager, T., Ravagnan, E., Dupont, S., 2016. Near-future ocean acidification impacts maintenance costs in sea-urchin larvae: Identification of stress factors and tipping points using a DEB modelling approach. J. Exp. Mar. Biol. Ecol. 474, 11–17.
Kahru, M., Kudela, R.M., Manzano-Sarabia, M., Mitchell, B.G., 2012. Trends in the surface chlorophyll of the California Current: merging data from multiple ocean color satellites. Deep-Sea Res 77–80 (Pt. II), 89–98.
Kanazawa, K.I., 1992. Adaptation of test shape for burrowing and locomotion in spatangoid echinoids. Palaeontology 35, 733–750.
Keller, A.A., Wallace, J.R., Horness, B.H., Hamel, O.S., Stewart, I.J., 2012. Variations in eastern North Pacific demersal fish biomass based on the U.S. west coast groundfish bottom trawl survey (2003–2010). Fish. B 110, 205–222.
Koslow, J.A., Goericke, R., Lara-Lopez, A., Watson, W., 2011. Impact of declining intermediate-water oxygen on deepwater fishes in the California Current. Mar. Ecol. Prog. Ser. 436, 207–218.
Koslow, J.A., Miller, E.F., McGowan, J.A., 2015. Dramatic declines in coastal and oceanic fish communities off California. Mar. Ecol. Prog. Ser. 538, 221–227.
Kroeker, K.J., Kordas, R.L., Crim, R., Hendriks, I.E., Ramajo, L., Singh, G.S., Duarte, C.M., Gattuso, J.P., 2013. Impacts of ocean acidification on marine organisms: quantifying sensitivities and interaction with warming. Glob. Change Biol. 19, 1884–1896.
Krumhansl, K.A., Scheibling, R.E., 2012. Production and fate of kelp detritus. Mar. Ecol. Progr. Ser. 467, 281–302.
Lange, C.B., Weinheimer, A.L., Reid, F.M., Tappa, E., Thunell, R.C., 2000. Response of siliceous microplankton from the Santa Barbara Basin to the 1997–98 El Niño event. Cal. Coop. Ocean. Fish. 41, 186–193.
Lebrato, M., Iglesias-Rodriguez, D., Feely, R.A., Greeley, D., Jones, D.O.B., Suarez-Bosche, N., Lampitt, R.S., Cartes, J.E., Green, D.R.H., Alker, B., 2010. Global contribution of echinoderms to the marine carbon cycle: $CaCO_3$ budget and benthic compartments. Ecol. Monogr. 80, 441–467.
Levin, L.A., Dayton, P.K., 2009. Ecological theory and continental margins: where shallow meets deep. Trends Ecol. Evol. 24, 606–617.
Levin, L.A., Liu, K.K., Emeis, K.C., Breitburg, D.L.,Cloern,J.,Deutsch, C., Giani, M., Goffart, A., Hofmann, E.E., Lachkar, Z., Limburg, K., Liu, S.M., Montes, E., Naqvi, W., Ragueneau, O., Rabouille, C., Sarkar, S.K., Swaney, D.P., Wassman, P., Wishner, K.F., 2015. Comparative biogeochemistry–ecosystem–human interactions on dynamic continental margins. J. Mar. Syst. 141, 3–17.
Lohrer, A.M., Thrush, S.F., Gibbs, M.M., 2004. Bioturbators enhance ecosystem function through complex biogeochemical interactions. Nature 431, 1092–1095.
Lohrer, A.M., Thrush, S.F., Hunt, L., Hancock, N., Lundquist, C., 2005. Rapid reworking of subtidal sediments by burrowing spatangoid urchins. J. Exp. Mar. Biol. Ecol. 321, 155–169.
Mantua, N.J., Hare, S.R., Zhang, Y., Wallace, J.M., Francis, R.C., 1997. A Pacific interdecadal climate oscillation with impacts on salmon production. Am. Meteorol. Soc. 78, 1069–1079.
McClatchie, S., Goericke, R., Cosgrove, R., Auad, G., Vetter, R., 2010. Oxygen in the Southern California Bight: multidecadal trends and implications for demersal fisheries. Geophys. Res. Lett. 37.
McGowan, J.A., Cayan, D.R., Dorman, L.M., 1998. Climate-ocean variability and ecosystem response in the northeast. Pac. Sci. 281, 210–217.
Miller, A.J., Song, H., Subramanian, A.C., 2015. The physical oceanographic environment during the CCE-LTER years: changes in climate and concepts. Deep-Sea Res 112 (Pt. II), 6–17.
Miller, E.E., Schiff, K., 2012. Descriptive trends in southern California bight demersal fish assemblages since 1994. Cal. Coop. Ocean. Fish. 53, 107–131.
Moffitt, S.E., Hill, T.M., Roopnarine, P.D., Kennett, J.P., 2015. Response of seafloor ecosystems to abrupt global climate change. Proc. Natl. Acad. Sci. USA 112, 4684–4689.
Nam, S., Kim, H.J., Send, U., 2011. Amplification of hypoxic and acidic events by La Niña conditions on the continental shelf off California. Geophys. Res. Lett. 38.
Nam, S., Takeshita, Y., Frieder, C.A., Martz, T., Ballard, J., 2015. Seasonal advection of Pacific Equatorial Water alters oxygen and pH in the Southern California Bight. J. Geophys. Res. 120, 5387–5399.
Netburn, A.N., Koslow, J.A., 2015. Dissolved oxygen as a constraint on daytime deep scattering layer depth in the southern California current ecosystem. Deep-Sea Res. Pt. I 104, 149–158.
Nichols, F.H., Cacchione, D.A., Drake, D.E., Thompson, J.K., 1989. Emergence of burrowing urchins from California continental shelf sediments—a response to alongshore current reversals? Estuar. Coast Shelf S29, 171–182.
Paine, R.T., 1966. Food web complexity and species diversity. Am. Nat. 100, 65–75. Pan, T.-C.F., Applebaum, S.L., Manahan, D.T., 2015. Experiment ocean acidification alters the allocation of metabolic energy. Proc. Natl. Acad. Sci. USA 112, 4696–4701.
Parmesan, C., 2006. Ecological and evolutionary responses to recent climate change. Annu. Rev. Ecol. Evol. Syst. 37, 637–669.
Parnell, P.E., Miller, E.F., Lennert-Cody, C.E., Dayton, P.K., Carter, M.L., Stebbins, T.D., 2010. The response of giant kelp (*Macrocystis pyrifera*) in southern California to low-frequency climate forcing. Limnol. Oceanogr. 55, 2686–2702.

Paulmier, A., Ruiz-Pino, D., Garcon, V., 2011. CO_2 maximum in the oxygen minimum zone (OMZ). Biogeosciences 8, 239–252.

Pisut D.P. The distance chemosensory behavior of the sea urchin Lytechinus variegatus, Masters Thesis, Georgia Institute of Technology, 2004.

Portner, H.O., Langenbuch, M., Michaelidis, B., 2005. Synergistic effects of temperature extremes, hypoxia, and increases in CO_2 on marine animals: from Earth history to global change. J. Geophys. Res. 110.

Prince, E.D., Goodyear, C.P., 2006. Hypoxia-based habitat compression of tropical pelagic fishes. Fish. Oceanogr. 15, 451–464.

Ramajo, L., Pérez-León, E., Hendriks, I.E., Marbà, N., Krause-Jensen, D., Sejr, M.K., Blicher, M.E., Lagos, N.A., Olsen, Y.S., Duarte, C.M., 2016. Food supply confers calcifiers resistance to ocean acidification. Sci. Rep. 6, 19374.

Reimers, C.E., Lange, C.B., Tabak, M., Bernhard, J.M., 1990. Seasonal spillover and varve formation in the Santa-Barbara Basin, California. Limnol. Oceanogr. 35, 1577–1585.

Reum, J.C.P., Alin, S.R., Harvey, C.J., Bednaršek, N., Evans, W., Feely, R.A., Hales, B., Lucey, N., Mathis, J.T., McElhany, P., Netwon, J., Sabine, C.L., 2016. Interpretation and design of ocean acidification experiments in upwelling systems in the context of carbonate chemistry co-variation with temperature and oxygen. ICES J. Mar. Sci 73, 582–595.

Seibel, B.A., 2011. Critical oxygen levels and metabolic suppression in oceanic oxygen minimum zones. The Journal of Experimental Biology 214, 326–336.

Sellanes, J., Neira, C., 2006. ENSO as a natural experiment to understand environmental control of meiofaunal community structure. Mar. Ecol 27, 31–43.

Send, U., Nam, S., 2012. Relaxation from upwelling: the effect on dissolved oxygen on the continental shelf. J. Geophys. Res. 117.

Somero, G.N., Beers, J.M., Chan, F., Hill, T.M., Klinger, T., Litvin, S.Y., 2016. What changes in the carbonate system, oxygen, and temperature portend for the northeastern Pacific ocean: a physiological perspective. BioScience 66, 14–26.

Stramma, L., Prince, E.D., Schmidtko, S., Luo, J.G., Hoolihan, J.P., Visbeck, M., Wallace, D.W.R., Brandt, P., Kortzinger, A., 2012. Expansion of oxygen minimum zones may reduce available habitat for tropical pelagic fishes. Nat. Clim. Change 2, 33–37.

Stumpp, M., Truebenbach, K., Brennecke, D., Hu, M.Y., Melzner, F., 2012.Resource allocation and extracellular acid-base status in the sea urchin *Strongylocentrotus droebachiensis* in response to CO_2 induced seawater acidification. Aquat. Toxicol. 110, 194–207.

Sydeman, W.J., Garcia-Reyes, M., Schoeman, D.S., Rykaczewski, R.R., Thompson, S.A., Black, B.A., Bograd, S.J., 2014. Climate change and wind intensification in coastal upwelling ecosystems. Science 345, 77–80.

Taylor, J.R., Lovera, C., Whaling, P.J., Buck, K.R., Pane, E.F., Barry, J.P., 2014. Physiological effects of environmental acidification in the deep-sea urchin *Strongylocentrotus fragilis*. Biogeosciences 11, 1413–1423.

Tegner, M.J., Dayton, P.K., 1987. El Niño effects on southern California kelp forest communities. Adv. Ecol. Res. 17, 243–279.

Thompson, B., Tsukada, D., Laughlin, J., 1993. Megabenthic assemblages of coastal shelves, slopes, and basins off southern California. Bull. South. Calif. Acad. Sci. 92, 25–42.

Thompson, B.E., Jones, G.F., 1987. Benthic macrofaunal assemblages of slope habitats in the southern California USA borderland. Allan Hancock Found. Occas., 1–21.

Thompson, B.E., Laughlin, J.D., Tsukada, D.T., 1983. Ingestion and oxygen consumption by slope echinoids. Annu. Rep. South. Calif. Coast. Water Res. Proj. 84, 93–107.

Thorsen, M.S., 1998. Microbial activity, oxygen status and fermentation in the gut of the irregular sea urchin *Echinocardium cordatum* (Spatangoida: Echinodermata). Mar. Biol. 132, 423–433.

Vetter, E.W., Dayton, P.K., 1998. Macrofaunal communities within and adjacent to a detritus-rich submarine canyon system. Deep-Sea Res 45 (Pt. II), 25–54.. Vopel, K., Vopel, A., Thistle, D., Hancock, N., 2007. Effects of spatangoid heart urchins on O_2 supply into coastal sediment. Mar. Ecol. Prog. Ser, 161–171.

Watts, S.A., McClintock, J.B., Lawrence, J.M., 2007. Ecology of *Lytechinus*. Dev. Aquac. Fish. Sci. 37, 473–497.

Wishner, K.F., Outram, D.M., Seibel, B.A., Daly, K.L., Williams, R.L., 2013. Zooplankton in the eastern tropical north Pacific: boundary effects of oxygen minimum zone expansion. Deep-Sea Res. 79 (Pt. I), 122–140.

Wolter, K., Timlin, M.S., 2011. El Niño/Southern Oscillation behaviour since 1871 as diagnosed in an extended multivariate ENSO index (MEI.ext). Int. J. Climatol. 31, 1074–1087.

Appendix 1.

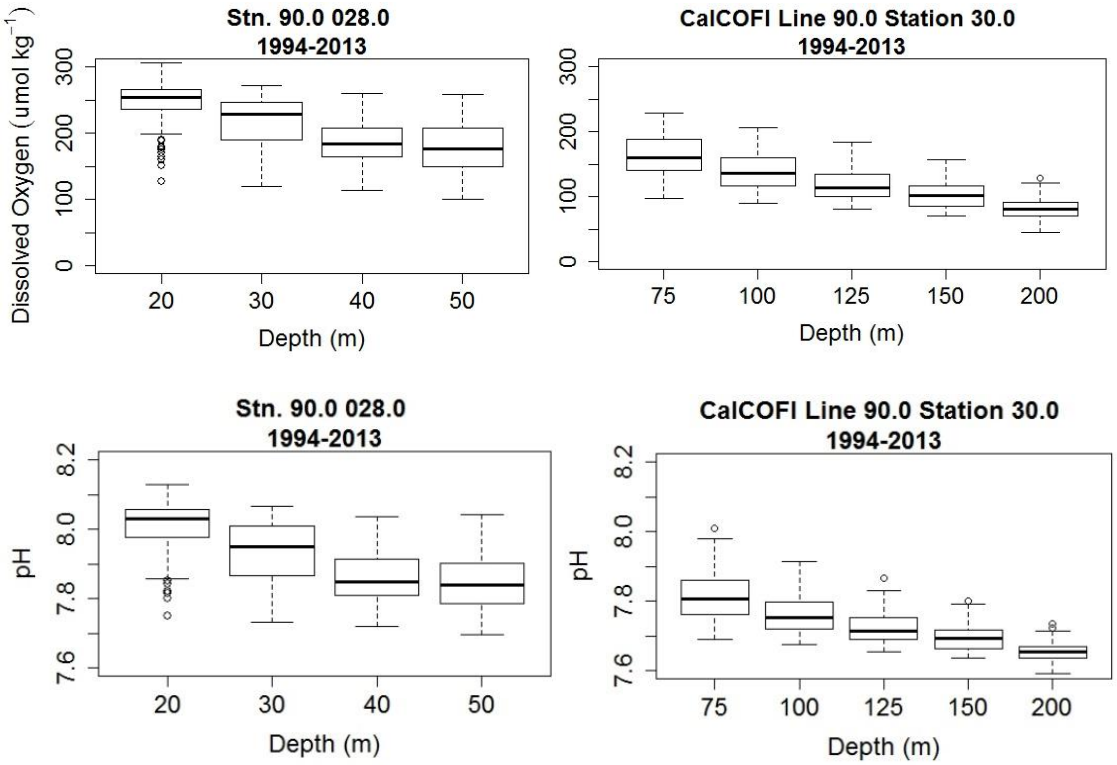
Stn. 90.0 028.0
1994-2013
Dissolved Oxygen (umol kg^{-1})
0
100
200
300
20
30
40
50
Depth (m)
CalCOFI Line 90.0 Station 30.0
1994-2013
0
100
200
300
75
100
125
150
200
Depth (m)
Stn. 90.0 028.0
1994-2013
pH
7.6
7.8
8.0
8.2
20
30
40
50
Depth (m)
CalCOFI Line 90.0 Station 30.0
1994-2013
pH
7.6
7.8
8.0
8.2
75
100
125
150
200
Depth (m)

This chapter, in full, is a reprint of the material as it appears in Deep Sea Research Part II: Topical Studies in Oceanography. Sato, Kirk N.; Levin, Lisa A.; Schiff, Kenneth, 2017. The dissertation author was the primary investigator and author of this material.

CHAPTER 3

Evaluating the promise and pitfalls of a potential climate change-tolerant sea urchin fishery in southern California

Abstract

Marine fishery stakeholders are beginning to consider and implement adaptation strategies in the face of growing consumer demand and potential deleterious climate change impacts such as ocean warming, ocean acidification, and deoxygenation. This study investigates the potential for development of a novel climate change-tolerant sea urchin fishery in southern California based on *Strongylocentrotus fragilis* (pink sea urchin). Here we outline potential criteria for a climate change-tolerant fishery by examining the distribution and life-history attributes of *S. fragilis* in southern California. We provide evidence of an environmental threshold using *in situ* observations and seasonality of marketable gonad production. The resiliency of *S. fragilis* to predicted future increases in acidity and decreases in oxygen was supported by positive growth rate estimates at extreme pH and oxygen conditions, which may provide assurances to stakeholders and managers regarding the suitability of this species for commercial exploitation, but further research on absolute growth rates is needed. Some marketable food quality properties of the *S. fragilis* roe (*e.g.*, color, texture) were comparable with those of the commercially exploited shallow-water red sea urchin (*Mesocentrotus franciscanus*). However, uncertain management challenges remain, and efforts to develop alternative adaptation strategies to climate change should be considered.

Introduction

Oxygen and pH regimes on the southern California shelf and slope are changing significantly with unknown consequences for the distributions and fitness of aerobic fishes and calcifying invertebrates (Gruber 2011, Gruber *et al.* 2012). In the Southern California Bight (SCB), expansion of low oxygen zones between 1984 and 2006 has led to a 20-30% decline in dissolved oxygen (DO) concentration on the upper slope and outer shelf and an inshore shoaling of up to 100 m of low-oxygen, high-CO_2 waters (Bograd *et al.* 2008, 2015). The climatological mechanisms of these trends in oxygen loss and CO_2 increase however, have not yet been determined (Bograd *et al.* 2015). Although evidence suggests that a natural strengthening of the CA Undercurrent source water over recent decades may result from low-frequency climate variability (Bograd *et al.* 2015), acidification (elevated CO_2) in the California Current System (CCS) is predicted to increase dramatically in future decades (Fabry *et al.* 2008). Biogeochemical models in the CCS predict that 100% of water in the twilight zone (60-120m) will be undersaturated with respect to the aragonitic form of calcium carbonate by 2050 (Gruber *et al.*, 2012). In addition, upwelling events, which are well known to bring deep, cold, and nutrient-rich water to shallower depths into coastal habitats are also characterized by relatively low oxygen, low pH, and low calcium carbonate saturation [Ω_{CaCO3}] (Feely *et al.* 2008, Send and Nam 2012, Booth *et al.* 2014). Such events have been observed in nearshore kelp forests of San Diego (Frieder *et al.* 2012), and potential sublethal effects on the reproductive output and structural integrity of key calcifying resources are expected to become far more widespread (Gaylord *et al.* 2011, Hofmann *et al.* 2014). Recent corrosive upwelling events have caused mortality in several oyster hatcheries on the U.S.

west coast in Oregon, resulting in major environmental projects to mitigate the effects of ocean acidification (Barton *et al.* 2012, 2015).

Among the many calcified inhabitants of the California margin, three species of Strongylocentrotid urchins occur between intertidal and bathyal depths off southern California: *Mesocentrotus franciscanus* (red urchins), *Strongylocentrotus purpuratus* (purple urchins) and *S. fragilis* (pink urchins). As important ecosystem engineers that efficiently graze on macroalgal species forming kelp forest habitat (Rogers-Bennett 2007), grazing urchins will remain key players in the management of coastal ecosystems in the face of future climate change. In southern California, these urchins experience a range of environmental conditions depending on depth and setting (*e.g.*, tidepools, submarine canyons), with the red and purple urchins generally occupying rocky intertidal and inner shelf reefs (Kato and Schroeter 1985, Rogers-Bennett 2007), and pink urchins occurring throughout the outer shelf and upper slope (Sato *et al.* 2017, Thompson *et al.* 1993).

Red urchins (*M. franciscanus*) make up the vast majority of urchin fishery landings on the west coast of North America. However, this sea urchin fishery is vulnerable to overfishing, disease, thermal stress, poor spawning seasons, and the supply of and demand for its roe (known as *uni* in sushi restaurants) (Botsford *et al.* 2004). Increased upwelling frequency over the next century may present challenges for urchin fishery management due to unknown species-specific and ecosystem-wide effects of multiple climate change drivers on fisheries (Gruber 2011). Additionally, potential deleterious effects of CO_2-acidified water due to ocean acidification on fertilization, larval development, and gene expression in red urchins could negatively impact

recruitment to the fishery, which depends on large, sexually mature individuals (O'Donnell *et al.* 2009, Frieder 2014, Hofmann *et al.* 2014, Kapsenberg *et al.* 2017). Early life-history stages have also been shown to be vulnerable to both acidification (Frieder 2014) and thermal stress (O'Donnell *et al.* 2009, Byrne and Przeslawski 2013). While the currently harvested urchin species (*M. franciscanus*) may suffer under future climate change scenarios, the deep-dwelling pink urchin, *S. fragilis*, is relatively more tolerant of low oxygen and pH (Sato *et al.* 2017, Taylor *et al.* 2014). This species appears to be extending its distribution into shallower water as low oxygen zones in the NE Pacific expand (Sato *et al.* 2017). Sea urchins are hand-picked by hookah divers primarily in southern California and secondarily in Mendocino County, CA. While the demand for sea urchins has increased domestically and internationally over recent years, the landings and value produced by the CA urchin fishery has been in continuous decline since 2000 (Figure 3.1). Therefore, it may be useful to consider alternative urchin species in order to reduce harvest stress on *M. franciscanus*.

An important adaptive management strategy under changing hydrographic conditions is to evaluate ways to shift fishery emphasis away from more vulnerable species to alternative resilient species (Ogier *et al.* 2016). Deep-sea fishery species (taken on the continental slope and seamounts) are conventionally thought to be non-sustainable due to long life spans, slow growth rates, and late maturity (Koslow *et al.* 2000, Norse *et al.* 2012). Indeed, few deep-sea fishery species have been sustainable, while most deep-sea fish stocks have experienced significant declines (Norse *et al.* 2012, Clark *et al.* 2016). However, species that naturally occur in stressful environments with respect to climate-change variables such as oxygen and pH may be adapted to future conditions that are

more hypoxic and acidic than at present. We investigated various adult characteristics of the pink urchin (*S. fragilis*), to evaluate the potential for developing this species as a climate change-tolerant fishery.

In this study, various fishery management criteria and food quality metrics of *S. fragilis* were evaluated in southern California populations in order to determine the feasibility of an emerging fishery. We addressed the following criteria for the potential management of a new climate change-tolerant *S. fragilis* fishery in southern California: (1) Resiliency evaluated as distribution and fitness traits in relation to multiple climate change variables, (2) accessibility evaluated as abundance across space and time, (3) habitat and ecosystems considered as habitat type, behavior, and food preference, and (4) acceptability (*i.e.*, marketable traits exemplifying food quality). In addition to these empirical data, we provide a rationale for the legalization of deep urchin bycatch take and the enhancement of aquaculture and novel food science practices for urchin fishery stakeholders to consider as alternative, long-term sustainable solutions in the face of environmental variation and climate change.

Methods

Field Sampling

Distribution and density

Availability of *Strongylocentrotus fragilis* urchins (*e.g.*, to fishers) is partly a function of both their depth distribution and density in the Southern California Bight (SCB). These were determined by analyzing benthic megafauna trawl survey datasets

collected during the summer months (July-September) of 2003, 2008, and 2013 by trained taxonomists of the Southern California Coastal Water Research Program. The gear type used during each survey year was a standardized 7.6 m head-rope semiballoon otter trawl net fitted with 1.25-cm cod-end mesh. Trawls were towed along open-coast isobaths for ~10 min at 1.5-2.0 nm hr^{-1} during daylight hours. Trawl distance was calculated from the start and stop fishing GPS coordinates, which acted as a proxy for the net's relative position. It was assumed the net remained on the bottom and was fishing the entire time (Allen *et al.* 2011). Upon retrieval, catches were sorted, identified to species, and enumerated. Each station was sampled once. Bay sites and sites at water depths <10 m were removed from this analysis in order to minimize zero inflated data (Thompson *et al.* 1993). The area swept by each trawl was calculated as the distance trawled (m) x 4.9 m (the width of the trawl) (Miller and Schiff 2012). Densities of *S. fragilis* were obtained per trawl by dividing the species count by the calculated area swept.

Historical densities and distributions of *S. fragilis* urchins between 10-500 m in the SCB are reported in Sato *et al.* (2017). A reanalysis of these data was conducted to identify the depths where *S. fragilis* occurs at densities above 0.001 indiv. m^{-2}, within smaller 50-m depth bins. *S. fragilis* density between 10-500 m was compared across survey years, while survey years were pooled in the 50-m depth bin analysis. The upper and lower depth limits, as well as the median, 25% quartile and 75% quartile depths were calculated by pooling all trawls with densities greater than 0.001 indiv. m^{-2} from the 3 surveys. Urchins often form feeding aggregations on kelp falls, which may bias density estimates, but the high number of trawls conducted is likely to capture this variability (Sato *et al.* 2017). One exception where kelp falls have been found to be more abundant

is in submarine canyons (Harrold *et al.* 1998), but in this study sites in canyons were avoided and sites were surveyed for flat, trawl-friendly ground prior to net deployment.

Abundance threshold depth and behavioral observations

Although *Strongylocentrotus fragilis* occurrence is present at depths of <100-1200 m in the SCB, the Oxygen Minimum Zone (OMZ) (O_2 < 20 μmol kg^{-1}) and associated food and climate variables limit most *S. fragilis* to the upper 500 m (Sato *et al.* 2017). To identify the threshold depth (and associated climate variables) where urchins are subjectively more abundant, we analyzed video footage from two cross-slope Remotely Operated Vehicle (ROV) transects on the San Diego shelf and slope. ROV surveys were conducted in August 2015 (Dive #1448) and December 2016 (Dive J-093) using two ROVs, the *Hercules* (Ocean Exploration Trust) and the *Jason* (Woods Hole Oceanographic Institution), aboard the R/V *Nautilus* and R/V *Sally Ride*, respectively. Each ROV was equipped with a Sea-Bird Electronics, Inc., Conductivity-Temperature-Depth (CTD) and an Aanderaa oxygen sensor, and these environmental data were thus simultaneously noted and reported. For each upslope transect, ROV pilots were instructed to maintain speed of 0.2-0.5 nmph and altitude above the seafloor between 1-2 m. Video cameras maintained the same direction, angle, and zoom throughout the duration of each dive. Video footage was paused every 30 s to 20 mins (0.5-10 m seafloor depth), and still frames were visually analyzed, to identify the deepest depth within the OMZ where *S. fragilis* urchins first appeared at high density. Urchins were counted within the visible area of each paused frame and recorded. To compare results across dives, urchin counts were calculated as a proportion of the highest count recorded during that dive. Feeding

aggregations were also observed, but not analyzed due to high uncertainty of urchin counts.

Spatiotemporal variability of edible gonads and growth

The spatial and seasonal variability of gonad production in *Strongylocentrotus fragilis* was compared across water depth zones on the shelf and slope in the SCB at various stations and depths throughout the species' distribution (Table 3.1). Local differences in *S. fragilis* gonad production were determined by separating the stations geospatially by latitude into three subregions (*i.e.* San Diego, Los Angeles, and Santa Barbara). *S. fragilis* individuals used in this spatial analysis were collected *via* otter trawls on various research cruises between July 2012 and June 2016 (Table 3.1). Subregional gonad data were further separated into 100-m depth bins and compared among subregions in the upper 500 m of the continental shelf and slope. To compare relative growth rates of *S. fragilis*, individuals were collected *via* otter trawl surveys in the San Diego region between 2012 and 2014. To determine the seasonality of *S. fragilis* gonad production, individuals were sampled by otter trawl from a single station (~340 m) off of Point Loma, CA (32.6986 °N, -117.3765 °W), at various times throughout the year, with the first trawl taking place in Summer 2012 and the twelfth and final trawl occurring in Summer 2016 (Table 3.2). During each collection, ~25 intact individuals were haphazardly selected from the trawl catch, sealed in a plastic bag, immediately frozen in a -20°C freezer on each ship, and transported to -20°C freezer in the lab until further analysis.

To obtain gonads for food quality analysis, live *S. fragilis* urchins were collected from 305 m water depth *via* otter trawl by the Los Angeles County Sanitation District on the R/V *Ocean Sentinel* in February 2015, near Palos Verdes, CA (33.6787 °N, -118.3276 °W). Live urchins were transported to the Kaplan Experimental Aquarium at Scripps Institution of Oceanography (La Jolla, CA) where they were fed *ad libitum* fronds of giant kelp (*Macrocystis pyrifera*) in flow-through seawater tanks at 8°C for approximately 4 weeks.

Hydrography Data

Hydrographic data for the study area were obtained during a multidisciplinary research cruise was carried out off the San Diego coast line on board the R/V *Melville* from 8-15 December, 2012 (Nam *et al.* 2015). A single profile of salinity, temperature, pressure, and dissolved oxygen (DO) at 1-m resolution was generated from the surface to 1,051 m (32.6901 °N, -117.5306 °W) using a Sea-Bird Electronics, Inc., CTD instrument (SBE9) and dissolved oxygen sensor (SBE43). Discrete water samples were collected every 50-100 m of water depth and analyzed for DO and pH following methods described by Nam *et al.* (2015). In brief, oxygen samples were analyzed following standard Winkler titration procedures (Dickson 1996), and pH samples were analyzed spectrophotometrically at 20° C using a custom automated system with m-cresol purple without further purification (Nam *et al.* 2015). Reported *in situ* pH was calculated from measured pH and dissolved inorganic carbon in CO2SYS (Van Heuven *et al.* 2011) using dissociation constants from Lueker *et al.* (2000).

Salinity, temperature, depth, and DO data were also collected from the ROV *Jason*, which was equipped with a CTD instrument (SBE19) that recorded data every second and an oxygen optode (Aanderaa 4831) that recorded oxygen every 30 seconds. The ROV *Hercules* was equipped with a CTD instrument (SBE FastCAT 49) and an oxygen optode (Aanderaa 3830), which recorded depth, salinity, temperature, and oxygen every second.

Lab Analyses

Gonad Index

Frozen *S. fragilis* urchins were thawed and rinsed clean of mud in the lab prior to dissection. Spines were removed prior to measurement of Total Length of the Diameter (TLD) via calibrated dial calipers to the nearest 0.1 mm. Wet weights of gonads (5 lobes) and each individual drained of its internal fluids were measured on a calibrated Sartorius digital balance (R160P) to the nearest 0.001 gram. The gonad index (GI) of a single individual was calculated by using the equation,

$$\mathrm{GI} = \frac{\mathrm{m_g}}{\mathrm{m}} \times 100,$$

where $\mathrm{m_g}$ is the total wet weight of the dissected gonads and m is the wet weight of the individual drained of its internal fluids.

Growth variability

Variability in relative growth was measured as a function of depth across the species' depth distribution (100-1200 m). Image analysis of growth bands was carried out on *Strongylocentrotus fragilis* individuals collected *via* otter trawl conducted at five depths in the San Diego region (Table 3.3). Frozen urchins were thawed in the laboratory, and individual ossicle plates from the interambulacral grooves of the aboral hemisphere were dissected using a scalpel under a dissecting microscope. Ossicle plates from each urchin were washed in a 2% bleach (NaClO) solution, placed on a shaker for 30 minutes to remove organic material from the plates, rinsed in DI water, and placed in a vial under a hood to dry for 24-48 hours. The ossicle plates were then charred in a muffled furnace for 3-5 minutes at 300°C and left to cool. Approximately 24 hours later, ossicles were set on a microscope slide and lightly coated with a clear epoxy for image analysis. Digital photographs were taken using a compound microscope fitted with a digital camera at 25x magnification. Images were digitally enhanced using Adobe Photoshop software in order to better identify alternating light and dark concentric bands on each ossicle (Figure 3.6).

The relative growth rate for each individual was calculated by using the equation,

$$\text{Rate of Growth} = \frac{x}{c},$$

where x is the TLD of the individual and c is the number of bands. Growth rate is reported as mm band^{-1} rather than mm year^{-1} because it is uncertain whether *S. fragilis* lays down annual or semiannual growth bands (Sumich and McCauley 1973). Other studies have attempted calcein marking of growth bands in red urchins (Pearse and Pearse 1975), but failed to determine urchin age due to inconsistencies of banding with seasonality (Kato

and Schroeter 1985). The growth zone analysis presented here provides a relative growth rate as a function of water depth, which can be relevant *S. fragilis* life history information for stakeholders and resource managers. The temperature, DO, and *in situ* pH values associated with each depth were determined using CTD data.

Roe Quality

To compare properties of *Strongylocentrotus fragilis* urchin roe quality to present seafood industry standards, freshly packaged *Mesocentrotus franciscanus* gonad lobes of the Grade B and B-minus quality were obtained from Catalina Offshore Products, Inc. (San Diego, CA). *M. franciscanus* individuals were collected from the wild by urchin divers, processed at Catalina Offshore Products Seafood, Inc., and gonad lobes were kept on ice until the moment of analysis. Prior to commercial sale, *M. franciscanus* gonads are typically placed in an anhydrous aluminum potassium sulfate ($AlK(SO_4)_2$), hereafter, Potassium Alum solution, which is used to commercially process urchin roe. The astringent is used for its ability to bind to proteins and prevent their breakdown, firming the roe (Kato and Schroeter 1985). For this study, gonads from *S. fragilis* and *M. franciscanus* were soaked for 20 minutes in a 0.5% Potassium Alum solution. Excess moisture was removed from *S. fragilis* and *M. franciscanus* gonads using paper towels, and gonads were weighed immediately prior to color and texture analyses. Individual gonad lobes from *M. franciscanus* were also weighed immediately prior to color and texture analyses.

Gonad color of *S. fragilis* and *M. franciscanus* roe was measured with a Konica-Minolta Colorimeter C-400 and recorded using SpectraMagic NX software. Gonads were

placed on transparent petri dishes and placed over the 8-mm diameter aperture of the colorimeter. Calibration of the colorimeter was carried out using a pure white color plate prior to each color measurement. The amount of red, the amount of yellow, and the lightness of the roe were measured 30 times per gonad lobe. The means of each color characteristic were used for statistical analysis. Red and yellow values represent on a scale of 0-100 the amount of red and yellow character a sample contains. Lightness is a measurement of how light or dark the sample is (white has the highest lightness character possible of $L^* = 60$). Total color change was recorded as the difference in overall color from pure white calibration plate (McBride *et al.* 2004). The difference between the color of the urchin gonad (Sample) and the white color calibration plate (Target) was calculated using the following equation:

$$\Delta E^*ab = ((L^*_{Target} - L^*_{Sample})^2 + (a^*_{Target} - a^*_{Sample})^2 + (b^*_{Target} - b^*_{Sample})^2)^{0.5},$$

where Δ^*ab = Total Color Change, L^* = Lightness, a^* = Redness, and b^* = Yellowness.

Texture was determined as a combination of gonad hardness and resilience using a TA.XT*Plus* texture analyzer with a 2" diameter metal cylinder probe. Hardness was recorded as the peak force (Newtons, kg m s^{-2}) required to compress the roe to half of its original height. Height of each gonad lobe was noted prior to texture analysis. The samples were compressed to a fixed distance of half their original height at a speed of 0.55 mm s^{-1} for a fixed duration of time. Resilience was then recorded as a function of the amount of time required for the roe to return to half of its original height after the roe's compression. Resilience was calculated by dividing the area under the curve during

the probe's withdrawal by the area under the curve during compression. The curve during withdrawal represented the decline in force as the probe returned to its starting height. The maximum force of the TA.XT*Plus* was set to its lowest setting (5 kg Load Cell), allowing for a force sensitivity of 0.1 g. The instrument was calibrated before every measurement using a 100 g weight.

Statistical Analyses

All response metrics were tested for normality using the Shapiro-Wilk test and homogeneity of variances using the Breusch–Pagan test. In each case where assumptions of normality and homoscedasticity were met, parametric tests such as linear regression or one-factor analysis of variance were employed. If the data violated these assumptions, the Box-Cox power transformation was used to correct the data. If the transformation did not improve normality or homoscedasticity of the data, then non-parametric tests were used. A Kruskal-Wallis test was used to compare density and gonad index across subregion, depth bin or season. If a significant difference was detected, a *post hoc* Dunn's test treated with a Bonferroni correction was conducted using the Pairwise Multiple Comparison of Mean Ranks Package in R. The Pearson product-moment correlation coefficient was determined for mean growth rate (evaluated as urchin test diameter in mm per band) with each depth-dependent environmental variable (*i.e.*, temperature, DO, and pH). To determine *S. fragilis* thresholds, mean environmental data (*i.e.*, depth, salinity, temperature, and DO) were calculated from data where abundances proportional to the maximum abundance were between 0.25 and 0.75.

Results

Distribution and density of *Strongylocentrotus fragilis*

Reasonably high density is a prerequisite for a viable fishery species, thus here we identify the distribution of *S. fragilis* in trawls where density exceeded 0.001 indiv. m^{-2}. The median and mean depths of trawls between 2003 and 2013 with *S. fragilis* densities >0.001 indiv. m^{-2} were 203 m and 250 m, respectively. Fifty percent of the trawls with these densities were found between depths 180.8 m (25% quartile) and 339 m (75% quartile) (Figure 3.2). The mean density of *S. fragilis* between 10 and 500 m did not vary significantly among the three survey years (Kruskal-Wallis Test: $\chi^2 = 5.967$, $p = 0.051$). As a result, the density data were pooled prior to further depth bin analysis. Density did not vary significantly across 50-m depth bins in the upper 500 m (Kruskal-Wallis Test: $\chi^2 = 8.263$, $p = 0.41$; Figure 3.2).

Abundance threshold and behavioral observations

Video analysis of two cross-slope benthic transects between ~450 and 650 m water depth using ship-based ROV deployments off San Diego, CA, revealed a consistent dramatic shift in *Strongylocentrotus fragilis* abundance with depth (Figure 3.3). In each case, a shift from 0-5 urchins per frame to a considerable abundance of 33-38 urchins per frame occurred over a short change in depth of <5 m. During the ROV *Hercules* dive in August 2015, this increase in *S. fragilis* occurred between 485-490 m water depth. During the ROV *Jason* dive in December 2016, the community changed abruptly to a *S. fragilis*

urchin-dominated community from an asteroid-dominated community between 505-510 m water depth. Table 3.4 shows the mean environmental conditions in which *S. fragilis* abundances were 25-75% of the maximum abundances counted during each dive.

We observed *S. fragilis* urchins aggregating around kelp falls (<500 m) consistently during both dives with estimated densities of up to ~200 indiv. m^{-2} (Figure 3.3). Active feeding on giant kelp (*Macrocystis pyrifera*) was confirmed by collections of urchins clinging to the kelp and gut contents. Drift *M. pyrifera* was observed without aggregating urchins at ~600 m where no *S. fragilis* urchins were present (Figure 3.3).

Spatiotemporal variability of edible gonads

Mean gonad index (GI) of *Strongylocentrotus fragilis* collected in the upper 500 m varied significantly among all three subregions (Kruskal-Wallis Test: $\chi^2 = 56.89$, $p < 0.0001$). While the mean depths from which the urchins originated significantly differed among subregions (Kruskal-Wallis Test: $\chi^2 = 74.18$, $p < 0.0001$), these depths did not differ between Los Angeles and San Diego (*post hoc* Dunn's test: $p = 0.76$). The mean depth of trawls in the Santa Barbara subregion was significantly shallower (219 m) than Los Angeles (302 m) and San Diego (310 m). The mean GI from Santa Barbara was 26% greater than those from Los Angeles and 94% greater than those from San Diego (Figure 3.4). Gonad indices decreased linearly with increasing depth (75-1100 m) in the SCB (Pearson: $r_{37} = -0.43$, $p = 0.007$) (Figure 3.4). When separated into 100-m depth bins, peak GI was found in different depth bins for each subregion with the highest mean GI

occurring in Santa Barbara between 200 and 300 m water depth (Figure 3.4). Within each subregion, mean GI varied significantly among depth bins (Figure 3.4).

Seasonal variability of gonad production in *S. fragilis* was observed over the sampling period (2012-2016) at a 340-m water depth site near Point Loma, San Diego, CA (Figure 3.5). When seasons were pooled across years, GI in *S. fragilis* exhibited significant seasonality (Kruskal-Wallis Test: $\chi^2 = 79.822$, $p < 0.001$) (Figure 3.5). Mean Winter GI was 86% higher than the global mean (4.11 ± 0.18 SE) and was reduced by 62-64% in the Spring and Summer (Figure 3.5). Mean Summer GI was significantly different across years (Kruskal-Wallis Test: $\chi^2 = 10.851$, $p = 0.013$), with Summer 2013 GI 48% higher than in Summer 2015 (*post hoc* Dunn's test: $p = 0.01$) (Figure 3.5). In addition, GI in Fall of 2015 was 58% lower than in 2013 and 55% lower than in 2012 (*post hoc* Dunn's test: $p < 0.001$).

Growth variability

Relative growth rate analysis of *Strongylocentrotus fragilis*, as determined from band counts, demonstrated positive growth at all depths. *S. fragilis* collected from 100-m water depth had the highest growth rate relative to those urchins living at greater water depths (Figure 3.6). The mean growth rate at 700m was 66% lower than at 100m (Table 3.3). Growth rate was positively correlated with dissolved oxygen (Pearson's correlation: $r_3 = 0.93$, $p = 0.022$) (Figure 3.6a) and pH (Pearson's correlation: $r_3 = 0.95$, $p = 0.014$) (Figure 3.6), but there was no significant relationship with temperature

(Pearson's correlation: $r_3 = 0.71$, $p = 0.183$) (Figure 3.6c) or depth (Pearson's correlation: $r_3 = -0.74$, $p = 0.152$).

Roe Quality – Color and Texture

Strongylocentrotus fragilis mean gonad lobe weight (2.38 g ± 0.33 S.E.) was 80% lower than the weight of gonad lobes of *Mesocentrotus franciscanus* (11.95 g ± 0.76 S.E.; Kruskal-Wallis Test: $\chi^2 = 14.778$, $p = 0.0001$). Color differences among the three types of gonad (*i.e. S. fragilis*, *M. fransciscanus* Grade B and B-minus) were observed (Figure 3.7), with *M. fransicanus* gonads exhibiting more total color change than *S. fragilis* gonads (1-way ANOVA: $F_{2, 29} = 32.49$, $p < 0.001$; Figure 3.7). *S. fragilis* gonads did not significantly differ in lightness and redness from *M. franciscanus* B-grade gonads (Figure 3.7a), nor did they significantly differ in yellowness from *M. franciscanus* B-minus grade gonads (Figure 3.7). The most distinctive difference in texture between the two species was the peak hardness of their gonads (Figure 3.7). On average, *S. fragilis* gonads were 85% softer than *M. franciscanus* B-grade gonads (Kruskal-Wallis Test: $\chi^2 = 12.231$, $p < 0.001$; Figure 3.7), but there was no significant difference in the resilience between the species (Kruskal-Wallis Test: $\chi^2 = 3.316$, $p = 0.07$; Figure 3.7).

Discussion

The development of sustainable climate-tolerant fisheries is one of several management adaptation strategies that stakeholders may pursue to limit the deleterious negative effects of climate change (FAO, 2016). This study uniquely provides

spatiotemporal analyses of an unfished species of sea urchin (*Strongylocentrotus fragilis*) and describes relevant food quality properties in order to inform various stakeholders about the feasibility of developing a *S. fragilis* fishery in southern California. The management criteria that we investigated (resiliency, accessibility, *S. fragilis* habitat and behavior, and acceptability) may inform the sea urchin industry, management, and scientific communities about *S. fragilis* should it be considered as a viable fishery in the future. The sheer abundance (Figure 3.3) and positive growth (Figure 3.6) of *S. fragilis* urchins throughout its vast spatial distribution at water depths (485-510 m) subject to low oxygen (11.7-16.9 µmol kg^{-1}) and pH (<7.44) in southern California (Bograd *et al.* 2008, Gruber *et al.* 2012, Nam *et al.* 2015) demonstrate the species' tolerance to stressful environments with respect to climate change variables. Our findings suggest that *S. fragilis* is abundant in the upper 500 m with a peak density occurring between 200 and 300 m. As a species tolerant to relatively acidic and hypoxic conditions, *S. fragilis* may become more accessible at shallower depths as the OMZ expands into shallower waters (Sato *et al.* 2017).

Multiple studies have suggested that important sea urchin fishery species are vulnerable to the effects of climate change and ocean acidification (O'Donnell *et al.* 2009, Reuter *et al.* 2011, Frieder 2014). In contrast to the conclusions of these experiments on currently fished sea urchin species, our results suggest that *S. fragilis* currently exhibits higher growth rates at the deepest site (1,096 m) with the lowest temperature (Figure 3.6) than in the OMZ core (700 m) where dissolved oxygen and pH were 9.187 µmol kg^{-1} and 7.39, respectively (Figure 3.6). The DO concentration at 700 m was 93% lower than at 100m (Table 3.3), and the simultaneously reduced pH and dissolved oxygen conditions

in the OMZ are predicted to shoal as the ocean becomes increasingly more acidic and deoxygenated (Bograd *et al.* 2008, Gruber *et al.* 2012). Our findings support the results of Taylor *et al.* (2014), which demonstrated that *S. fragilis* collected from the OMZ has limited ability to regulate internal acid-base balance under simulated ocean acidification conditions (pH_{Total} <7.5), with little effect on their feeding rates and righting times. The range of pH and dissolved oxygen concentrations at the San Diego sites where abundant populations of *S. fragilis* persist (Figure 3.3) demonstrates the resilience of this species to extreme pH and oxygen conditions.

However, there are lessons to consider from the existing urchin fisheries. Understanding the size- and age-dependent responses to low oxygen and low pH environments is important for establishing or adjusting size limits for the *Mesocentrotus franciscanus* urchin fishery (Kato and Schroeter 1985, Rogers-Bennett 2007). Larger *M. franciscanus* serve as nursery habitat for younger urchins that are more vulnerable to predation (Tegner and Levin 1983, Tegner and Dayton 1991), while younger urchins may not be reproductive. We were unable to observe this behavior in *S. fragilis* using trawl and ROV imagery, and this possibility warrants further investigation.

Although sea urchin gonads are often considered delicacies in various cuisines worldwide, the demand for and fishing pressure on sea urchins continues to increase (Andrew *et al.* 2002, Botsford *et al.* 2004, Knapp and Rubino 2016). In order to provide enough sea urchins for this growing demand, finding alternative sources of supply should be a priority for managers and stakeholders, especially given the known vulnerability of *M. franciscanus* populations to overfishing (Andrew *et al.* 2002, Botsford *et al.* 2004) and unfavorable environmental conditions. For example, El Niño or anomalously warm

ocean conditions (*e.g*., summer 2014 "warm blob" in the Southern CA Bight) are hypothesized to reduce the availability of nutrients and inhibit the growth of the primary urchin food source of harvested sea urchins, giant kelp (*Macrocystis pyrifera*) (Reed *et al.* 2016). These warm ocean conditions can subsequently affect the gonad production and recruitment of sea urchins into the fishery (Tegner and Dayton 1991, Arntz *et al.* 2006, Rogers-Bennett 2007, Vasquez 2007) and may have explained the decrease in *S. fragilis* gonad production in Fall 2015 (Figure 3.5, c). As these conditions are predicted to become more frequent due to ocean warming (Sweetman *et al.* 2017), it is critical for stakeholders to consider alternative sources of sea urchins including increased imports, aquaculture, or other alternative food production techniques.

The United States currently imports approximately 90% of its seafood (by value), and the country's trade deficit continues to increase (Kite-Powell *et al.* 2013, Knapp and Rubino 2016). In order to maintain food security, especially in the face of climate change, increasing domestic fishery production (*via* alternative species or aquaculture) may provide some economic relief. Based on the criteria we present, *S. fragilis* may be a possible viable alternative fishery to supplement the current southern CA fishery, but further consideration and research will be required. Although the gonad weight of *S. fragilis* gonads was on average 80% lower than *M. franciscanus* gonads and significantly softer (Figure 3.7e), the color and resilience were comparable. These results suggest that *S. fragilis* gonads may not be suitable for direct consumption as *uni*, but other potential uses for *S. fragilis* gonads could include garnish and flavoring.

Our results suggest that the peak density of *S. fragilis* was in the 251-300 m depth bin, 130% higher than the density of the 201-250 m depth bin and 29% higher than the

density in the 301-350 m depth bin (Figure 3.3). *S. fragilis* is currently caught as bycatch in baited traps that target the valuable spot prawn (*Pandalus platyceros*) at a mean depth of 250 m (Phil Zerofski, Personal Communication). Spot prawn fishers however, are not permitted to catch sea urchins and are prohibited from taking non-target species (CDFG 2008). The *P. platyceros* fishery season in southern CA is open during the spring and summer months when *S. fragilis* gonad production is low and closed during the fall and winter months when *S. fragilis* gonad production is high (Figure 3.5). Legalizing bycatch or opening a *S. fragilis* fishery during fall and winter months could provide an additional source of income for fishers in the region. Baited traps are a less destructive type of gear than bottom trawls and would minimize costs to fishers and ecosystem impact (Clark *et al.* 2016). However, the type of bait used for *S. fragilis* could be switched to *M. pyrifera* kelp in order to minimize impact on *P. platyceros* during its closure season. These issues could complicate the development of future fishery activity for *S. fragilis* and warrant further discussion.

In addition, the aquaculture industry provides added food security to economies, particularly when unfavorable environmental conditions reduce and negatively affect wild-caught production. Marketable sea urchin products depend on gonad indices around 10-15%, and thus an abundance of food in the wild. We documented on several occasions using ROVs that *S. fragilis* aggregated in large numbers on *M. pyrifera*, the seemingly most important and favorable *S. fragilis* food source. Given the co-dependence of southern CA sea urchins (*i.e.*, *S. fragilis* and *M. franciscanus*) on healthy *M. pyrifera* in the wild, aquaculture may be a more realistic and lucrative industry for *M. franciscanus* than for *S. fragilis*. Although *S. fragilis* can be cultured, the production cost associated

with maintaining a shallow-water sea urchin aquaculture facility for *M. franciscanus* would likely be significantly less than that of *S. fragilis* due to the difference in production weight of valuable gonads between the two species. In addition, *S. fragilis* would require a much cooler environment to be sustained during growth. While the average age of *M. fransicanus* in the fishery is approximately 4-5 years (Kato and Schroeter 1985), the absolute age of *S. fragilis* remains uncertain, and a comparative study to test effects on absolute growth rates and gonad production would be required.

Acknowledgements

We acknowledge the Southern California Coastal Water Research Project, the National Oceanic and Atmospheric Administration's West Coast Groundfish Bottom Trawl Survey, and the University of California Ship Funds Program for providing KNS with access to data and ship time for sample collection. We especially thank Phil Zerofski and Natalya Gallo for their field assistance, and Daniel Jio, Katie Kelsoe, Stephanie Luong, and Marissa Mangelli for their assistance in the laboratory. We thank Randy Bunney (Konica Minolta Sensing Americas, Inc.) for assistance with color analysis and Kelly Lane (San Diego State University) for access to and assistance with texture analysis. KNS and LAL were supported by the Edna Bailey Sussman Foundation Internship and National Oceanic and Atmospheric Administration (NOAA) Grant No. NA14OAR4170075, California Sea Grant College Program Project No. R/SSFS-02 through NOAA's National Sea Grant College Program, U.S. Department of Commerce. JAP was supported by the Scripps Undergraduate Research Fellowship and National Institute of Health (NIH) MARC U-STAR Grant No. GM08228 as an undergraduate at California State University Los Angeles. The statements, findings, conclusions and recommendations are those of the authors and do not necessarily reflect the views of California Sea Grant, NOAA, or NIH. This chapter, in full, has been submitted for publication of the material as it may appear in ICES Journal of Marine Science, 2017, Sato, Kirk N.; Powell, Jackson; Rudie, David; Levin, Lisa A. The dissertation author was the primary investigator and author of this material.

References

Allen, M. J., D. Cadien, E. Miller, D. W. Diehl, K. Ritter, S. L. Moore, C. Cash, D. J. Pondella, V. Raco-Rands, C. Thomas, R. Gartman, W. Power, A. K. Latker, J. Williams, J. L. Armstrong, and K. Schiff. 2011. Southern California Bight 2008 Regional Monitoring Program: Volume IV. Demersal Fishes and Megabenthic Invertebrates. Southern California Coastal Water Research Project, Costa Mesa, CA:153 pp.

Andrew, N., Y. Agatsuma, E. Ballesteros, A. Bazhin, E. Creaser, D. Barnes, L. Botsford, A. Bradbury, A. Campbell, J. Dixon, and S. Einarsson. 2002. Status and management of world sea urchin fisheries. Oceanography and Marine Biology: An Annual Review 40:343–425.

Arntz, W. E., V. A. Gallardo, D. Gutiérrez, E. Isla, L. A. Levin, J. Mendo, C. Neira, G. T. Rowe, J. Tarazona, and M. Wolff. 2006. El Niño and similar perturbation effects on the benthos of the Humboldt, California, and Benguela Current upwelling ecosystems. Advances in Geosciences 6:243–265.

Barton, A., B. Hales, G. G. Waldbusser, C. Langdon, and R. A. Feely. 2012. The Pacific oyster, *Crassostrea gigas*, shows negative correlation to naturally elevated carbon dioxide levels: Implications for near-term ocean acidification effects. Limnology and Oceanography 57:698–710.

Barton, A., G. Waldbusser, R. Feely, S. Weisberg, J. Newton, B. Hales, S. Cudd, B. Eudeline, C. Langdon, I. Jefferds, T. King, A. Suhrbier, and K. McLauglin. 2015. Impacts of coastal acidification on the Pacific Northwest shellfish industry and adaptation strategies implemented in response. Oceanography 25:146–159.

Bograd, S. J., M. P. Buil, E. Di Lorenzo, C. G. Castro, I. D. Schroeder, C. R. Anderson, C. Benitez-Nelson, and F. A. Whitney. 2015. Changes in source waters to the Southern California Bight. Deep Sea Research Part II: Topical Studies in Oceanography 112:42–52.

Bograd, S. J., C. G. Castro, E. Di Lorenzo, D. M. Palacios, H. Bailey, W. Gilly, F. P. Chavez, C. G. Castro, E. Di Lorenzo, D. M. Palacios, H. Bailey, W. Gilly, and F. P. Chavez. 2008. Oxygen declines and the shoaling of the hypoxic boundary in the California Current. Geophysical Research Letters 35:L12607.

Booth, J. A. T., C. B. Woodson, M. Sutula, F. Micheli, S. B. Weisberg, S. J. Bograd, A. Steele, J. Schoen, and L. B. Crowder. 2014. Patterns and potential drivers of declining oxygen content along the southern California coast. Limnology and Oceanography 59:1127–1138.

Botsford, L. W., A. Campbell, and R. Miller. 2004. Biological reference points in the management of North American sea urchin fisheries. Canadian Journal of Fisheries

and Aquatic Sciences 61:1325–1337.

Byrne, M., and R. Przeslawski. 2013. Multistressor impacts of warming and acidification of the ocean on marine invertebrates' life histories. Integrative and Comparative Biology 53:582–596.

CDFG. 2008. Status of the Fisheries Report Through 2006, Spot Prawn.

Clark, M. R., F. Althaus, T. A. Schlacher, A. Williams, D. A. Bowden, and A. A. Rowden. 2016. The impacts of deep-sea fisheries on benthic communities: A review. ICES Journal of Marine Science 73:i51–i69.

Dickson, A. G. 1996. Determination of dissolved oxygen in sea water by Winkler titration. World Hydrographic Program 91–1:1–13.

Fabry, V. J., B. A. Seibel, R. A. Feely, and J. C. Orr. 2008. Impacts of ocean acidification on marine fauna and ecosystem processes. ICES Journal of Marine Science 65:414–432.

Feely, R. A., C. L. Sabine, J. M. Hernandez-Ayon, D. Ianson, and B. Hales. 2008. Evidence for upwelling of corrosive "acidified" water onto the continental shelf. Science 320:1490–1492.

Frieder, C. A. 2014. Present-day nearshore pH differentially depresses fertilization in congeneric sea urchins. Biological Bulletin 226:1–7.

Frieder, C. A., S. H. Nam, T. R. Martz, and L. A. Levin. 2012. High temporal and spatial variability of dissolved oxygen and pH in a nearshore California kelp forest. Biogeosciences 9:3917–3930.

Gaylord, B., T. M. Hill, E. Sanford, E. A. Lenz, L. A. Jacobs, K. N. Sato, A. D. Russell, and A. Hettinger. 2011. Functional impacts of ocean acidification in an ecologically critical foundation species. Journal of Experimental Biology 214:2586–2594.

Gruber, N. 2011. Warming up, turning sour, losing breath: ocean biogeochemistry under global change. Philosophical Transactions of the Royal Society of London A: Mathematical, Physical and Engineering Sciences 369:1980–1996.

Gruber, N., C. Hauri, Z. Lachkar, D. Loher, T. L. Frolicher, and G. K. Plattner. 2012. Rapid progression of ocean acidification in the California Current System. Science 337:220–223.

Harrold, C., K. Light, and S. Lisin. 1998. Organic enrichment of submarine-canyon and continental-shelf benthic communities by macroalgal drift imported from nearshore kelp forests. Limnology and Oceanography 43:669–678.

Van Heuven, S., D. Pierrot, J. W. B. Rae, E. Lewis, and D. W. Wallace. 2011. MATLAB Program Developed for CO_2 System Calculations. ORNL/CDIAC-105b.

Hofmann, G. E., T. G. Evans, M. W. Kelly, J. L. Padilla-Gamiño, C. A. Blanchette, L. Washburn, F. Chan, M. A. Mcmanus, B. A. Menge, B. Gaylord, T. M. Hill, E. Sanford, M. Lavigne, J. M. Rose, L. Kapsenberg, and J. M. Dutton. 2014. Exploring local adaptation and the ocean acidification seascape – studies in the California Current Large Marine Ecosystem. Biogeosciences 11:1053–1064.

Kapsenberg, L., D. K. Okamoto, J. M. Dutton, and G. E. Hofmann. 2017. Sensitivity of sea urchin fertilization to pH varies across a natural pH mosaic. Ecology and Evolution:1–14.

Kato, S., and S. C. Schroeter. 1985. Biology of the red sea rrchin, *Strongylocentrotus franciscanus*, and its fishery in California. Marine Fisheries Reviews 47:1–20.

Kite-Powell, H. L., M. C. Rubino, and B. Morehead. 2013. The future of U.S. seafood supply. Aquaculture Economics and Management 17:228–250.

Knapp, G., and M. C. Rubino. 2016. The political economics of marine aquaculture in the United States. Reviews in Fisheries Science and Aquaculture 24:213–229.

Koslow, J. A., G. W. Boehlert, J. D. M. M Gordon, R. L. Haedrich, P. Lorance, and N. Parin. 2000. Continental slope and deep-sea fisheries: implications for a fragile ecosystem. ICES Journal of Marine Science 57:548–557.

Lueker, T. J., A. G. Dickson, and C. D. Keeling. 2000. Ocean pCO_2 calculated from dissolved inorganic carbon, alkalinity, and equations for K_1 and K_2 : validation based on laboratory measurements of CO_2 in gas and seawater at equilibrium. Marine Chemistry 70:105–119.

McBride, S. C., R. J. Price, P. D. Tom, J. M. Lawrence, and A. L. Lawrence. 2004. Comparison of gonad quality factors: color, hardness and resilience, of *Strongylocentrotus franciscanus* between sea urchins fed prepared feed or algal diets and sea urchins harvested from the Northern California fishery. Aquaculture 233:405–422.

Miller, E. F., and K. Schiff. 2012. Descriptive trends in southern California bight demersal fish assemblages since 1994. California Cooperative Oceanic Fisheries Investigations Reports 53:107–131.

Nam, S., Y. Takeshita, C. A. Frieder, T. Martz, and J. Ballard. 2015. Seasonal advection of Pacific Equatorial Water alters oxygen and pH in the Southern California Bight. Journal of Geophysical Research: Oceans 120:5387–5399.

Norse, E. A., S. Brooke, W. W. L. Cheung, M. R. Clark, I. Ekeland, R. Froese, K. M.

Gjerde, R. L. Haedrich, S. S. Heppell, T. Morato, L. E. Morgan, D. Pauly, R. Sumaila, and R. Watson. 2012. Sustainability of deep-sea fisheries. Marine Policy 36:307–320.

O'Donnell, M. J., L. M. Hammond, and G. E. Hofmann. 2009. Predicted impact of ocean acidification on a marine invertebrate: elevated CO_2 alters response to thermal stress in sea urchin larvae. Marine Biology 156:439–446.

Ogier, E. M., J. Davidson, P. Fidelman, M. Haward, A. J. Hobday, N. J. Holbrook, E. Hoshino, and G. T. Pecl. 2016. Fisheries management approaches as platforms for climate change adaptation: Comparing theory and practice in Australian fisheries. Marine Policy 71:82–93.

Pearse, J. S., and V. B. Pearse. 1975. Growth zones in the echinoid skeleton. American Zoologist 15:731–751.

Reed, D., L. Washburn, A. Rassweiler, R. Miller, T. Bell, and S. Harrer. 2016. Extreme warming challenges sentinel status of kelp forests as indicators of climate change. Nature Communications 7:13757.

Reuter, K. E., K. E. Lotterhos, R. N. Crim, C. A. H. Thompson, and C. D. G. Harley. 2011. Elevated pCO_2 increases sperm limitation and risk of polyspermy in the red sea urchin *Strongylocentrotus franciscanus*. Global Change Biology 17:163–171.

Rogers-Bennett, L. 2007. The ecology of *Strongylocentrotus franciscanus* and *Strongylocentrotus purpuratus*. Pages 393–425 *in* J. M. Lawrence, editor. Edible sea urchins: Biology and Ecology. Second edition. Elvesier.

Sato, K. N., L. A. Levin, and K. Schiff. 2017. Habitat compression and expansion of sea urchins in response to changing climate conditions on the California continental shelf and slope (1994–2013). Deep Sea Research Part II: Topical Studies in Oceanography 137:377–389.

Send, U., and S. Nam. 2012. Relaxation from upwelling: The effect on dissolved oxygen on the continental shelf. Journal of Geophysical Research: Oceans 117:C04024.

Sumich, J. L., and J. E. McCauley. 1973. Growth of a sea urchin, *Allocentrotus fragilis*, off the Oregon coast. Coastal Pacific Science 27:156–167.

Sweetman, A. K., A. R. Thurber, C. R. Smith, L. A. Levin, C. Mora, C.-L. Wei, A. J. Gooday, D. O. B. Jones, M. Rex, M. Yasuhara, J. Ingels, H. A. Ruhl, C. A. Frieder, R. Danovaro, L. Würzberg, A. Baco, B. M. Grupe, A. Pasulka, K. S. Meyer, K. M. Dunlop, L.-A. Henry, and J. M. Roberts. 2017. Major impacts of climate change on deep-sea benthic ecosystems. Elementa 5:4.

Taylor, J. R., C. Lovera, P. J. Whaling, K. R. Buck, E. F. Pane, and J. P. Barry. 2014.

Physiological effects of environmental acidification in the deep-sea urchin *Strongylocentrotus fragilis*. Biogeosciences 11:1413–1423.

Tegner, M. J., and P. K. Dayton. 1991. Sea urchins, El Niños, and the long term stability of Southern California kelp forest communities. Marine Ecology Progress Series 77:14.

Tegner, M. J., and L. A. Levin. 1983. Spiny lobsters and sea urchins: Analysis of a predator-prey interaction. Journal of Experimental Marine Biology and Ecology 73:125–150.

Thompson, B., D. Tsukada, and J. Laughlin. 1993. Megabenthic assemblages of coastal shelves, slopes, and basins off southern California. Bulletin of the Southern California Academy of Sciences 92:25–42.

Vasquez, J. A. 2007. Ecology of *Loxechinus albus*. Pages 227–241 *in* J. M. Lawrence, editor. Edible sea urchins: Biology and Ecology. Second edition. Elvesier.

Table 3.1. Subregion within the Southern California Bight, collection date, GPS coordinates, and depths of stations where Strongylocentrotus fragilis were sampled via otter trawl and dissected for gonad index measurement.

Subregion	Date Collected	Latitude (°)	Longitude (°)	Depth (m)
Los Angeles	8/14/2013	33.7668	-118.4600	130
	9/4/2013	33.9340	-118.5905	200
	8/14/2013	33.6941	-118.3460	253
	8/16/2013	33.7215	-118.4180	293
	2/13/2014	33.6959	-118.3509	305
		33.6787	-118.3276	305
	7/21/2014	33.5045	-118.0396	458
	8/16/2013	33.6761	-118.3320	470
San Diego	8/6/2013	32.5954	-117.3286	136
	8/1/2013	32.6434	-117.4277	150
	8/8/2013	32.8254	-117.3660	182
	8/7/2013	32.9092	-117.2951	184
	7/27/2014	32.8211	-117.3690	200
		32.6720	-117.3542	200
	11/3/2012	32.6736	-117.3602	215
	7/27/2013	32.6694	-117.3975	300
	12/15/2012	32.6916	-117.3758	300
	4/20/2014	32.6986	-117.3765	300
	12/12/2012	32.8100	-117.4004	300
	7/8/2012	32.8786	-117.3436	300
	6/13/2015	32.7209	-117.3737	325
	3/13/2016	32.7035	-117.3776	340
	11/1/2014	32.7070	-117.3760	340
	11/2/2014	32.7070	-117.3760	340
	10/18/2015	32.7244	-117.3660	340
	4/12/2015	32.6908	-117.6908	340
	7/9/2016	32.7015	117.3796	340
	7/26/2014	32.7010	-117.3852	360
	12/12/2012	32.8100	-117.4004	400
	12/9/2012	32.9471	-117.3416	400
	8/13/2013	33.0938	-117.4172	400
	10/19/2013	32.7461	-117.4159	427
	8/1/2013	32.6683	-117.4197	435
	7/14/2014	33.1547	-117.5011	439
	7/16/2014	32.8990	-118.6182	475
	7/29/2014	32.8908	-117.4745	697
	4/18/2015	32.8828	-117.4830	715
	10/14/2014	32.8230	-118.0330	758
		32.8327	-118.0292	768
	7/9/2016	32.8706	-117.5941	900
	7/1/2014	33.2165	-118.2318	1096
Santa Barbara	7/16/2014	34.0069	-118.9009	77
	7/15/2014	34.0720	-119.6489	90
	8/22/2013	34.2068	-119.6353	154
	8/23/2013	34.1327	-119.3699	172
		34.1072	-119.3190	195
	8/21/2013	34.2251	-119.7320	196
		34.2778	-119.7183	200
	8/22/2013	34.1690	-119.5420	237
	8/21/2013	34.1186	-119.6305	260
	8/20/2013	33.9774	-118.8764	493

Table 3.2. Collection date, season, and mean gonad index (± 1 S.E.) of *Strongylocentrotus fragilis* collected *via* otter trawl at a single station (~340 m) off of Point Loma, San Diego, CA.

Year	Season	Date	Gonad Index (± 1 S.E.)
2012	Summer	7/8/2011	3.114 ± 0.237
	Winter	12/12/2012	7.815 ± 0.913
2013	Summer	7/27/2013	3.547 ± 0.306
	Winter	2/13/2014	8.487 ± 0.825
2014	Spring	4/20/2014	3.923 ± 0.304
	Summer	7/26/2014	3.448 ± 0.487
	Fall	11/1/2014	5.583 ± 0.525
2015	Spring	4/12/2015	2.107 ± 0.226
	Summer	6/13/2015	2.402 ± 0.292
	Fall	10/18/2015	3.545 ± 0.274
2016	Spring	3/13/2016	2.880 ± 0.267

Table 3.3. Collection sites of *Strongylocentrotus fragilis* individuals in the Southern California Bight that were analyzed in the lab for growth rate. Hydrographic data (depth, dissolved oxygen, temperature and *in situ* pH) were measured from a single vertical profile in December 2012 (32.69012° N, -117.53061° W) (Nam *et al.*, 2015).

Depth of Urchin (m)	**Mean Growth (± S.D.)**	**Latitude (°)**	**Longitude (°)**	**Depth of CTD (m)**	**Oxygen ($\mu mol\ kg^{-1}$)**	**Temperature (°C)**	***in situ* pH**
100	5.21 ± 1.63	32.9641	-117.3136	100	138.198	11.442	7.75
300	2.75 ± 0.69	32.9523	-117.3184	300	46.815	8.1301	7.46
400	2.12 ± 0.52	32.9471	-117.3416	400	26.355	7.2387	7.44
700	1.78 ± 0.39	32.8128	-117.4676	700	9.187	5.1982	7.39
1096	1.86 ± 0.41	33.2165	-118.2318	1051	19.336	4.0242	7.42

Table 3.4. *Strongylocentrotus fragilis* threshold results from *in situ* visual surveys conducted by remotely operated vehicles. Mean environmental conditions over which *S. fragilis* abundances were 25-75% of the maximum abundances counted during each dive. Values in brackets are standard deviations.

Vehicle	Vessel	Date	Mean Latitude (°N)	Mean Longitude (°W)	Depth (m)	Salinity (PSU)	Temperature (°C)	O2 (µmol kg^{-1})	Proportion of Max Abundance	No. of Frames Analyzed
Hercules	E/V *Nautilus*	8/1/2015	32.8134	-117.4121	487.1 [3.3]	34.326 [0.001]	7.52 [0.01]	16.945 [0.077]	0.46 [0.14]	38
Jason	R/V *Sally Ride*	12/3/2016	32.7085	-117.4144	478.6 [30.7]	34.290 [0.015]	6.34 [0.21]	13.614 [2.467]	0.54 [0.11]	31

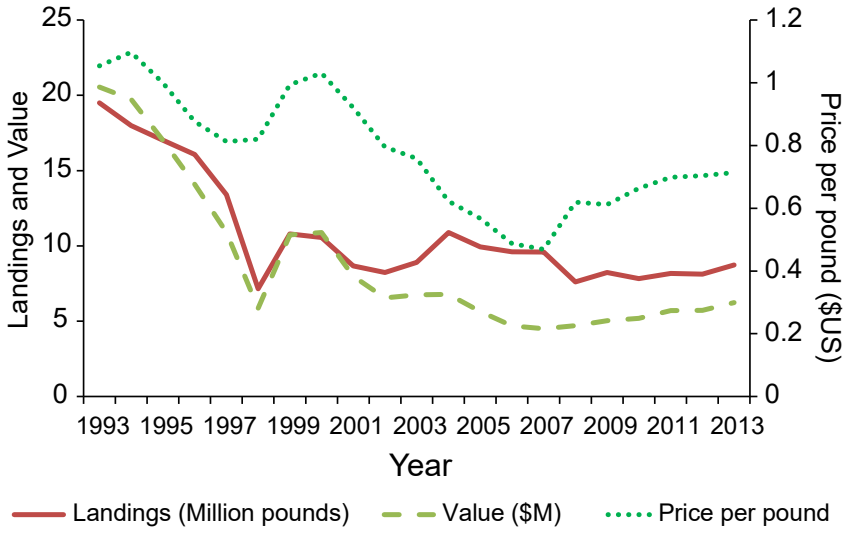

Figure 3.1. 20-year time series of *Mesocentrotus franciscanus* (red urchin) fishery data in southern CA. Commercial landings in million pounds (red line), ex-vessel value in millions of US dollars (green dashed line), and price per urchin pound (green dotted line). Data source: http://www.dfg.ca.gov/marine/seaurchin/index.asp.

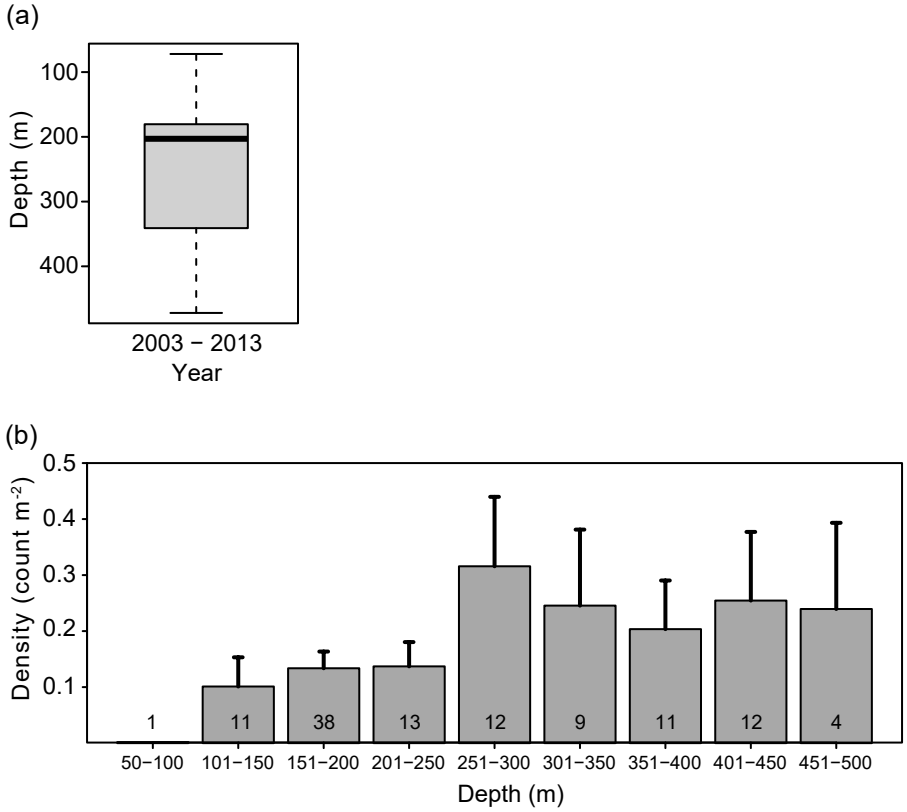

Figure 3.2. Pooled *Strongylocentrotus fragilis* data collected during three trawl surveys throughout southern California (2003, 2008, and 2013). (a) Depth distribution of otter trawls with S. fragilis densities >0.001 indiv. m^{-2}. Boxplot shows upper and lower limits, 25% and 75% quartile depths, and median depth of trawls. (b). Mean density (± 1 SE) of *S. fragilis* across 50-m depth bins.

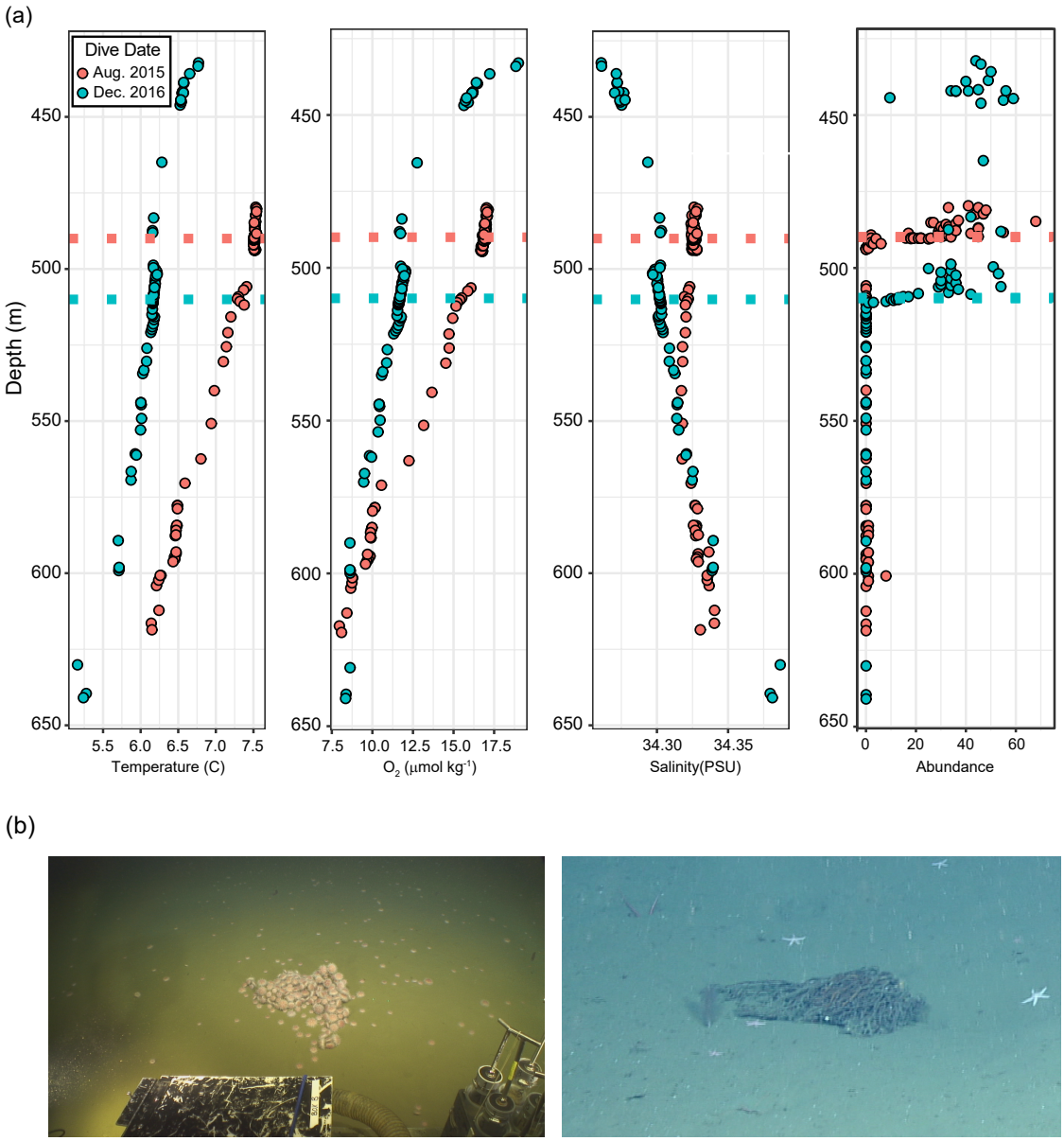

Figure 3.3. Abundance thresholds of *Strongylocentrotus fragilis* from two remotely operated vehicle (ROV) dives conducted on the San Diego slope. (a) Depth of *S. fragilis* observations as functions of water temperature (°C), dissolved oxygen (µmol kg^{-1}), salinity (PSU), and *S. fragilis* abundance determined during the ROV *Hercules* dive in August 2015 (red circles) and the ROV *Jason* dive in December 2016 (blue circles). Colored dotted lines indicate depths at which S. fragilis abundance dramatically increased. (b) All images were taken during the ROV Jason dive. Left: feeding aggregation of S. fragilis at 485 m was estimated to have an approximate density of 200 indiv. m^{-2}. Right: holdfast of *Macrocystis pyrifera* kelp at ~625 m unoccupied by *S. fragilis*.

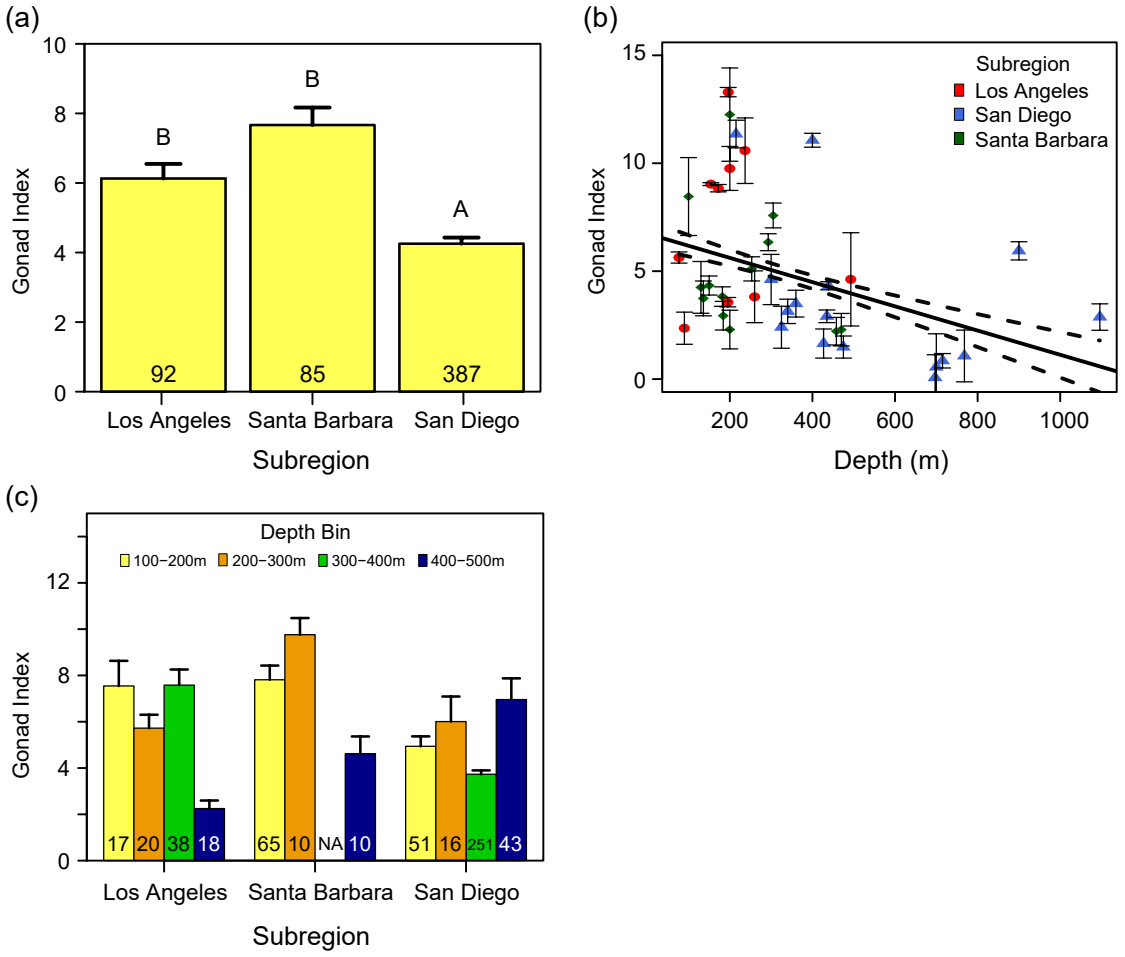

Figure 3.4. *Strongylocentrotus fragilis* gonad indices collected from Los Angeles, Santa Barbara, and San Diego subregions in the Southern California Bight. (a) Mean (+1 S.E.) gonad index from urchins collected in the upper 500 m. Letters indicate significant difference based on Dunn's test treated with a Bonferroni correction ($p < 0.05$). Numbers indicate replicate number of urchins dissected. (b) Relationship between gonad index (±1 S.E.) and depth in Los Angeles (red circles), San Diego (blue triangles), and Santa Barbara (green diamonds). Linear regression (solid line) and 95% confidence intervals (dashed lines) represents trend across all data. (c) Mean GI (+1 S.E.) separated into 100 m depth bins across subregions.

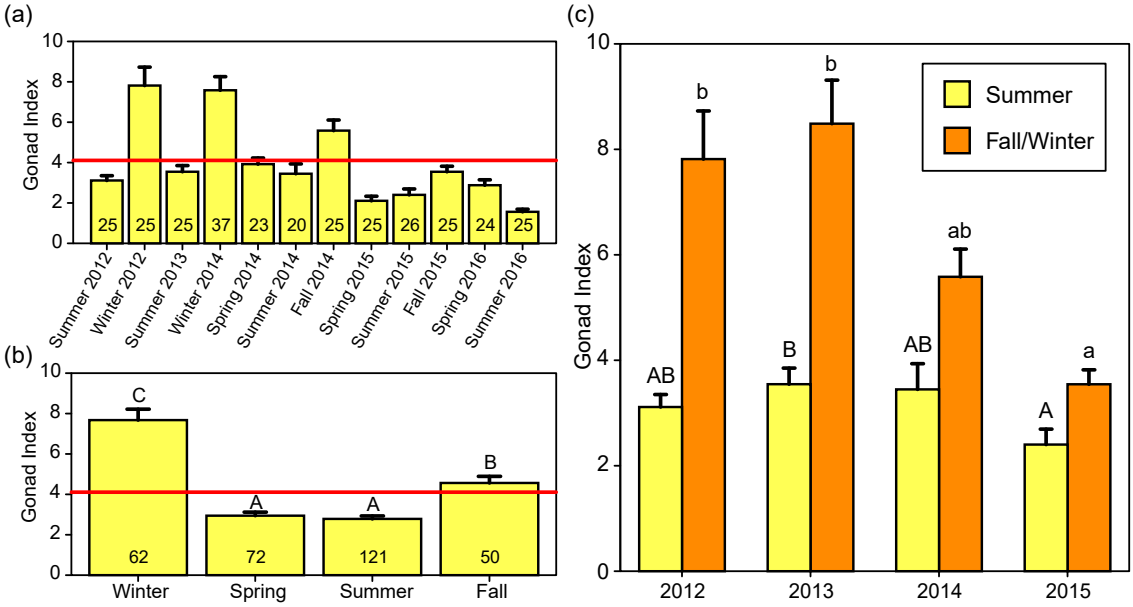

Figure 3.5. Gonad indices (GI) of *Strongylocentrotus fragilis* collected from a repeat trawl station at 340 m water depth near Point Loma, San Diego, CA. Red line indicates the dataset mean measured across 12 collections spanning 4.5 years. Letters represent significant differences ($p < 0.05$) as determined from *post hoc* Dunn's tests. (a) Seasonality of GI (+1 S.E.) from Winter 2012 to Summer 2016. (b) Seasonality of GI (+1 S.E.) pooled across years. (c) Comparison of GI between Summer and either Fall or Winter seasons across years to show the difference between seasons with relatively high and low GI.

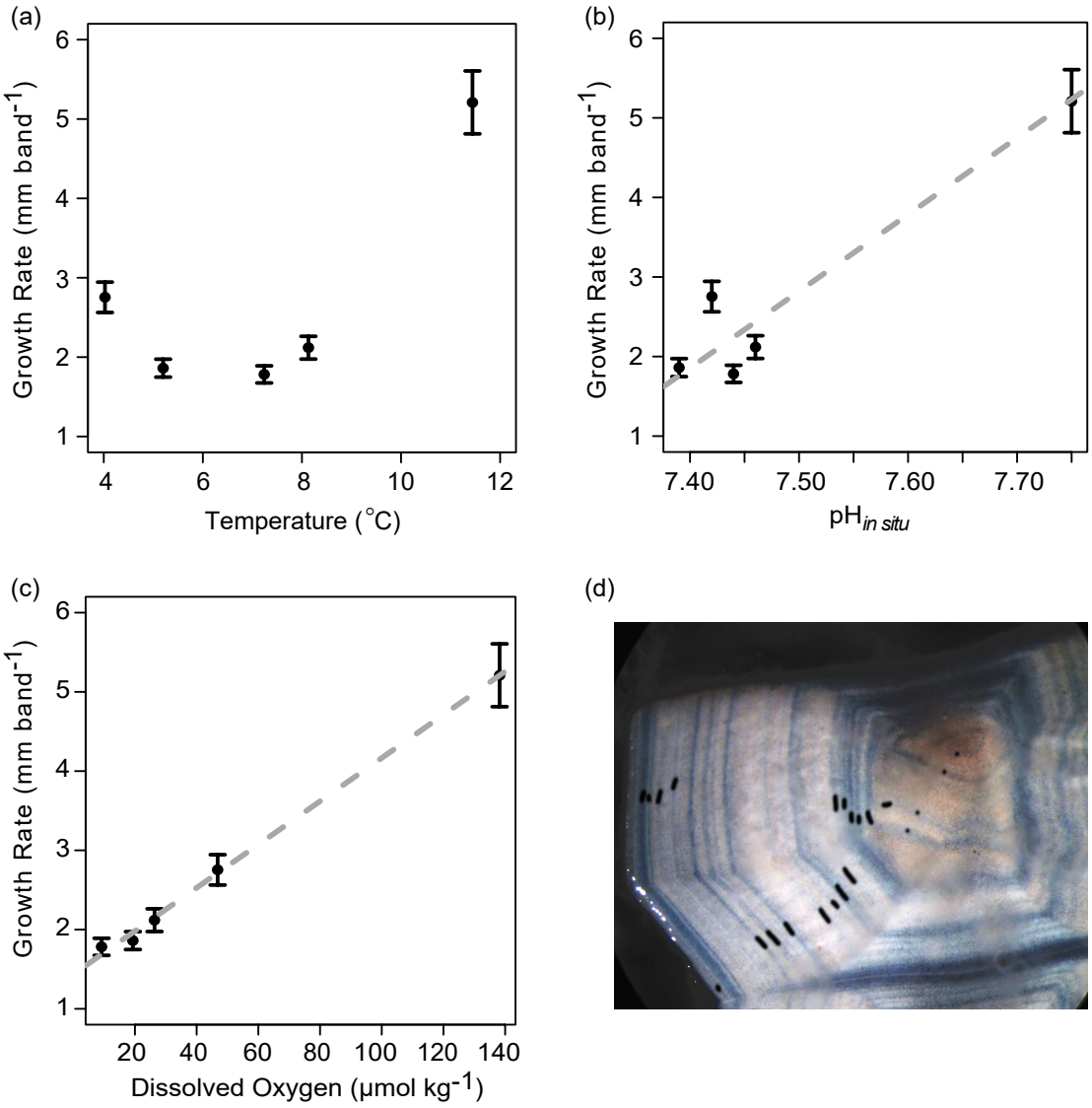

Figure 3.6. Mean growth rates of *Strongylocentrotus fragilis* (± 1 S.E.) as functions of (a) temperature (°C), (b) dissolved oxygen (µmol O_2 kg^{-1}), and (c) *in situ* pH. (d) Growth rates are presented as diameter length (mm) per growth band by counting the number of dark bands within treated interambulacral plate ossicles. Depths of each trawl and CTD cast are presented in Table 3.3. Gray dashed line indicates a significant correlation between growth rate and environmental variable (see text for details).

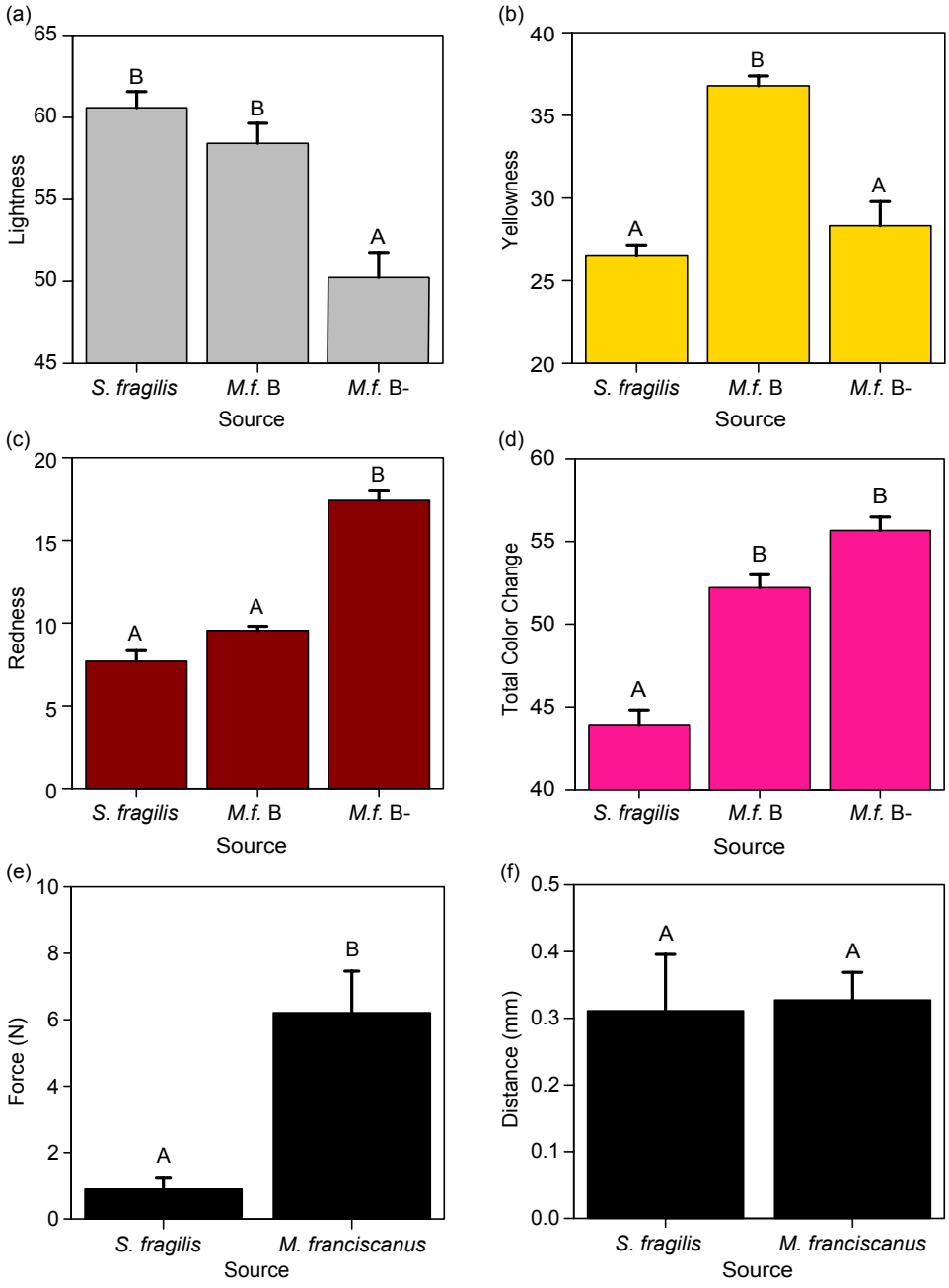

Figure 3.7. Mean (+1 S.E.) color and texture properties of individual gonad lobes from *Strongylocentrotus fragilis* and *Mesocentrotus franciscanus* (B and B-minus grade). (a) Lightness, (b) yellowness, (c) redness, and (d) total color change. Letters indicate significant differences among sources of gonads as indicated by Dunn's tests. (e) Mean peak hardness (+1 S.E.) and (f) resilience (+1 S.E.) of individual lobes from *S. fragilis* and *M. franciscanus* (B grade). Letters indicate significant differences between the two sources as the results of either a 1-way analysis of variance (peak hardness) or Kruskal-Wallis test (resilience).

CHAPTER 4

Microscale variability in geochemical, biomechanical, and structural properties in the pink fragile urchin, *Strongylocentrotus fragilis*, along natural environmental gradients

Abstract

Calcifiers in the ocean are among the taxa hypothesized to be most vulnerable to environmental changes associated with anthropogenic climate change. The presence of the pink fragile sea urchin, *Strongylocentrotus* (formerly *Allocentrotus*) *fragilis* (Jackson, 1912) along the shelf and slope in southern California motivated the examination of how geochemical, microstructural, and biomechanical properties vary with depth and natural gradients in temperature, salinity, oxygen, and pH. This study examines empirical relationships between size, potential reproductive fitness (gonad index), and various climate change parameters in the juvenile and adult stages of *S. fragilis*. Although *S. fragilis* may be mostly tolerant of future climatic change, observed increases in porosity and mean pore size coupled with decreases in mechanical hardness and stiffness of the calcitic endoskeleton structure in individuals collected from low pH_{Total} (7.57-7.59) and low dissolved oxygen (13-42 µmol kg^{-1}) environments suggest *S. fragilis* may be especially vulnerable to crushing predators under these conditions. Elemental composition determined using inductively coupled plasma-mass spectrometry (ICP-MS) indicates that *S. fragilis* has a skeleton composed of the low Mg-calcite mineral phase of calcium carbonate (mean Mg/Ca= 0.02 mol mol^{-1}) and appears to contain higher amounts of trace metals (Fe, Cd, Ni, Zn) than the surrounding seawater.

Introduction

> *"*[*Strongylocentrotus*] *fragilis*, thanks to its brightly colored test and whitish short spines, has been termed the most beautiful of the sea urchins. Perhaps because of the fragility of the almost paper-thin test and the depths at which this sea urchin lives there was no study of the species before that of Jackson in 1912…" A.R. Moore (1959).

Continental margin ecosystems along eastern boundary upwelling systems experience sharp natural gradients in temperature, salinity, dissolved oxygen (DO), and pH over short vertical distances (Figure 4.1; Feely *et al.* 2008, Levin and Sibuet 2012, Sperling *et al.*, 2016). These gradients originate from a combination of respiration of abundant sinking organic matter and reduced influence of oxygenated water masses (Gilly *et al.* 2013). These coupled oceanographic and biological processes produce a persistent and dynamic midwater Oxygen Minimum Zone (OMZ) with better oxygenated water masses that occur above and below (Nam *et al.* 2015). In the SCB, two intermediate water mass end-members converge to produce upwelled source water: the relatively cool, less saline, high-DO, high pH Pacific Subarctic Upper Water (PSUW) advected from the north and the relatively warm, salty, low-DO, low-pH Pacific Equatorial Water (PEW) advected from the south (Figure 4.1; Nam *et al.* 2015).

OMZs are defined as midwater areas where DO levels are < 22 µmol kg^{-1} (< 0.5 ml l^{-1}), although many species experience biological or distribution limitation at higher and lower oxygen values (Gilly *et al.* 2013, Somero *et al.* 2016). Above the OMZ is the Oxygen

Limited Zone (OLZ; 22-60 µmol kg^{-1}; Gilly *et al.* 2013). OMZ features (*e.g.*, thickness, boundary depths, seasonality, oxygen minima values) vary geographically (reviewed in Gallo and Levin, 2016) and are formed *via* natural processes as opposed to coastal hypoxia, which is primarily caused by eutrophication (Diaz and Rosenberg 2008, Breitburg *et al.* 2009). OMZs are highly dynamic over glacial-interglacial periods (Moffitt *et al.* 2015), but they appear to be expanding in tropical and subtropical regions in recent decades (Stramma *et al.* 2010, Schmidtko *et al.* 2017). In southern California, for example, the upper boundary (60 µmol kg^{-1}) of the OLZ has shoaled by as much at 100 m over the past 25 years (Bograd *et al.* 2008, 2015). This change coincides with an upslope expansion of deep-water sea urchin species, including the pink sea urchin, *Strongylocentrotus fragilis*, and an apparent habitat compression for a shallower urchin species, *Lytechinus pictus* (Sato *et al.* 2017). The pink urchin, *S. fragilis*, which is the dominant megafaunal species on the outer shelf (120-200 m) and upper slope (200-500 m) in southern California (Thompson *et al.* 1993, Sato *et al.* 2017, Walther *et al.* 2017), is also present in the OMZ core (~700 m) and in the Lower OMZ (LOMZ) where DO and pH increase down to basin depths (900-1,200 m) (Sumich and McCauley 1973, Taylor *et al.* 2014, Barry *et al.* 2014).

To better understand the evolutionary and ecological consequences of multiple climate change drivers in the ocean such as ocean acidification and deoxygenation, it is critical to characterize environmental effects on the variability of traits linked to fitness *in situ* within key species (*i.e.*, phenotypic buffering) (Reusch 2014, Sunday *et al.* 2014). According to life-history theory, the variability of key life-history traits, including organism body size, gonad index, and material and structural properties confer intraspecific fitness (Lack 1947, Smith and Fretwell 1974, Denny *et al.* 1985, Fabian and Flatt 2012).

This makes continental margin communities and species, like *S. fragilis*, excellent candidates to investigate patterns that coincide with concomitant drivers associated with anthropogenic climate change such as warming, ocean acidification (OA) and deoxygenation (Gruber 2011). The upper and lower boundaries of OMZs on upwelling margins exhibit strong vertical zonation of benthic communities, with rapid shifts in species composition occurring often in a threshold-like manner (Levin 2003, Gooday *et al.* 2010). Only recently has there been investigation of the interplay of temperature, oxygen and pH effects on benthos in these areas (Sperling *et al.* 2016). *S. fragilis* serves as a model species to evaluate how multiple climate change factors (*e.g.*, temperature, DO, and pH) potentially influence sublethal fitness traits on both macro- and microscale levels (Taylor *et al.* 2014).

Echinoid sea urchins are important benthic grazers (Pearse 2006) and deposit feeders (Lohrer *et al.* 2005). Biocalcification rates by echinoderms (*e.g.*, sea urchins, sea stars, brittle stars, crinoids) contribute significantly to calcium carbonate production on a global scale (Lebrato *et al.* 2010). Meta-analyses of experimental results suggest that multiple life-history stages of calcifying benthic megafaunal organisms will respond negatively to simulated OA conditions (Dupont *et al.* 2010, Kroeker *et al.* 2010, Dubois 2014). However, the vast majority of the studies used in these meta-analyses have been conducted on shallow-water species, and recent evidence suggests some species can acclimate to OA levels expected under "business-as-usual" fossil fuel emission scenarios (Hofmann *et al.* 2011, Dupont *et al.* 2013, Collard *et al.* 2014). Notably, some deep-water echinoderms distributed across the globe have been found to be surprisingly tolerant of

waters undersaturated with respect to the species-specific seawater mineral saturation state ($\Omega_{Mg\text{-}x} < 1$) (Lebrato *et al.* 2016).

There is compelling evidence that demonstrates how projected future changes in ocean temperature, carbonate chemistry, and DO may affect morphological function of calcified hard parts and fitness success. For example, weaker structures in intertidal mussel larvae (Gaylord *et al.* 2011), crustaceans (Taylor *et al.* 2015, deVries *et al.* 2016, Lowder *et al.* 2017), coccolithophorids (Ziveri *et al.* 2014), and sea urchins (Presser *et al.* 2010, Collard *et al.* 2016) could increase vulnerability to predation. Sea urchins produce ellipsoid-shaped, calcitic skeletal structures called tests, as well as calcitic spines, both of which provide the organism with a variety of critical functions such as protection against predators, sensing, locomotion, and feeding (Pearse 2006).

Compared to shallow-water urchin species, *S. fragilis* appears to have a more limited ability to regulate acid-base balance of its extracellular fluids in response to month-long exposure to decreased pH_{Total} (~7.2) levels, which were suggested to represent OMZ conditions in the "far future" (approx. 2300) (Taylor *et al.* 2014). In contrast, a temperate shallow urchin species (*Paracentrotus lividus*) was shown to regulate extracellular pH by compensating coelomic fluid acidosis with both bicarbonate and non-bicarbonate buffers (Collard *et al.* 2013, 2014) and exhibited no significant differences in the mechanical properties of its skeletal test after long-term exposure (12 months) to future pCO_2 scenarios (Collard *et al.* 2016). An improved understanding of the relationship between material properties (*e.g.*, hardness, stiffness) of *S. fragilis* skeletal tests and the environmental gradients they experience on the continental margin could provide valuable information

about *S. fragilis*' potential survival under climate change and its vulnerability to crushing predators (*e.g.*, crabs and fish).

Calcified sea urchin tests are typically composed primarily of calcite ($CaCO_3$) with significant amounts of incorporated magnesium (>4% $MgCO_3$), or Mg calcite. Organisms that produce high-Mg calcite (>12% $MgCO_3$), which is potentially the most soluble metastable form of $CaCO_3$ (Walter and Morse 1984), are likely to be among the organisms most vulnerable to future changes in the carbonate system linked to anthropogenic increases in atmospheric pCO_2 (Morse *et al.* 2006). While several datasets quantify % $MgCO_3$ in field-collected sea urchins (*e.g.*, Clarke and Wheeler 1917, Chave 1954, Kuklinski and Taylor 2009) and in controlled laboratory experiments (*e.g.*, Hermans *et al.* 2010, Lavigne *et al.* 2013), few studies attempt to link spatiotemporal patterns of Mg content with material properties of calcified hard parts in the context of physicochemical variables affected by climate change.

Some evidence suggests that Mg content is related to the hardness of biogenic structures (Ma *et al.* 2009, Long *et al.* 2014). The Aristotle's Lantern – a complex feeding apparatus made up of both organic and inorganic components – is constantly being used, worn down, and regrown in selected echinoids (Wang *et al.* 1997). Of the 35 skeletal elements controlled by 40 muscles in the Aristotle's Lantern (Candia Carnevali *et al.* 1993), the stone part of each tooth can be made up of the highest Mg-calcite content (40-45% $MgCO_3$; Wang *et al.* 1997), which results in a hard tooth and the taxon's evolutionary success (Candia Carnevali *et al.* 1993, Reich and Smith 2009, Ma *et al.* 2009, Frank *et al.* 2015). The test biomineral Mg composition of *S. fragilis*, a potential climate change-tolerant species, has yet to be determined.

In addition to Mg, numerous other co-precipitated elements are differentially incorporated into biotic calcitic structures such as phosphorous (P; *e.g.*, calcium phosphate) and strontium (Sr; *e.g.*, strontium calcite) (Mackenzie *et al.* 1983). Some trace metals, such as iron (Fe) and zinc (Zn), have been found in biomineralized structures (*e.g.*, iron oxides, zinc oxides), which enhance mechanical properties of the material and inspire the development of anthropogenic biomaterials (Meyers *et al.* 2008, Ağaoğullari *et al.* 2012, Naleway *et al.* 2016). Other elements have been used as paleoceanographic environmental proxies to help reconstruct past seawater conditions (Hönisch and Allen 2013, Janssen *et al.* 2014) or in ecology as environmental markers to model dispersal and population connectivity (Levin 2006, Fodrie *et al.* 2011). Elements such as Strontium (Sr), Cadmium (Cd), Manganese (Mn), Boron (B), and Uranium (U) have been used as environmental proxies for seawater temperature, dissolved oxygen, and pH (Table 4.1; Marchitto *et al.* 2000, Russell *et al.* 2004, Tribovillard *et al.* 2006, Walther and Limburg 2012, Limburg *et al.* 2015). However, the underlying mechanisms for linking the environmental exposure history of the organism to these elements are still under study (Levin *et al.* 2015). At the same time, some of the aforementioned heavy metals (*e.g.*, Zn, Ni, and Cd) are considered to be toxic to marine organisms at low concentrations (Fairbairn *et al.* 2011, Chiarelli and Roccheri 2014, Kanold *et al.* 2016).

To elucidate the elemental attributes of calcified structures that correlate with material hardness and stiffness of *S. fragilis*, we set out to investigate the question: How do skeletal traits (morphological, biomineral element composition, material properties and microstructure) of *S. fragilis* vary with physicochemical variables (temperature, salinity, DO, and pH) across the southern California OMZ? Our main objective was to measure

variability of *S. fragilis* across depth zones and their associated differences in temperature, salinity, DO, and pH, for 5 potential fitness traits: 1) size (test diameter), 2) gonad index, 3) biomineral element composition, 4) material properties, and 5) test microstructure. We hypothesized that *S. fragilis* in the Shelf zone would exhibit the highest mean size and gonad index, strongest skeletal tests, and lowest porosity compared to congeners in OLZ, OMZ, and LOMZ depth bins because the unfavorable environmental conditions (lower T, O_2, pH and food availability) should limit calcification, growth, and gonadal production.

Methods

Field Sampling

Strongylocentrotus fragilis individuals were collected from various depths between 77 m and 1116 m throughout the Southern California Bight (SCB) using depth-stratified otter trawls over a period of four years between July 2012 and July 2016. For elemental, biomechanical, and porosity analyses, a subset of urchins were selected from the following four depth zones, corresponding to the concomitant environmental variables (Table 4.2 and 4.3): continental shelf (Shelf), Oxygen limited zone (OLZ), Oxygen minimum zone (OMZ), and Lower oxygen minimum zone (LOMZ). Urchins were collected in collaboration with the Southern California Coastal Water Research Project's Bight '13 Trawl Survey (2013) and the National Oceanic and Atmospheric Administration (NOAA) West Coast Groundfish Bottom Trawl Survey (2014). Additionally, urchins were collected from trawls conducted by Scripps Institution of Oceanography (SIO) courses and student cruises in 2014-2016 on the R/V *Robert Gordon Sproul*, the R/V *New Horizon*, and the R/V *Melville*. During each trawl, the GPS coordinates and bottom depth of the trawl start

location were recorded (Appendix 4.1). Upon retrieval, *S. fragilis* urchins were frozen at -20 °C on board and transported back to the laboratory.

Hydrographic Data

Each trawl was assigned a single value for temperature, salinity, DO, and pH near or on the seafloor bottom (0-10 m from seafloor). Hydrographic data were obtained in one of three ways. (1) During the 2014 NOAA survey cruise, conductivity, temperature, depth, and dissolved oxygen sensors (CTD-O_2) (Sea-Bird Scientific, Bellevue, WA, USA) were directly attached to the trawl net. These recorded *in situ* temperature (°C), salinity (PSU), and DO (µmol kg^{-1}). (2) During the SIO cruises, CTD-O_2 casts (Sea-Bird Scientific, Bellevue, WA, USA) were conducted immediately before the trawls were deployed. (3) Historical CTD-O_2 data from quarterly hydrographic cruises conducted by the California Cooperative Oceanic Fisheries Investigations (CalCOFI) were obtained for the CalCOFI station, sampling date and depth nearest in space and time to the trawl providing urchins.

Data for the negative logarithmic of the total hydrogen ion concentration, pH_{Total}, were obtained in one of two ways. (1) In the San Diego subregion, samples were collected from discrete bottle samples taken at depths corresponding to urchin trawls aboard the R/V *Melville* during the student-led San Diego Coastal Expedition cruises in June/July and December 2012. Briefly, water samples were collected in Pyrex serum bottles following standard procedures (Dickson *et al.* 2007). Within 4 h of collection, pH was analyzed spectrophotometrically onboard at 20 °C using unpurified *m*-cresol purple as indicator dye. The pH data were highly accurate (1 s.d. = 0.02) and precise (±0.0015) when calibrated with certified reference materials (Takeshita *et al.* 2015). For further discussion, see Nam

et al. (2015), Takeshita *et al.* (2015), and Chapter 3. (2) For urchin collection sites in the Santa Barbara subregion, $pH_{Seawater}$ was calculated using an empirical relationship with temperature and dissolved oxygen concentration determined by Alin *et al.* (2012). $pH_{Seawater}$ values were converted to the pH_{Total} scale using the 'pHconv' function in the R package *seacarb*. All pH_{Total} values were corrected to reflect *in situ* conditions using the 'pHinsi' function with dissociation constants from Lueker *et al.* (2000) and Dickson (1990).

Laboratory Analyses

Size and Gonad Index

Frozen *Strongylocentrotus fragilis* urchins were thawed and rinsed clean in the laboratory prior to dissection. Spines were removed prior to measurement of the total length of the urchin test diameter (TLD) *via* calibrated dial calipers to the nearest 0.1 mm. Gonad measurement methodologies are reported in Chapter 3. Briefly, wet weights of gonads (5 lobes) were measured and reported as the weight percent of each individual drained of its internal fluids to the nearest 0.001 gram.

Biomineral Element Composition of Tests

For each urchin test, a maximum of 10 interambulacral ossicles located 3-4 plates from the apex were dissected and stored in glass vials tubes. Ossicles were transferred to a trace element clean room and placed in 5 mL plastic vials pre-washed with 10% nitric acid. They were then soaked in a clean solution of 15% Optima grade hydrogen peroxide (Fisher Chemical) buffered with 0.05 M Suprapur sodium hydroxide (EMD Chemicals) for

approximately 24 hours to remove organic tissue, rinsed in ultrapure water three times, and set to dry under a Class-100 laminar flow hood for approximately 48 hours. Between 1-5 ossicles were weighed (4-15 mg total weight) and placed in Teflon vials for digestion with 1 ml of concentrated Teflon-distilled (TD) nitric acid (14.7 M HNO_3) on a hotplate at 100 °C for >24 h. Digested samples were dried down, re-acidified with 0.5 mL TD HNO_3, doped with a 1 ppm indium solution (to monitor instrumental drift), and diluted with 3 mL of ultrapure water to achieve a dilution factor of 250x. Samples were again diluted to achieve a final dilution factor of 8,000x prior to analysis using a *ThermoScientific iCAPq*c inductively coupled plasma-mass spectrometer (ICP-MS; Thermo Fisher Scientific GmbH, Bremen, Germany), in standard mode. Masses of each element and Calcium (Ca) were measured for 30 ratios, resulting in internal precision of <2% (2 s.d.). Elements were corrected for total mole fraction. Total procedural blanks were made during the acidification process and represented <3% of the measurement for all elements. Raw data were corrected off line for instrument background and drift. Samples were bracketed by internal standards of crab carapace (n = 4), which allowed for calculation of absolute values. The crab standards yielded external precision of better than 2% for each element, including Ca (2 s.d.).

Biomechanical Properties

Hardness and stiffness (*i.e.*, elastic modulus) of each test plate ossicle were measured using a nanoindentation materials testing machine (Nano Hardness Tester, Nanovea, Irvine, CA, USA) equipped with a 200-µm diameter spherical tip. Surfaces were smoothed using ultra fine sandpaper (P6000) and then rinsed with MilliQ water and dried

under a hood. Flattened ossicles were mounted with super glue onto a steel block (Figure 4.2). Indentations were performed by penetrating into each ossicle with a load of 30 mN, and loading and unloading rates of 60 mN min^{-1}. A total of 3-5 indents were made on 1-2 ossicles from each individual (n = 8-15 indiv. depth $zone^{-1}$).

Porosity Analyses

Additional ossicles (also 3-4 interambulacral plates away from the apex) from the same individual were sliced vertically across the plate using a razor blade, cleaned using a brush under a microscope, mounted vertically on the tip to reveal a cross-section (Figure 4.3), and secured with adhesive tape to direct electrical current. Samples were coated with iridium for 15 seconds using a deposition current of 85 mA in an Emitech sputter coater (K575X). Images of urchin plate cross-sections were haphazardly obtained at 300x-400x magnification using a FEI XL-30 SFEG Scanning Electron Microscope (SEM) set to an accelerating potential of 5 kV to achieve a resolution of 2.5 nm. SEM micrographs were analyzed for porosity (%) by calculating the ratio of pore area to total area of the micrograph using ImageJ (Figure 4.3; Schneider *et al.*, 2012). The color threshold for each 2-D SEM micrograph was adjusted using either a mixed or traditional segmentation algorithm in the DiameterJ Segmentation plugin (Hotaling *et al.* 2015). For each micrograph (3 per plate), the output result that best fit the original was manually determined from 16 possible black and white images. The outlines of segments or pores (pore size area: 0-infinity μm^2) were determined automatically, and the area (μm^2) of each pore was calculated (Figure 4.3). Outlined areas were visually inspected for detection errors and manually traced using the polygon tool if needed. The mean 2-D porosity for each ossicle

(*i.e.*, individual urchin), and the mean porosity and variance for each zone (n = 5 indiv. urchins per depth zone) were calculated.

High-resolution micro-computed tomography (HR-μCT) was used to explore the spatial variability of porosity within individual ossicles and to obtain more accurate estimations of three-dimensional porosity. One ossicle plate from 333 m and 1116 m were selected to represent a broad range in physicochemical environments, embedded in epoxy, scanned with an isotropic voxel size of 400 nm at a 40 kV acceleration voltage. The rotation angle and tilt increment were set at 360° and 0.2°, respectively, using a MicroXCT-200 scanner (Xradia, Pleasanton, CA) at the National Center for Microscopy and Imaging Research facility (University of California, San Diego). Each scan was selected for visualization using Amira software (FEI Visualization Sciences Group, Burlington, MA). Distribution of surface porosity was visualized by creating volume renderings of each ossicle by adjusting the threshold range limits (*i.e.*, average range threshold limits and upper range (low porosity) threshold limits). To quantify 3-D porosity for each sample, a 200-μm sided box was haphazardly placed inside the initial scan file, additional volume renderings were created, and the percent porosity was calculated from Material Statistics outputs.

Statistical Analyses

To examine the environmental relationships (*e.g.*, depth, temperature, salinity, DO, pH_{Total}) and zonal effects (*e.g.*, Shelf, OLZ, OMZ, and LOMZ) on size, gonad index, single element concentrations, hardness, stiffness, and porosity, the data were tested for normality using the Shapiro-Wilk test and homogeneity of variances using the Breusch–Pagan test.

In each univariate analysis, where assumptions of normality and homoscedasticity were met, parametric tests such as linear regression with hydrographic variables as explanatory factors or one-factor analysis of variance with depth zone as a factor were employed. If the data violated these assumptions, the Box-Cox power transformation in R was used to correct the data. If the transformation did not improve normality or homoscedasticity of the data, then non-parametric tests were used.

Non-metric multidimensional scaling (NMDS) ordinations were employed to evaluate the multi-elemental biomineral composition patterns among urchins collected from different depth zones, sites, and regions. Urchin samples were organized and analyzed based on their origin of collection: subregion (*e.g.*, Santa Barbara, San Diego), trawl site, and the four depth- and oxygen-related zones (*e.g.*, Shelf, OLZ, OMZ, and LOMZ). Mole fraction ratios of element to calcium were converted to mmol mol^{-1} or µmol mol^{-1} (for standardization purposes) and square-root transformed prior to Bray-Curtis distance similarity matrix calculation using the *vegan* package (v. 2.4-2) in R (Oksanen *et al.* 2017). Elements and hydrographic variables were tested for ordination significance based on a permutation test with 999 iterations using the function 'envfit' (*vegan* package) with equally weighted 'sites' (*i.e.*, indiv. urchins). Vectors of variables with a significance of $p < 0.05$ were scaled relative to their correlation coefficient and plotted onto the 2-D ordination space. Analysis of similarities (ANOSIM) was employed to determine whether elemental composition differed across subregion, trawl site, and depth zone.

Results

Size and Gonad Index

Strongylocentrotus fragilis total length of the diameter (TLD) ranged from 22.3-88.1 mm (Table 4.2; n = 656 indiv.; 58 sites). Mean TLD was negatively related to depth (Figure 4.5A; Linear Regression: $r^2 = 0.17$, $p = 0.011$), DO (Figure 4.5B; $r^2 = 0.17$, $p = 0.016$), temperature (Figure 4.5C; $r^2 = 0.17$, $p = 0.040$), and pH (Figure 4.5D; $r^2 = 0.14$, $p = 0.004$). TLD was significantly different between Shelf, OLZ, and OMZ (Figure 4.5E; Kruskal-Wallis: $\chi^2 = 111.11$, $p < 0.001$), but not OLZ and LOMZ. The mean TLD of *S. fragilis* in the Shelf zone was 24% greater than in the OLZ, 32% greater than in the OMZ, and 17% greater than in the LOMZ (Dunn's test: $p \leq 0.001$). On average, *S. fragilis* TLD in the OMZ were 6% smaller than in the OLZ and 11% smaller than in the LOMZ ($p < 0.05$).

Mean gonad index (GI) of *S. fragilis* was negatively related to depth (Figure 4.6A; Linear Regression: $p = 0.002$, $r^2 = 0.25$), DO (Figure 4.6B; $p = 0.015$, $r^2 = 0.12$), temperature (Figure 4.6C; $p = 0.04$, $r^2 = 0.09$), pH (Figure 4.6D; $p = 0.039$, $r^2 = 0.07$), and was significantly different among depth zones (Figure 4.6E; Kruskal-Wallis: $\chi^2 = 107.35$, $p < 0.001$). Mean GI in the Shelf zone was 37% greater than in the OLZ, 256% greater than in the OMZ, and 58% greater than in the LOMZ (Dunn's test: $p \leq 0.001$). Mean GI in the OMZ was 61% lower than in the OLZ and 55% lower than in the LOMZ (Dunn's test: $p \leq 0.006$). There was no significant difference in mean GI between the OLZ and the LOMZ (Dunn's test: $p = 0.12$). The square-root transform of gonad index exhibited a positive linear relationship to TLD (Linear Regression: $r^2 = 0.33$, $p < 0.001$), but also demonstrated a logistic growth curve (Figure 4.6F).

Biomineral Element Composition

For a total of 70 out of 103 samples, each element was detected without being flagged for having more than 2% internal precision. Sr/Ca in *S. fragilis* calcified test plates was positively related to temperature (Figure 4.7A; Linear Regression: $r^2 = 0.34$, $p = 0.028$) and DO (Figure 4.7B; Linear Regression: $r^2 = 0.41$, $p = 0.014$), but not salinity, pH or depth. Magnesium to calcium ratios (mol mol Ca^{-1}) of all *S. fragilis* were < 0.025 (Table 4.3). Magnesium was positively related to temperature (Figure 4.7C; Linear Regression: $r^2 = 0.39$, $p = 0.018$) and negatively related to salinity (Figure 4.7D; Linear Regression: $r^2 = 0.46$, $p = 0.018$), but there was no relationship with dissolved oxygen, pH, or depth. There were no significant relationships of the remaining element to Ca ratios (Fe, Zn, Ni, Cd, U, and P) with any environmental variables. Mean molar ratios (± 1 s.e.) of all elements to Ca are shown in Table 4.3.

NMDS ordination analysis resulted in significant correlations of multiple elements within the 2-D ordination space (Figure 4.8; 2D stress = 0.11). ANOSIM results of element to calcium ratios revealed significant differences in elemental composition across depth-related zones (Figure 4.8A-D; ANOSIM: $R^2 = 0.19$, $p = 0.001$), trawl sites (Figure 4.8E; $R^2 = 0.32$, $p = 0.001$), and Santa Barbara and San Diego subregions (Figure 4.8F; $R^2 = 0.28$, $p = 0.001$). Positive element-loading vector lengths and directions with respect to NMDS axis-1 indicate that zonal differences were driven primarily by Mg, cadmium (Cd), phosphorous (P), and uranium (U). A significant difference between the elemental composition of *S. fragilis* originating from Santa Barbara and San Diego was also suggested (Figure 4.11F). Zinc (Zn) appeared to be the primary driver explaining this difference (NMDS axis-2), with San Diego urchins incorporating 93% more Zn (Mean =

12.54 nmol mol Ca^{-1}) into their tests than Santa Barbara urchins on average (Welch's t-test: $t_{49} = -4.01$, $p < 0.001$).

There were significant relationships between the concentrations in *S. fragilis* tests and seawater of two metals, Fe and Cd (Figure 4.9). We found increases in the Fe concentration in *S. fragilis* tests in response to increasing concentrations in seawater (Figure 4.9H; $r^2 = 0.99$; $p < 0.001$), and decreases in the Cd concentration in *S. fragilis* tests in response to increasing Cd concentrations in seawater (Figure 4.9G; $r^2 = 0.99$; $p < 0.001$). Although similar positive (Mg, U, Ni) and negative (Sr, P, Zn) trends were observed in other elements, these relationships were not significant (Linear Regression: $p > 0.05$).

Using seawater Element/Ca ratios from published datasets collected from coastal ocean sites (Biller and Bruland 2013), the partition coefficients for each element (E) in urchin tests were calculated according to $D_E = (E/Ca)_{urchins}/ (E/Ca)_{seawater}$. The D_E was > 1 for Ni, Zn, Cd and Fe, and < 1 for Mg, Sr, P and U (Figure 4.10). For elements with D_E > 1, D_E was highest in *S. fragilis* from the Shelf and lowest in urchins from the OMZ.

Mechanical Properties

Strongylocentrotus fragilis skeletal test plates from the Shelf zone were approximately 188% harder than those in the OMZ and 110% harder than those collected from the OLZ and the LOMZ (Figure 4.11A; 1-way ANOVA: $F_{3,42} = 11.22$, $p < 0.001$; Tukey HSD: $p \leq 0.005$). Mean hardness of OMZ urchin plates was 32% lower than those from the LOMZ, but this was not statistically significant (Figure 4.11A; Tukey HSD: $p > 0.05$).

Mean stiffness (*i.e.*, elastic modulus) of *S. fragilis* test plates were square-root transformed, and significant differences were found among depth zones (1-way ANOVA: $F_{3,42} = 17.78$, $p < 0.001$). Mean stiffness of the plates from Shelf zone urchins was between 140-280% greater than that of plates of urchins from the other three depth zones (Figure 4.11B; Tukey HSD: $p < 0.001$).

Porosity

Two-dimensional porosity (% pore area) of cross sections of *Strongylocentrotus fragilis* test plates ranged from 36% in samples collected from the Shelf to >45% in LOMZ samples (Table 4.3) and differed significantly across depth zones based on 1-way analysis of variance (Figure 4.11C; 1-way ANOVA: $F_{3, 15} = 9.143$, $p = 0.001$). Mean 2-D porosity of Shelf urchin test plates was 19% lower than OMZ urchin test plates (Tukey HSD: $p = 0.004$) and 22% lower than LOMZ urchin ossicles ($p = 0.001$). Consistent with the change in porosity, the mean pore size was significantly different across depth zones (Figure 4.11D; 1-way ANOVA: $F_{3, 15} = 9.542$, $p < 0.001$). Mean pore size in the LOMZ was almost double the per pore area of the Shelf urchins (Tukey HSD: $p < 0.001$).

Analysis of HR-µCT scans for 3-D assessment revealed significant variability in porosity across the outer surface of *S. fragilis* ossicles and within the sponge-like stereom of the ossicle (Figure 4.12). However, 3-D porosity analysis from 200-µm-sided volume renderings of both urchins from 333 m and 1116 m exhibited ~80% pore space compared to the 2-D porosity estimates of 35-45% (Figure 4.11D).

2-D Ordination Space

NMDS ordination analysis resulted in significant correlations of multiple elements and mechanical response variables within the 2-D ordination space (Figure 4.13; 2-D stress = 0.08). Magnesium does not appear to influence nanohardness as originally hypothesized (Long *et al.* 2014). Instead, Sr/Ca and Ni/Ca appear to positively correlate with *S. fragilis* test hardness and stiffness, although this does not imply cause. Cd/Ca appeared to negatively correlate with test hardness and stiffness. U/Ca appeared to be positively correlated with pore size and total porosity within the test structure. The elements P, B, Ba, and Mn were not included in the NMDS analysis due to flagged data with more than 2% internal precision.

Discussion

Sea urchins are generally thought to be vulnerable to secular chemical changes in marine systems associated with the acidification, and presumed deoxygenation, of intermediate waters (Dupont *et al.* 2010, Kroeker *et al.* 2010, Kurihara *et al.* 2013). The observed shoaling of low oxygen zones coupled with predicted acidification and undersaturation of subsurface waters with respect to distinct mineral phases of calcium carbonate (Gruber *et al.* 2012, Bograd *et al.* 2015) present the impetus to better understand the functional implications of multiple climate drivers on key taxa in southern California.

Some sea urchins, not all (Presser *et al.* 2010), produce skeletal tests composed of high-magnesium calcite (Chave 1954, Andersson *et al.* 2008, Lavigne *et al.* 2013, Lebrato *et al.* 2016), a mineral phase of calcium carbonate that is more soluble than low-Mg calcite. ICP-MS analysis of *S. fragilis* skeletal test plates collected across all sites spanning

multiple environmental gradients revealed surprisingly low mean (±1 s.e.) concentrations of Mg (0.01918 ± 0.0012 mol mol Ca^{-1}), which suggests that *S. fragilis* skeletal tests have the lowest Mg calcite among all other documented sea urchin species collected from kinetically unfavorable conditions (Lebrato *et al.* 2016). Calcite with lower amounts of Mg is less soluble than other common biogenic mineral phases of calcium carbonate such as aragonite, which is deposited by corals (Andersson and Mackenzie 2012) and pteropods (Bednaršek *et al.* 2016). These results support previous conclusions about *S. fragilis* tolerance to carbonate-undersaturated waters in the southern CA OMZ (Sato *et al.* 2017), but further analyses are required on whole individuals, spines, and life-history stages to fully characterize the variability of Mg incorporation by *S. fragilis* (Lavigne *et al.* 2013).

Despite such small variation in Mg (s.d. = 0.5%), we detected positive relationships of Mg in *S. fragilis* with temperature and salinity (Figure 4.8C, D) and of Sr content with temperature and oxygen (Figure 4.8A, B). These relationships are consistent with results of previous studies on echinoid urchins and other calcifying taxa (Chave 1954, Moberly 1968, Mackenzie *et al.* 1983, Levin *et al.* 2015, Williams *et al.* 2017). The positive linear relationship between Sr content and dissolved oxygen (Figure 4.8A) is also consistent with the linear relationship between growth rate and oxygen content described in Chapter 3 (Figure 3.6; Hermans *et al.* 2010). The important influences of relative growth rates and other biologically mediated vital effects on Mg and Sr incorporation during skeletogenesis confound the utilization of environmental proxy development in *S. fragilis* (Chave 1954, Weiner and Dove 2003). However, our ability to detect linear trends of small variations in Mg/Ca and Sr/Ca over a broad spatial range and environmental conditions combined with trace metal incorporation warrants further hypothesis testing under controlled laboratory

conditions. Calcification mechanisms in echinoids and other calcifiers are poorly understood (but see Politi *et al.*, 2004 and Von Euw *et al.*, 2017), and the validity of proxy development using calcitic *S. fragilis* tests depends on the extent to which *S. fragilis* controls calcification biologically.

While the focus of this chapter has been on *S. fragilis* phenotypic change among depth zones (and associated climate drivers), there are likely to be regional differences in morphology, gonad production, and microscale and geochemical traits due to differences in environmental variability and kelp production. A significant separation of clusters based on subregion (Santa Barbara and San Diego) and trawl sites suggests that the elemental composition of *S. fragilis* skeletal test could be influenced by water mass properties associated with different physicochemical variables or food availability (Figure 4.8A-D). In addition, significant dissimilarity among trawl sites within the same depth zone suggests that movement of adult *S. fragilis* among trawl sites within different depth zones may be limited (Figure 4.8E). Although Zn was shown to be 93% higher in urchins from San Diego than in those from Santa Barbara, Zn was not correlated with variation of any of the mechanical and structural response variables (Figure 4.13).

Food availability likely plays an important role in the trait differences seen in *S. fragilis* from the Shelf compared to other zones. A subtropical urchin species, *Hemicentrotus pulcherrimus*, exposed to elevated pCO_2 (1000 µatm) for 16 days exhibited an initial suppression of food intake and a subsequent delay in gonad production and reproductive phenology after longer-term exposure to elevated CO_2 conditions (Kurihara *et al.* 2013). Since no effect was found on growth rate or respiration rate, the authors suggest the reduced feeding could negatively affect the quality of *H. pulcherrimus* eggs

(egg size and nutrient content). Although we did not investigate the quality of *S. fragilis* eggs, it is quite likely that OMZ urchins received less food input in the form of allochthonous kelp than those in the Shelf zone, as reflected by their smaller size and lower gonad index.

The observed increases in 2-D porosity and mean pore size seen at OLZ, OMZ, and LOMZ depths relative to conspecifics from Shelf depths (Figure 4.11C, D) are consistent with the hypothesis that sublethal tradeoffs between form and function may occur under energetically stressful conditions (Todgham and Hofmann 2009, Byrne *et al.* 2014). While a 3-D correction needs to be applied to SEM images, higher 2-D porosity and larger pore sizes in the OLZ, OMZ, and LOMZ compared to those at Shelf depths suggest these properties may be negatively correlated with growth rate. Alternatively, the critical proteins, glycoproteins, and polysaccharides responsible for biomineral crystal nucleation may be in higher demand within the organic matrix that fills the pores during *S. fragilis* skeletogenesis at deeper depths (Hermans *et al.* 2010, Addadi and Weiner 2014). Comparative analysis between proteomes of *S. fragilis* and the shallow-water congener, *S. purpuratus* by Oliver *et al.* (2010) concluded that genes responsible for skeletal development and sulfur metabolism (*e.g.*, carbohydrate sulfotransferases) are more strongly selected for in *S. fragilis* relative to *S. purpuratus*. The greater demand to produce precursor macromolecules for skeletogenesis coupled with extracellular acid-base regulation of internal fluids (Taylor *et al.* 2014) are both likely to be energetically costly at deeper depths (Mann *et al.* 2008, Oliver *et al.* 2010). *S. fragilis* may respond to unfavorable future acidification and deoxygenation by either shrinking in size (Figure 4.5E), as seen in

other animals (Piersma and Drent 2003), including *S. purpuratus* (Ebert 1967, 1968), by limiting gonad production (Figure 4.6), or by growing slower (*sensu* Chapter 3).

Partition coefficients (D_E) greater than 1 (Ni/Ca, Zn/Ca, Cd/Ca, and Fe/Ca) could suggest that *S. fragilis* may actively control the incorporation of these trace metals into the test (Figure 4.10). Alternatively, *S. fragilis* may actively remove these elements from the test organic matrix to avoid the potential lethal effects of toxic dissolved metal ions (*e.g.*, Zn^{2+} and $CdCl^{+}$), which have been demonstrated in other urchin species (Fairbairn *et al.* 2011, Chiarelli and Roccheri 2014). For these trace metals, higher partition coefficients in urchins from the Shelf relative to those in deeper depth bins may also suggest a decrease in the efficiency of elemental uptake during calcification in unfavorable conditions (Figure 4.10). However, the lower partition coefficients in OLZ and OMZ depth bins may support an alternative non-biological uptake hypothesis that foreign ions precipitate inorganically from the calcification fluid as a result of variable growth rates and by extension, calcification rates (Lavigne *et al.* 2013).

Although the D_{Metal} in *S. fragilis* appears to be exceptionally high for several elements (Figure 4.10), it is likely that the seawater concentration of these metals is significantly higher in the benthic boundary layer where urchins live relative to the adjacent water column (Biller and Bruland 2013). The higher concentrations of Fe and other scavenged elements (*e.g.*, Mn, Co, Cu) in the benthic boundary layer found by Biller and Bruland (2013) could influence these partition coefficient results, and needs to be investigated in more detail. This knowledge gap about the microenvironment in which the soft-sediment urchins grow limits our ability to fully understand how vital effects control incorporation of trace metals into *S. fragilis* tests.

The opposing directions of the relationships between $E/Ca_{calcite}$ and E/Ca_{SW} in Cd and Fe (Figures 4.11G and H) raise hypotheses about potential reasons why *S. fragilis* differentially incorporates these trace metals into the skeletal test (Milton and Chenery 2001). Although the negative correlation between material properties of *S. fragilis* tests and $Cd/Ca_{calcite}$ (Figure 4.12) suggests that Cd could have a direct or indirect effect on the hardness and stiffness of the skeletal calcite, further study is required to test this hypothesis. *S. fragilis* calcite from Shelf urchins on average, exhibit approximately 100% more Cd than OMZ urchins and ~30% more Cd than OLZ urchins (Table 4.3), but the direct correlation between Cd and material properties was not determined. The tight coupling between dissolved Cd and the nutrient, PO_4^{3-}, is well known in well-oxygenated waters (> 75 µmol kg^{-1}), but this coupling breaks down in oxygen-deprived zones (< 75 µmol kg^{-1}) because Cd sulfide (CdS) precipitates where sulfide is present, especially in OLZ and OMZ sediments (Janssen *et al.* 2014). Although sulfur was not measured in the urchin calcite, *S. fragilis* is capable of metabolizing sulfur as demonstrated by strong gene selection for carbohydrate sulfotransferase (Oliver *et al.* 2010). This suggests a potential mechanism in need of further study to better understand the linkages between higher porosity, softer tests, smaller test size, and lower gonad production and low oxygen/low pH zones.

Our results suggest *S. fragilis* may be more vulnerable to the future upslope expansion of OMZs and calcium carbonate undersaturated waters than previously thought. Higher porosity, larger pore sizes, and softer, weaker skeletal tests found in persistently low pH (pH_{Total} (7.57-7.59) and low dissolved oxygen (13-42 µmol kg^{-1}) zones could make *S. fragilis* more vulnerable to crushing predators. It is possible that maintenance of low Mg-calcite (0.02 mol mol^{-1}) and calcification in the OLZ, OMZ, and LOMZ, occurs at the

expense of other fitness-related traits such as size, reproductive potential, and growth. Although temperature and pressure could be important parameters that affect shelf and slope animal traits like growth rates and respiration, the linear correlations of oxygen and pH with several *S. fragilis* characteristics (growth, size, gonad index, hardness, stiffness) suggest oxygen and pH are likely major drivers affecting this species.

Acknowledgements

We thank NOAA, SCCWRP, UC Ship Funds, and CCE-LTER for the ship time necessary to conduct field work and Andrew Mehring for constructive conversations. We are grateful to the various crew and volunteers who helped KNS collect urchins, especially Phil Zerofski and Natalya Gallo. Katy Kelsoe, Stephanie Luong, Marissa Mangelli, Jackson Powell, and Ximena Trujillo assisted in the laboratory. We especially thank Daniel Jio, Michael Frank, and Jae-Yung Jung for their assistance in preparing and imaging urchin samples. Funding was provided by the Tegner Fellowship and Sussman Fellowship to KNS. Funding to Lisa A. Levin and KNS was provided by National Oceanic and Atmospheric Administration (NOAA) Grant No. NA14OAR4170075, California Sea Grant College Program Project No. R/SSFS-02 through NOAA's National Sea Grant College Program, U.S. Department of Commerce. The statements, findings, conclusions and recommendations are those of the authors and do not necessarily reflect the views of California Sea Grant or NOAA.

Chapter 4, in part, is currently being prepared for submission for publication of the material. Sato, Kirk N.; Day, James M. D.; Taylor, Jennifer R. A.; Andersson, Andreas J.; Frank, Michael; Jung, Jae-Young; McKittrick, Joanna; Levin, Lisa A. The dissertation author was the primary investigator and author of this material.

References

Addadi, L., and S. Weiner. 2014. Biomineralization: mineral formation by organisms. Physica Scripta 89:98003.

Ağaoğullari, D., D. Kel, H. Gökçe, I. Duman, M. L. Öveçoglu, A. T. Akarsubaşi, D. Bilgic, and F. N. Oktard. 2012. Bioceramic Production from Sea Urchins. Acta Physica Polonica, A 121:23–26.

Alin, S. R., R. A. Feely, A. G. Dickson, J. M. Hernández-Ayón, L. W. Juranek, M. D. Ohman, and R. Goericke. 2012. Robust empirical relationships for estimating the carbonate system in the southern California Current System and application to CalCOFI hydrographic cruise data (2005-2011). Journal of Geophysical Research: Oceans 117:C05033.

Andersson, A. J., and F. T. Mackenzie. 2012. Revisiting four scientific debates in ocean acidification research. Biogeosciences 9:893–905.

Andersson, A. J., F. T. Mackenzie, and N. R. Bates. 2008. Life on the margin: Implications of ocean acidification on Mg-calcite, high latitude and cold-water marine calcifiers. Marine Ecology Progress Series 373:265–273.

Barry, J. P., C. Lovera, K. R. Buck, E. T. Peltzer, J. R. Taylor, P. Walz, P. J. Whaling, and P. G. Brewer. 2014. Use of a Free Ocean CO_2 Enrichment (FOCE) System to Evaluate the Effects of Ocean Acidification on the Foraging Behavior of a Deep-Sea Urchin. Environmental Science & Technology 48:9890–9897.

Bednaršek, N., C. J. Harvey, I. C. Kaplan, R. A. Feely, and J. Možina. 2016. Pteropods on the edge: Cumulative effects of ocean acidification, warming, and deoxygenation. Progress in Oceanography 145:1–24.

Biller, D. V., and K. W. Bruland. 2013. Sources and distributions of Mn, Fe, Co, Ni, Cu, Zn, and Cd relative to macronutrients along the central California coast during the spring and summer upwelling season. Marine Chemistry 155:50–70.

Bograd, S. J., M. P. Buil, E. Di Lorenzo, C. G. Castro, I. D. Schroeder, C. R. Anderson, C. Benitez-Nelson, and F. A. Whitney. 2015. Changes in source waters to the Southern California Bight. Deep Sea Research Part II: Topical Studies in Oceanography 112:42–52.

Bograd, S. J., C. G. Castro, E. Di Lorenzo, D. M. Palacios, H. Bailey, W. Gilly, and F. P. Chavez. 2008. Oxygen declines and the shoaling of the hypoxic boundary in the California Current. Geophysical Research Letters 35:L12607.

Breitburg, D. L., D. W. Hondorp, L. A. Davias, and R. J. Diaz. 2009. Hypoxia, Nitrogen,

and Fisheries: Integrating Effects Across Local and Global Landscapes. Annual Review of Marine Science 1:329–349.

Byrne, M., A. M. Smith, S. West, M. Collard, P. Dubois, A. Graba-Landry, and S. A. Dworjanyn. 2014. Warming influences Mg^{2+} content, while warming and acidification influence calcification and test strength of a sea urchin. Environmental Science and Technology 48:12620–12627.

Candia Carnevali, M. D., I. C. Wilkie, E. Lucca, F. Andrietti, and G. Melone. 1993. The Aristotle's lantern of the sea-urchin *Stylocidaris affinis* (Echinoida, Cidaridae): functional morphology of the musculo-skeletal system. Zoomorphology 113:173–189.

Chave, K. E. 1954. Aspects of the Biogeochemistry of magnesium, 1. Calcareous marine organisms. Journal of Geology 62:266–283.

Chiarelli, R., and M. C. Roccheri. 2014. Marine Invertebrates as Bioindicators of Heavy Metal Pollution. Open Journal of Metal 4:93–106.

Clarke, F. W., and W. D. Wheeler. 1917. The inorganic constituents of marine constituents of marine invertebrates. U.S. Geological Survey 102:56 pp.

Collard, M., A. Dery, F. Dehairs, and P. Dubois. 2014. Euechinoidea and Cidaroidea respond differently to ocean acidification. Comparative Biochemistry and Physiology Part A: Molecular & Integrative Physiology 174:45–55.

Collard, M., K. Laitat, L. Moulin, A. I. Catarino, P. Grosjean, and P. Dubois. 2013. Buffer capacity of the coelomic fluid in echinoderms. Comparative Biochemistry and Physiology Part A: Molecular & Integrative Physiology 166:199–206.

Collard, M., S. P. S. Rastrick, P. Calosi, Y. Demolder, J. Dille, H. S. Findlay, J. M. Hall-Spencer, M. Milazzo, L. Moulin, S. Widdicombe, F. Dehairs, and P. Dubois. 2016. The impact of ocean acidification and warming on the skeletal mechanical properties of the sea urchin *Paracentrotus lividus* from laboratory and field observations. ICES Journal of Marine Science 73:727–738.

Denny, M., T. Daniel, and M. Koehl. 1985. Mechanical Limits to Size in Wave-Swept Organisms. Ecological Monographs 55:69–102.

deVries, M. S., S. J. Webb, J. Tu, E. Cory, V. Morgan, R. L. Sah, D. D. Deheyn, and J. R. A. Taylor. 2016. Stress physiology and weapon integrity of intertidal mantis shrimp under future ocean conditions. Scientific Reports 6:1–15.

Diaz, R. J., and R. Rosenberg. 2008. Spreading Dead Zones and Consequences for Marine Ecosystems. Science 321:926–929.

Dickson, A. G. 1990. Standard potential of the reaction: $AgCl_{(s)} + 1/2\ H_{2(g)} = Ag_{(s)} + HCl_{(aq)}$, and the standard acidity constant of the ion HSO_4^- in synthetic sea water from 273.15 to 318.15 K. Journal of Chemical Thermodynamics 22:113–127.

Dickson, A. G., C. L. Sabine, and J. R. Christian, editors. 2007. Guide to Best Practices for Ocean CO_2 Measurements. Third edition. PICES Special Edition.

Dubois, P. 2014. The Skeleton of Postmetamorphic Echinoderms in a Changing World. Biological Bulletin 226:223–236.

Dupont, S., N. Dorey, M. Stumpp, F. Melzner, and M. Thorndyke. 2013. Long-term and trans-life-cycle effects of exposure to ocean acidification in the green sea urchin *Strongylocentrotus droebachiensis*. Marine Biology 160:1835–1843.

Dupont, S., O. Ortega-Martínez, and M. Thorndyke. 2010. Impact of near-future ocean acidification on echinoderms. Ecotoxicology 19:449–462.

Ebert, T. A. 1967. Negative growth and longevity in the purple sea urchin Strongylocentrotus purpuratus (Stimpson). Science 157:557–558.

Ebert, T. A. 1968. Growth rates of the sea urchin *Strongylocentrotus purpuratus* related to food availability and spine abrasion. Ecology 49:1075–1091.

Von Euw, S., Q. Zhang, V. Manichev, N. Murali, J. Gross, L. C. Feldman, T. Gustafsson, C. Flach, R. Mendelsohn, and P. G. Falkowski. 2017. Biological control of aragonite formation in stony corals. Science 356:933–938.

Fabian, D., and T. Flatt. 2012. Life History Evolution. Nature Education Knowledge 3:24.

Fairbairn, E. A., A. A. Keller, L. Mädler, D. Zhou, S. Pokhrel, and G. N. Cherr. 2011. Metal oxide nanomaterials in seawater: Linking physicochemical characteristics with biological response in sea urchin development. Journal of Hazardous Materials 192:1565–1571.

Feely, R. A., C. L. Sabine, J. M. Hernandez-Ayon, D. Ianson, and B. Hales. 2008. Evidence for upwelling of corrosive “acidified” water onto the continental shelf. Science 320:1490–1492.

Fodrie, F. J., B. B. J., L. A. Levin, K. Gruenthal, and P. McMillan. 2011. Connectivity clues from short-term variability in settlement and geochemical tags of mytilid mussels. Journal of Sea Research 65:141–150.

Frank, M., S. Naleway, J.-Y. Jung, T. Wirth, C. Cheung, F. Loera, S. Medina, K. Sato, J. Taylor, and J. McKittrick. 2015. A Protocol for Bioinspired Design: A Ground Sampler Based on Sea Urchin Jaws. Journal of Visualized Experiments 110:e53554.

Gallo, N. D., and L. A. Levin. 2016. Fish Ecology and Evolution in the World's Oxygen Minimum Zones and Implications of Ocean Deoxygenation. Advances in Marine Biology 74:117–198.

Gaylord, B., T. M. Hill, E. Sanford, E. A. Lenz, L. A. Jacobs, K. N. Sato, A. D. Russell, and A. Hettinger. 2011. Functional impacts of ocean acidification in an ecologically critical foundation species. Journal of Experimental Biology 214:2586–2594.

Gilly, W. F., J. M. Beman, S. Y. Litvin, and B. H. Robison. 2013. Oceanographic and Biological Effects of Shoaling of the Oxygen Minimum Zone. Annual Review of Marine Science 5:393–420.

Gooday, A. J., B. J. Bett, E. Escobar, B. Ingole, L. A. Levin, C. Neira, A. V. Raman, and J. Sellanes. 2010. Habitat heterogeneity and its influence on benthic biodiversity in oxygen minimum zones. Marine Ecology 31:125–147.

Gruber, N. 2011. Warming up, turning sour, losing breath: ocean biogeochemistry under global change. Philosophical Transactions of the Royal Society of London A: Mathematical, Physical and Engineering Sciences 369:1980–1996.

Gruber, N., C. Hauri, Z. Lachkar, D. Loher, T. L. Frolicher, and G. K. Plattner. 2012. Rapid progression of ocean acidification in the California Current System. Science 337:220–223.

Hermans, J., C. Borremans, P. Willenz, L. Andre, and P. Dubois. 2010. Temperature, salinity and growth rate dependences of Mg/Ca and Sr/Ca ratios of the skeleton of the sea urchin *Paracentrotus lividus* (Lamarck): an experimental approach. Marine Biology 157:1293–1300.

Hofmann, G. E., J. E. Smith, K. S. Johnson, U. Send, L. A. Levin, F. Micheli, A. Paytan, N. N. Price, B. Peterson, Y. Takeshita, P. G. Matson, E. D. Crook, K. J. Kroeker, M. C. Gambi, E. B. Rivest, C. A. Frieder, P. C. Yu, and T. R. Martz. 2011. High-Frequency Dynamics of Ocean pH: A Multi-Ecosystem Comparison. PLoS ONE 6:e28983.

Hönisch, B., and K. A. Allen. 2013. Paleoceanography, physical and chemical proxies: Carbon Cycle Proxies (δ11B, $\delta 13C_{calcite}$, $\delta 13C_{organic}$, Shell Weights, B/Ca, U/Ca, Zn/Ca, Ba/Ca). Pages 849–858Encyclopedia of Quaternary Science.

Hotaling, N. A., K. Bharti, H. Kriel, and C. G. Simon. 2015. DiameterJ: A validated open source nanofiber diameter measurement tool. Biomaterials 61:327–338.

Jackson, R. T. 1912. Phylogeny of the Echini, with a revision of Palaeozoic species. Memoirs of the Boston Society of Natural History.

Janssen, D. J., T. M. Conway, S. G. John, J. R. Christian, D. I. Kramer, T. F. Pedersen, and J. T. Cullen. 2014. Undocumented water column sink for cadmium in open ocean oxygen-deficient zones. Proceedings of the National Academy of Sciences of the United States of America 111:6888–6893.

Kanold, J. M., J. Wang, F. Brümmer, and L. Siller. 2016. Metallic nickel nanoparticles and their effect on the embryonic development of the sea urchin *Paracentrotus lividus*. Environmental Pollution 212:224–229.

Kroeker, K. J., R. L. Kordas, R. N. Crim, and G. G. Singh. 2010. Meta-analysis reveals negative yet variable effects of ocean acidification on marine organisms. Ecology Letters 13:1419–1434.

Kuklinski, P., and P. D. Taylor. 2009. Mineralogy of Arctic bryozoan skeletons in a global context. Facies 55:489–500.

Kurihara, H., R. Yin, G. N. Nishihara, K. Soyano, and A. Ishimatsu. 2013. Effect of ocean acidification on growth, gonad development and physiology of the sea urchin *Hemicentrotus pulcherrimus*. Aquatic Biology 18:281–292.

Lack, D. 1947. The significance of clutch size. Ibis 89:302–352.

Lavigne, M., T. M. Hill, E. Sanford, B. Gaylord, A. D. Russell, E. A. Lenz, J. D. Hosfelt, and M. K. Young. 2013. The elemental composition of purple sea urchin (*Strongylocentrotus purpuratus*) calcite and potential effects of pCO_2 during early life stages. Biogeosciences 10:3465–3477.

Lebrato, M., A. J. Andersson, J. B. Ries, R. B. Aronson, M. D. Lamare, W. Koeve, A. Oschlies, M. D. Iglesias-Rodriguez, S. Thatje, M. Amsler, S. C. Vos, D. O. B. Jones, H. A. Ruhl, A. R. Gates, and J. B. McClintock. 2016. Benthic marine calcifiers coexist with $CaCO_3$ -undersaturated seawater worldwide. Global Biogeochemical Cycles 30:1038–1053.

Lebrato, M., D. Iglesias-Rodriguez, R. A. Feely, D. Greeley, D. O. B. Jones, N. Suarez-Bosche, R. S. Lampitt, J. E. Cartes, D. R. H. Green, and B. Alker. 2010. Global contribution of echinoderms to the marine carbon cycle: $CaCO_3$ budget and benthic compartments. Ecological Monographs 80:441–467.

Levin, L. A. 2003. Oxygen Minimum Zone benthos: adaptation and community response to hypoxia. Oceanography and Marine Biology: an Annual Review 41:1–45.

Levin, L. A. 2006. Recent Progress in Understanding Larval Dispersal: New Directions and Digressions. Integrative and Comparative Biology 46:282–297.

Levin, L. A., B. Hönisch, and C. A. Frieder. 2015. Geochemical proxies for estimating

faunal exposure to ocean acidification. Oceanography 28:62–73.

Levin, L. A., and M. Sibuet. 2012. Understanding Continental Margin Biodiversity: A New Imperative. Annual Review of Marine Science 4:79–112.

Limburg, K. E., B. D. Walther, Z. Lu, G. Jackman, J. Mohan, Y. Walther, A. Nissling, P. K. Weber, and A. K. Schmitt. 2015. In search of the dead zone: Use of otoliths for tracking fish exposure to hypoxia. Journal of Marine Systems 141:167–178.

Lohrer, A. M., S. F. Thrush, L. Hunt, N. Hancock, and C. Lundquist. 2005. Rapid reworking of subtidal sediments by burrowing spatangoid urchins. Journal of Experimental Marine Biology and Ecology 321:155–169.

Long, X., Y. Ma, and L. Qi. 2014. Biogenic and synthetic high magnesium calcite – A review. Journal of Structural Biology 185:1–14.

Lowder, K. B., M. C. Allen, J. M. D. Day, D. D. Deheyn, and J. R. A. Taylor. 2017. Assessment of ocean acidification and warming on the growth, calcification, and biophotonics of a California grass shrimp. ICES Journal of Marine Science 74:1150–1158.

Lueker, T. J., A. G. Dickson, and C. D. Keeling. 2000. Ocean pCO_2 calculated from dissolved inorganic carbon, alkalinity, and equations for K_1 and K_2 : validation based on laboratory measurements of CO_2 in gas and seawater at equilibrium. Marine Chemistry 70:105–119.

Ma, Y., B. Aichmayer, O. Paris, P. Fratzl, A. Meibom, R. A. Metzler, Y. Politi, L. Addadi, P. U. P. . Gilbert, and S. Weiner. 2009. The grinding tip of the sea urchin tooth exhibits exquisite control over calcite crystal orientation and Mg distribution. Proceedings of the National Academy of Sciences of the United States of America 106:6048–6053.

Mackenzie, F. T., W. D. Bischoff, F. C. Bishop, M. Loijens, J. Schoonmaker, and R. Wollast. 1983. Mg-calcites: low temperature occurrence, solubility and solid-solution behavior. Pages 97–143 *in* R. J. Reeder, editor. Reviews in Mineralogy, Carbonates: Mineralogy and Chemistry. Mineralogical Society of America.

Mann, K., A. Poustka, and M. Mann. 2008. The sea urchin (*Strongylocentrotus purpuratus*) test and spine proteomes. Proteome Science 6:22.

Marchitto, T. M., W. B. Curry, and D. W. Oppo. 2000. Zinc concentrations in benthic foraminfera reflect seawater chemistry. Paleoceanography 15:299–306.

Meyers, M. A., P.-Y. Chen, A. Y.-M. Lin, and Y. Seki. 2008. Biological materials: Structure and mechanical properties. Progress in Materials Science 53:1–206.

Milton, D. A., and S. R. Chenery. 2001. Sources and uptake of trace metals in otoliths of juvenile barramundi (*Lates calcarifer*). Journal of Experimental Marine Biology and Ecology 264:47–65.

Moberly, R. 1968. Composition of magnesian calcites of algae and pelecypods by electron microprobe analysis. Sedimentology 11:61–82.

Moffitt, S. E., R. A. Moffitt, W. Sauthoff, C. V. Davis, K. Hewett, and T. M. Hill. 2015. Paleoceanographic Insights on Recent Oxygen Minimum Zone Expansion: Lessons for Modern Oceanography. PLOS ONE 10:e0115246.

Moore, A. R. 1959. On the embryonic development of the sea urchin Allocentrotus fragilis. Biological Bulletin 117:492–496.

Morse, J. W., A. J. Andersson, and F. T. Mackenzie. 2006. Initial responses of carbonate-rich shelf sediments to rising atmospheric pCO_2 and "ocean acidification": Role of high Mg-calcites. Geochimica et Cosmochimica Acta 70:5814–5830.

Naleway, S. E., J. R. A. Taylor, M. M. Porter, M. A. Meyers, and J. McKittrick. 2016. Structure and mechanical properties of selected protective systems in marine organisms. Materials Science & Engineering C: Materials for Biological Applications 59:1143–1167.

Nam, S., Y. Takeshita, C. A. Frieder, T. Martz, and J. Ballard. 2015. Seasonal advection of Pacific Equatorial Water alters oxygen and pH in the Southern California Bight. Journal of Geophysical Research: Oceans 120:5387–5399.

Oksanen, J., F. G. Blanchet, M. Friendly, R. Kindt, P. Legendre, D. McGlinn, P. Minchin, R. B. O'Hara, G. L. Simpson, P. Solymos, M. H. H. Stevens, E. Szoecs, and H. Wagner. 2017. vegan: Community Ecology Package. https://cran.r-project.org/package=vegan.

Oliver, T. A., D. A. Garfield, M. K. Manier, R. Haygood, G. A. Wray, and S. R. Palumbi. 2010. Whole-genome positive selection and habitat-driven evolution in a shallow and a deep-sea urchin. Genome Biology and Evolution 2:800–814.

Pearse, J. S. 2006. Ecological role of purple sea urchins. Science 314:940–941.

Piersma, T., and J. Drent. 2003. Phenotypic flexibility and the evolution of organismal design. Trends in Ecology & Evolution 18:228–233.

Politi, Y., T. Arad, E. Klein, S. Weiner, and L. Addadi. 2004. Sea Urchin Spine Calcite Forms via a Transient Amorphous Calcium Carbonate Phase. Science 306:1161–1164.

Presser, V., K. Gerlach, A. Vohrer, K. G. Nickel, and W. F. Dreher. 2010. Determination of the elastic modulus of highly porous samples by nanoindentation: A case study on sea urchin spines. Journal of Materials Science 45:2408–2418.

Reich, M., and A. B. Smith. 2009. Origins and biomechanical evolution of teeth in echinoids and their relatives. Palaeontology 52:1149–1168.

Reusch, T. B. H. 2014. Climate change in the oceans: Evolutionary versus phenotypically plastic responses of marine animals and plants. Evolutionary Applications 7:104–122.

Russell, A. D., B. Hönisch, H. J. Spero, and D. W. Lea. 2004. Effects of seawater carbonate ion concentration and temperature on shell U, Mg, and Sr in cultured planktonic foraminifera. Geochimica et Cosmochimica Acta 68:4347–4361.

Sato, K. N., L. A. Levin, and K. Schiff. 2017. Habitat compression and expansion of sea urchins in response to changing climate conditions on the California continental shelf and slope (1994–2013). Deep Sea Research Part II: Topical Studies in Oceanography 137:377–389.

Schmidtko, S., L. Stramma, and M. Visbeck. 2017. Decline in global oceanic oxygen content during the past five decades. Nature 542:335–339.

Schneider, C. A., W. S. Rasband, and K. W. Eliceiri. 2012. NIH Image to ImageJ: 25 years of image analysis. Nature Methods 9:671–675.

Smith, C. C., and S. D. Fretwell. 1974. The optimal balance between size and number of offspring. The American Naturalist 108:499–506.

Somero, G. N., J. M. Beers, F. Chan, T. M. Hill, T. Klinger, and S. Y. Litvin. 2016. What Changes in the Carbonate System, Oxygen, and Temperature Portend for the Northeastern Pacific Ocean: A Physiological Perspective. BioScience 66:14–26.

Sperling, E. A., C. A. Frieder, and L. A. Levin. 2016. Biodiversity response to natural gradients of multiple stressors on continental margins. Proceedings of the Royal Society of London B: Biological Sciences 283:20160637.

Stramma, L., S. Schmidtko, L. A. Levin, and G. C. Johnson. 2010. Ocean oxygen minima expansions and their biological impacts. Deep Sea Research Part I: Oceanographic Research Papers 57:587–595.

Sumich, J. L., and J. E. McCauley. 1973. Growth of a sea urchin, *Allocentrotus fragilis*, off the Oregon coast. Coastal Pacific Science 27:156–167.

Sunday, J. M., P. Calosi, S. Dupont, P. L. Munday, J. H. Stillman, and T. B. H. Reusch. 2014. Evolution in an acidifying ocean. Trends in Ecology & Evolution 29:117–125.

Takeshita, Y., C. A. Frieder, T. R. Martz, J. R. Ballard, R. A. Feely, S. Kram, S. Nam, M. O. Navarro, N. N. Price, and J. E. Smith. 2015. Including high-frequency variability in coastal ocean acidification projections. Biogeosciences 12:5853–5870.

Taylor, J. R. A., J. M. Gilleard, M. C. Allen, and D. D. Deheyn. 2015. Effects of CO_2-induced pH reduction on the exoskeleton structure and biophotonic properties of the shrimp *Lysmata californica*. Scientific Reports 5:10608.

Taylor, J. R., C. Lovera, P. J. Whaling, K. R. Buck, E. F. Pane, and J. P. Barry. 2014. Physiological effects of environmental acidification in the deep-sea urchin *Strongylocentrotus fragilis*. Biogeosciences 11:1413–1423.

Thompson, B., D. Tsukada, and J. Laughlin. 1993. Megabenthic assemblages of coastal shelves, slopes, and basins off southern California. Bulletin of the Southern California Academy of Sciences 92:25–42.

Todgham, A. E., and G. E. Hofmann. 2009. Transcriptomic response of sea urchin larvae *Strongylocentrotus purpuratus* to CO_2-driven seawater acidification. Journal of Experimental Biology 212:2579–2594.

Tribovillard, N., T. J. Algeo, T. Lyons, and A. Riboulleau. 2006. Trace metals as paleoredox and paleoproductivity proxies: An update. Chemical Geology 232:12–32.

Walter, L. M., and J. W. Morse. 1984. Reactive Surface Area of Skeletal Carbonates During Dissolution: Effect of Grain Size. Journal of Sedimentary Research 54:1081–1090.

Walther, B. D., and K. E. Limburg. 2012. The use of otolith chemistry to characterize diadromous migrations. Journal of Fish Biology 81:796–825.

Walther, S. M., J. P. Williams, A. Latker, D. B. Cadien, D. W. Diehl, E. Miller, K. Patrick, R. Gartman, and K. Schiff. 2017. Southern California Bight 2013 Regional Monitoring Program: Volume VIII. Demersal Fishes and Megabenthic Invertebrates. Southern California Coastal Water Research Project, Costa Mesa, CA.

Wang, R. Z., L. Addadi, and S. Weiner. 1997. Design strategies of sea urchin teeth: Structure, Composition, and micromechanical relations to function. Philosophical Transactions of the Royal Society B 352:469–480.

Weiner, S., and P. M. Dove. 2003. An Overview of Biomineralization Processes and the Problem of the Vital Effect. Reviews in Mineralogy and Geochemistry 54:1–29.

Williams, B., J. Halfar, K. L. Delong, E. Smith, R. Steneck, P. A. Lebednik, D. E. Jacob, J. Fietzke, and G. W. K. Moore. 2017. North Pacific twentieth century decadal-scale variability is unique for the past 342 years. Geophysical Research Letters 44.

Ziveri, P., M. Passaro, A. Incarbona, M. Milazzo, R. Rodolfo-Metalpa, and J. M. Hall-Spencer. 2014. Decline in Coccolithophore Diversity and Impact on Coccolith Morphogenesis Along a Natural CO_2 Gradient. Biological Bulletin 226:282–290.

Table 4.1. Use of elements in biological carbonate structures as marine environmental proxies. Modified after Levin (2006).

Environmental Variable	**Proxy Elements (standardized to [Ca])**	**References**
Temperature	Mg, Sr	Levin (2006)
pH	Mn, Zn, B, U	Hönisch and Allen (2013) Frieder et al. (2014)
$[CO_3^{2-}]$	Zn, U	Marchitto et al. (2000) Russell et al. (2004)
Upwelling	Cd	Fodrie et al. (2011)
$[O_2]$	Mn, Cd	Levin (2006) Limburg et al. (2015)
Productivity	Ba, U	Tribovillard et al. (2006)
Salinity	Ba, Sr	Walther and Limburg (2012)
Structural Properties (e.g., Hardness, Elastic Modulus)	Mg, Fe, P, Ni, Pb	Long et al. (2014) Naleway et al. (2016)

Table 4.2. Mean values (± 1 SE) of hydrographic variables (Depth, Temperature, Salinity, Oxygen, and *in situ* pHTotal) and gonad index (% weight) and Total length of the test diameter of *Strongylocentrotus fragilis* urchins separated by depth zone bin. Shelf = <200 m; OLZ = Oxygen Limited Zone (22-60 µmol oxygen kg-1); OMZ = Oxygen Minimum Zone core (< 22 µmol oxygen kg-1); LOMZ = Lower Oxygen Minimum Zone (>750 m where dissolved oxygen begins to increase).

Zone	n	Depth (m)	Temp (°C)	Salinity	Oxygen (µmol kg^{-1})	*in situ* pH_{Total}	Gonad Index	TLD (mm)
Shelf	134	155.4 ± 3.431	9.643 ± 0.051	33.975 ± 0.015	85.050 ± 1.927	7.695 ± 0.002	6.574 ± 0.377	60.463 ± 1.172
OLZ	403	328.3 ± 2.326	8.426 ± 0.031	34.253 ± 0.003	41.879 ± 0.599	7.594 ± 0.001	4.788 ± 0.186	48.260 ± 0.403
OMZ	95	590.2 ± 13.334	6.216 ± 0.107	34.287 ± 0.010	15.827 ± 0.557	7.567 ± 0.002	1.846 ± 0.176	45.494 ± 0.823
LOMZ	24	1014.3 ± 20.149	4.331 ± 0.027	34.460 ± 0.002	13.321 ± 0.491	7.628 ± 0.002	4.152 ± 1.014	51.079 ± 2.884

Table 4.3. Mean values (± 1 SE) of hydrographic variables (Depth, Temperature, Salinity, Oxygen, and *in situ* pH_{Total}) and $E/Ca_{calcite}$ ratios of *Strongylocentrotus fragilis* urchin tests separated by depth zone bin. Shelf = <200 m; OLZ = Oxygen Limited Zone (22-60 µmol oxygen kg^{-1}); OMZ = Oxygen Minimum Zone core (< 22 µmol oxygen kg^{-1}); LOMZ = Lower Oxygen Minimum Zone (>750 m where dissolved oxygen begins to increase).

Zone	n	Depth (m)	Temp (°C)	Salinity	Oxygen (µmol kg^{-1})	*in situ* pH_{Total}
Shelf	24	174.2 ± 10.5	9.440 ± 0.173	33.985 ± 0.051	90.392 ± 8.530	7.697 ± 0.015
OLZ	20	362.5 ± 8.1	8.057 ± 0.105	34.292 ± 0.008	33.080 ± 0.774	7.574 ± 0.002
OMZ/ LOMZ	26	681.8 ± 32.4	5.559 ± 0.195	34.363 ± 0.012	14.613 ± 0.710	7.576 ± 0.006

		Urchin (µmol mol Ca^{-1})					Urchin (mmol mol Ca^{-1})			
Zone	n	Zn	Ni	Cd	U	P	n	Mg	Sr	Fe
Shelf	24	12.665 ± 1.893	10.566 ± 0.070	0.983 ± 0.088	0.224 ± 0.023	9.458 ± 1.407	24	19.858 ± 0.221	5.903 ± 0.038	6.932 ± 0.124
OLZ	20	8.629 ± 0.874	10.506 ± 0.036	0.738 ± 0.037	0.127 ± 0.011	1.334 ± 0.188	20	19.876 ± 0.179	5.929 ± 0.033	7.284 ± 0.119
OMZ//LOMZ	26	9.698 ± 1.482	10.528 ± 0.094	0.613 ± 0.066	0.116 ± 0.013	4.475 ± 0.636	26	18.486 ± 0.132	5.788 ± 0.028	6.941 ± 0.155

Table 4.4. Mean values (± 1 SE) of mechanical and structural properties (Hardness, Elastic Modulus, Porosity, and Pore Size) of *Strongylocentrotus fragilis* urchin tests separated by depth zone bin. Shelf = <200 m; OLZ = Oxygen Limited Zone (22-60 μmol oxygen kg^{-1}); OMZ = Oxygen Minimum Zone core (< 22 μmol oxygen kg^{-1}); LOMZ = Lower Oxygen Minimum Zone (>750 m where dissolved oxygen begins to increase).

Zone	Hardness (GPa)			Elastic Modulus (GPa)			% Porosity			Pore Size (μm^2)		
Shelf	0.179	±	0.022	10.096	±	1.438	30.76	±	5.40	184.032	±	13.405
OLZ	0.073	±	0.007	3.916	±	0.544	40.93	±	1.97	277.517	±	31.251
OMZ	0.063	±	0.007	2.694	±	0.297	44.32	±	1.64	267.009	±	10.098
LOMZ	0.092	±	0.024	2.946	±	0.629	45.98	±	0.59	350.625	±	25.491

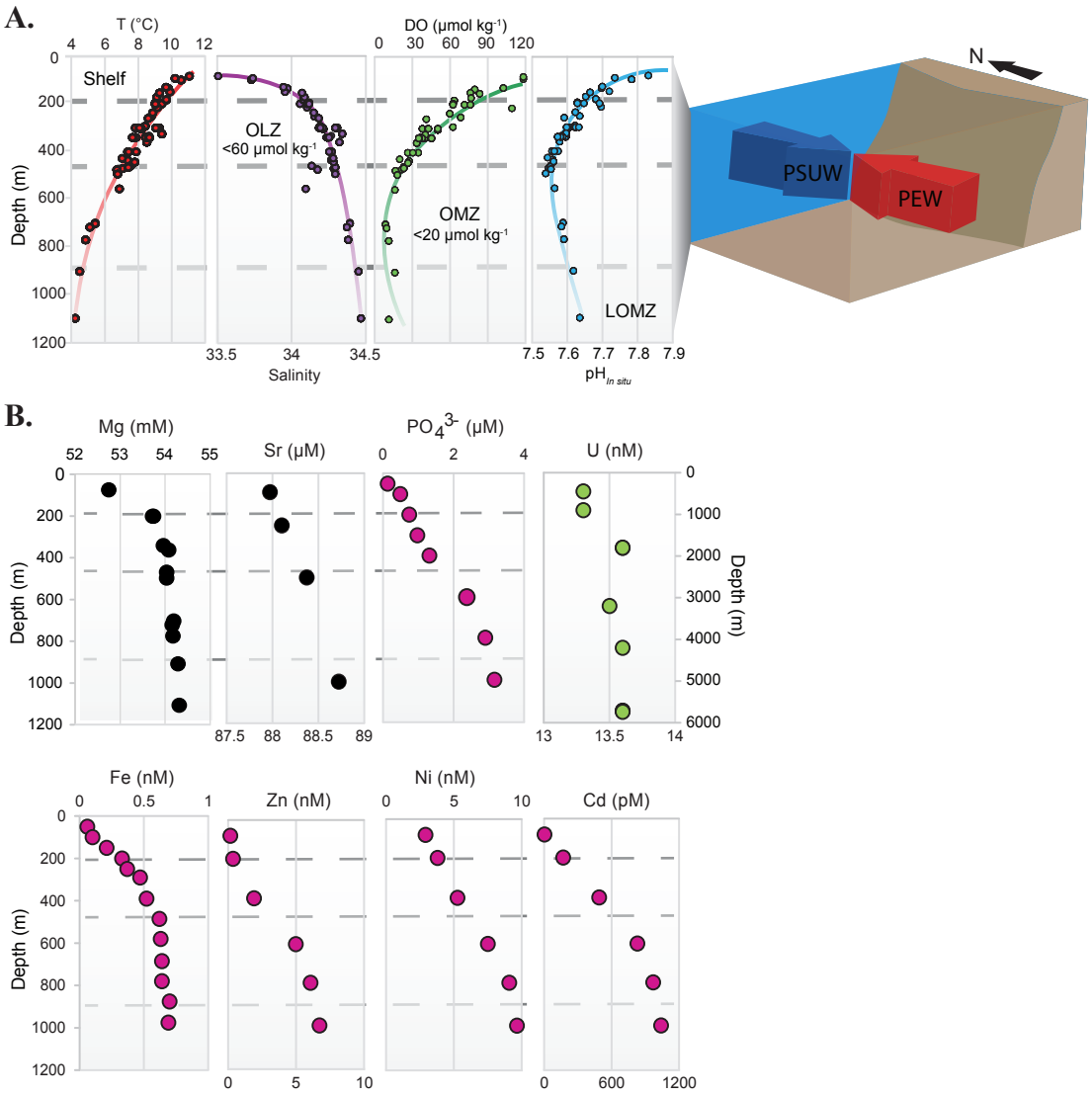

Figure 4.1. **A)** Depth profiles for temperature (T), salinity, dissolved oxygen (DO), and *in situ* pH_{Total} in southern California, indicating the vertical structure of key climate change variables (Left). Horizontal gray dashed lines separate the continental margin into 4 depth zones: Shelf, Oxygen Limited Zone, Oxygen Minimum Zone, and Lower Oxygen Minimum Zone. Right image depicts the convergence of intermediate source waters. Pacific Equatorial Water (PEW) originates from the south, and is warmer, saltier, and lower in DO and pH than Pacific Subarctic Upper Water (PSUW) advected from the north. **B)** Elemental concentrations of various elements in seawater in the upper 1,000 m of the water column (except Uranium). Pink dots indicate elements that demonstrate a nutrient-like profile. Elemental sample locations and concentration data were extracted from Biller and Bruland (2013) and Dr. Kenneth Johnson's *Periodic Table of Elements in the Ocean*. Available online at: http://www.mbari.org/science/upper-ocean-systems/chemical-sensor-group.

Figure 4.2. Image of a dried plate from the test of *Strongylocentrotus fragilis* that has been sanded flat and mounted to a steel block prior to nanoindentation tests.

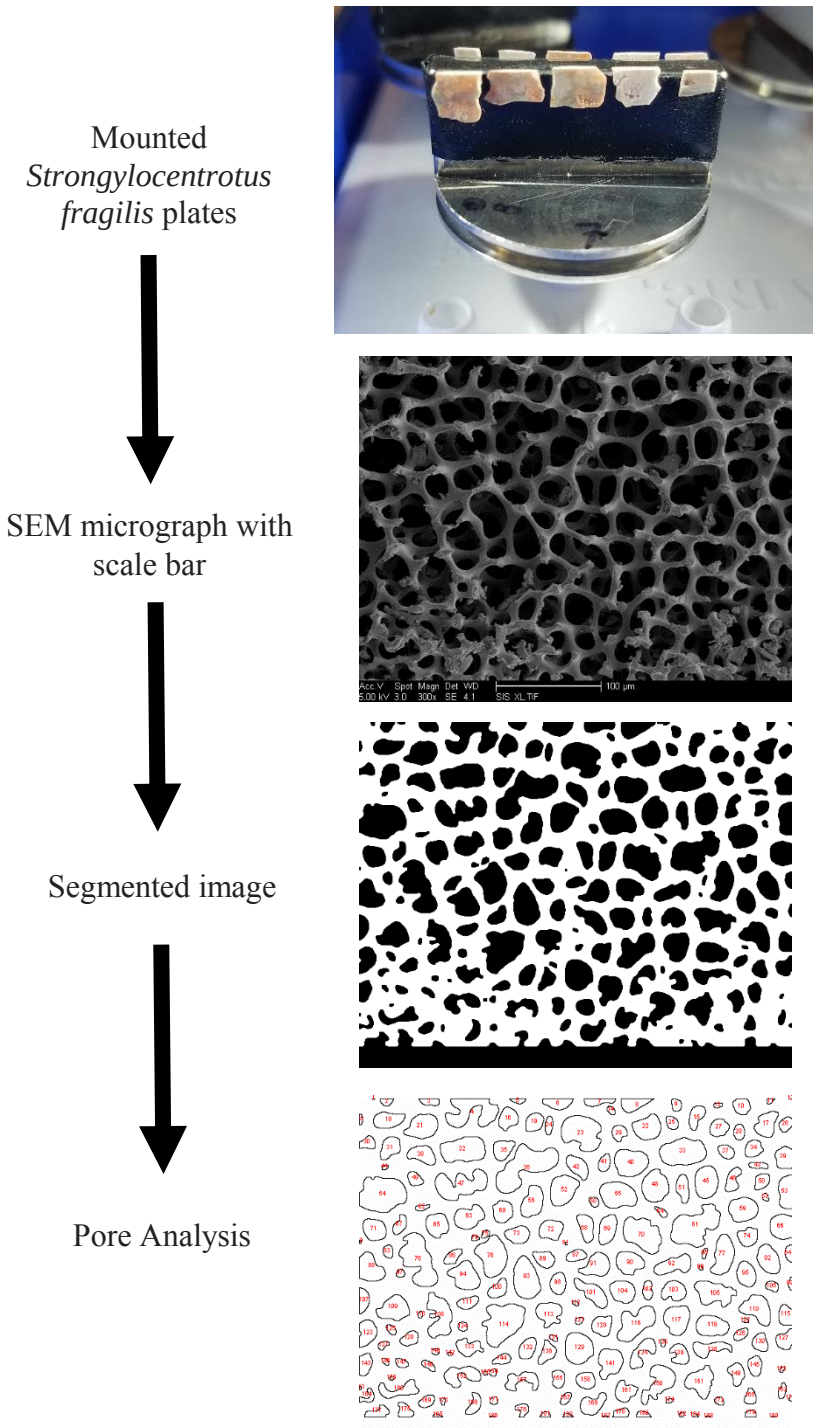

Figure 4.3. Flow chart of methods used for quantification of porosity and pore size from Scanning Electron Microscopy images. Segmented image and particle analysis were carried out in ImageJ. Scale bar: 100 µm.

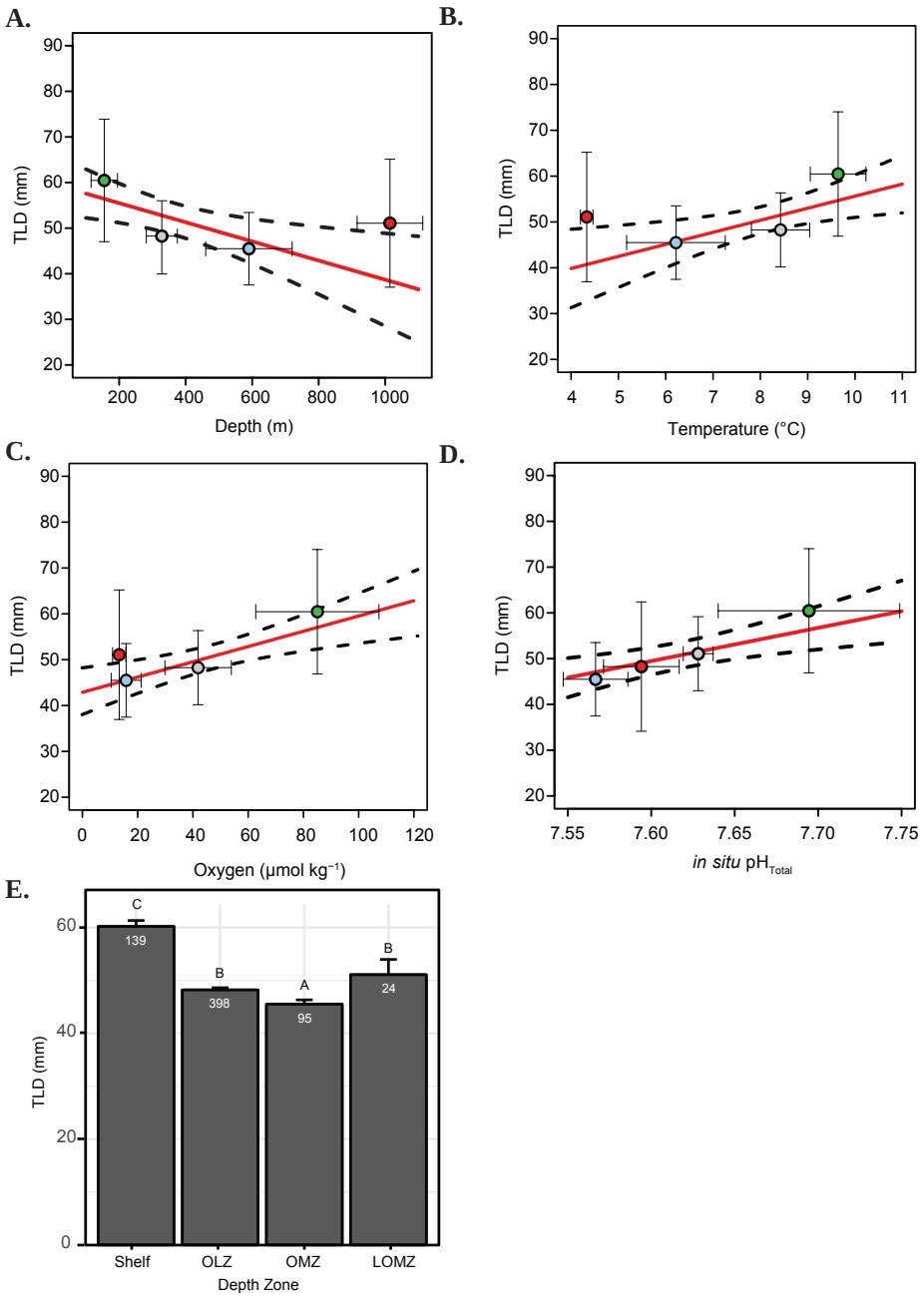

Figure 4.4. Total length of diameter (TLD; mm) of *Strongylocentrotus fragilis* tests collected throughout the SCB and its relationship with **A.** depth (m), **B.** dissolved oxygen (µmol kg^{-1}), **C.** temperature (°C), **D.** *in situ* pH_{Total}, and **E.** variation across depth zones. Green: Shelf = <200 m; Gray: OLZ = Oxygen Limited Zone (22-60 µmol oxygen kg^{-1}); Blue: OMZ = Oxygen Minimum Zone core (< 22 µmol oxygen kg^{-1}); Red: LOMZ = Lower Oxygen Minimum Zone (>750 m where dissolved oxygen begins to increase). Error bars are standard errors and numbers in barplots are numbers of dissected urchins. Dashed lines indicate 95% confidence intervals.

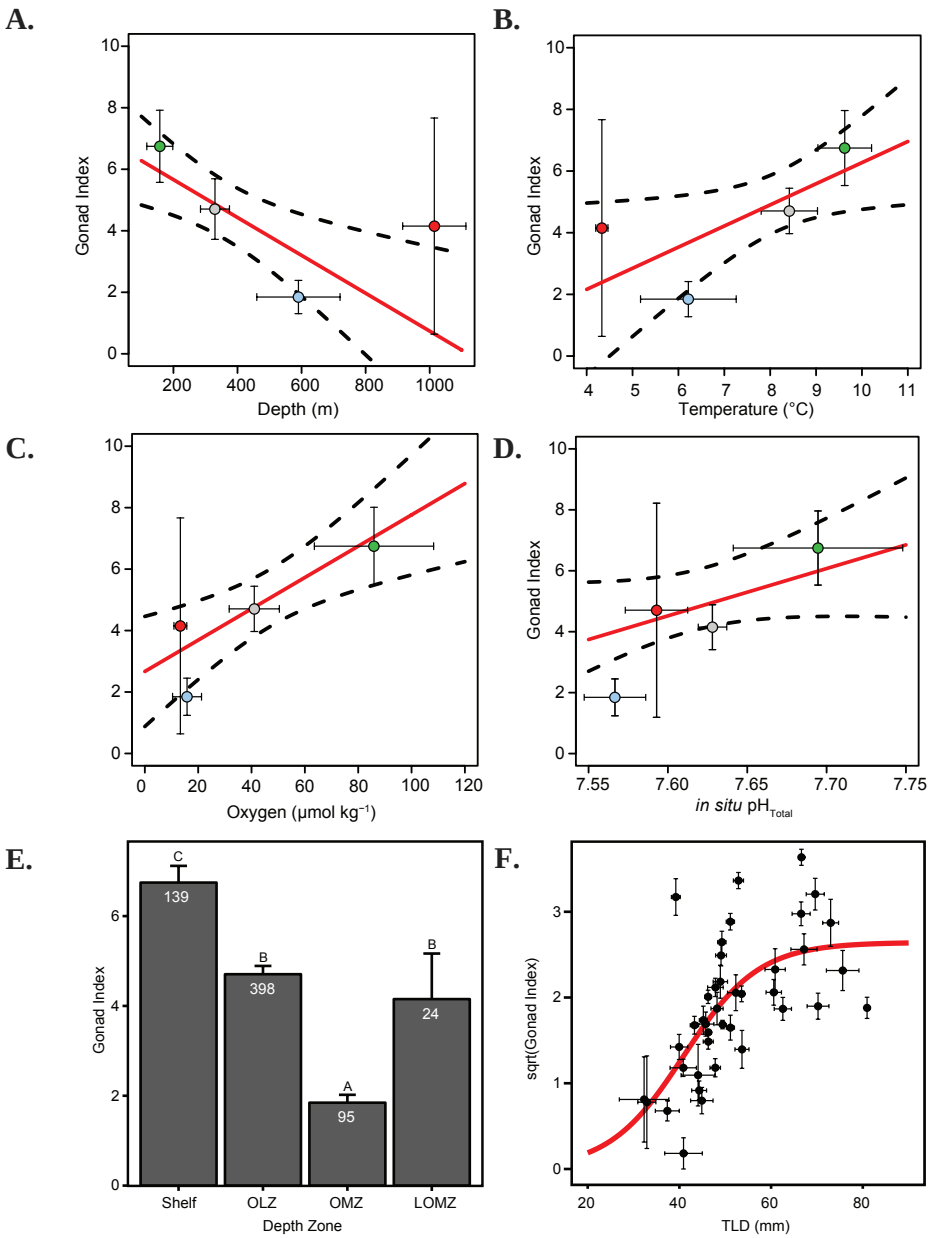

Figure 4.5. Gonad index of *Strongylocentrotus fragilis* tests collected throughout the SCB and its relationship with **A)** depth (m), **B)** dissolved oxygen (µmol kg^{-1}), **C)** temperature (°C), **D)** *in situ* pH_{Total}, and **E)** variation across depth zones. **F)** Curvilinear relationship between gonad index and mean total length diameter. Error bars are standard errors. Red lines indicate lines of best fit, and dashed lines indicate 95% confidence intervals. Numbers in barplots are numbers of dissected urchins and letters indicate differences resulting from a Tukey HSD *post hoc* test ($p < 0.05$). Green: Shelf = <200 m; Grey: OLZ = Oxygen Limited Zone (22-60 µmol oxygen kg-1); Blue: OMZ = Oxygen Minimum Zone core (< 22 µmol oxygen kg-1); Red: LOMZ = Lower Oxygen Minimum Zone (>750 m where dissolved oxygen begins to increase).

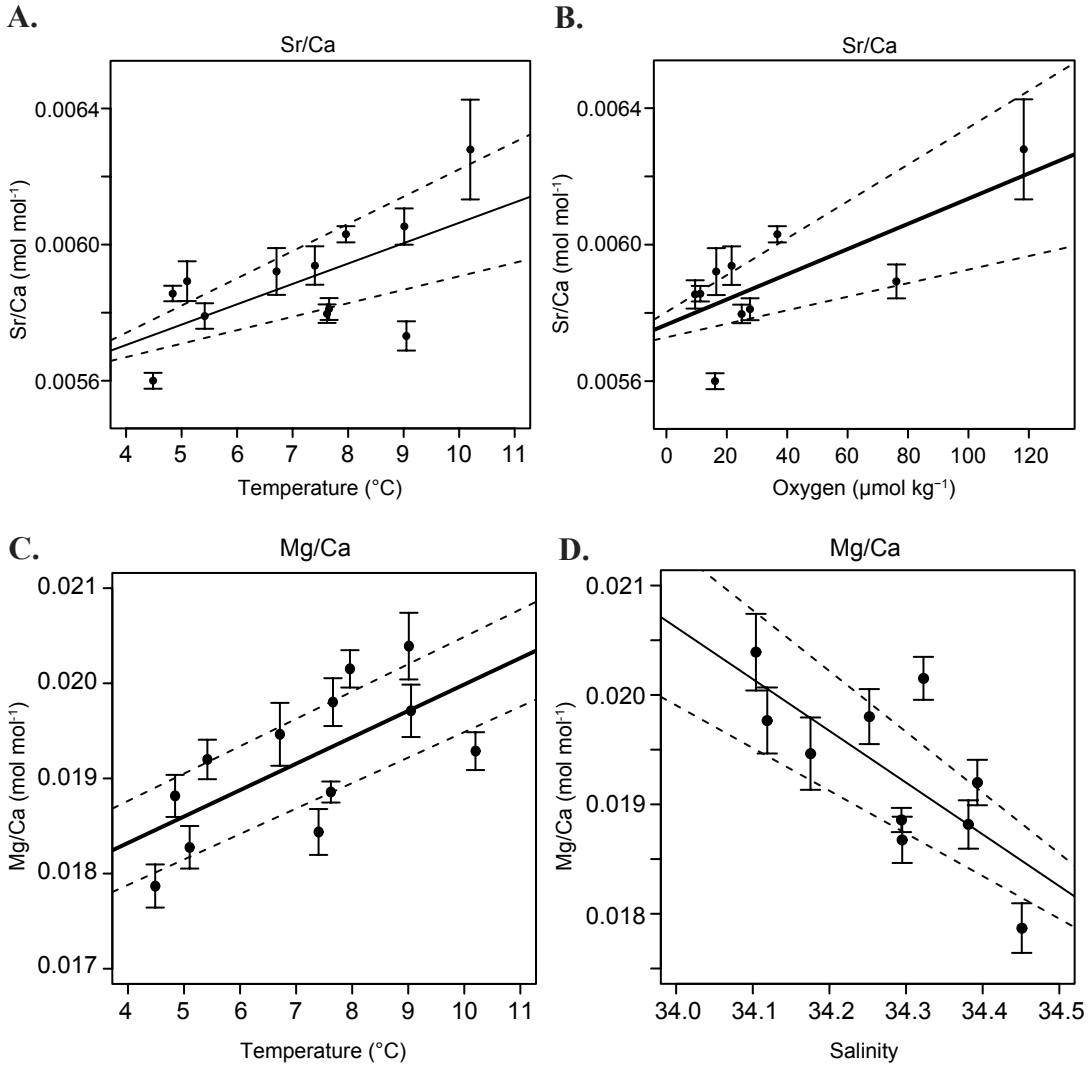

Figure 4.6. Significant relationships of *Strongylocentrotus fragilis* test ossicles elemental concentrations and hydrographic variables. Ratios of Sr to Ca (mol mol^{-1}) with **A)** temperature and **B)** dissolved oxygen. Ratios of Mg to Ca (mol mol^{-1}) with **C)** temperature and **D)** salinity. Black solid lines indicate the best fit line resultant of linear regression. Dashed lines indicate 95% confidence intervals. Error bars are ± 1 standard error.

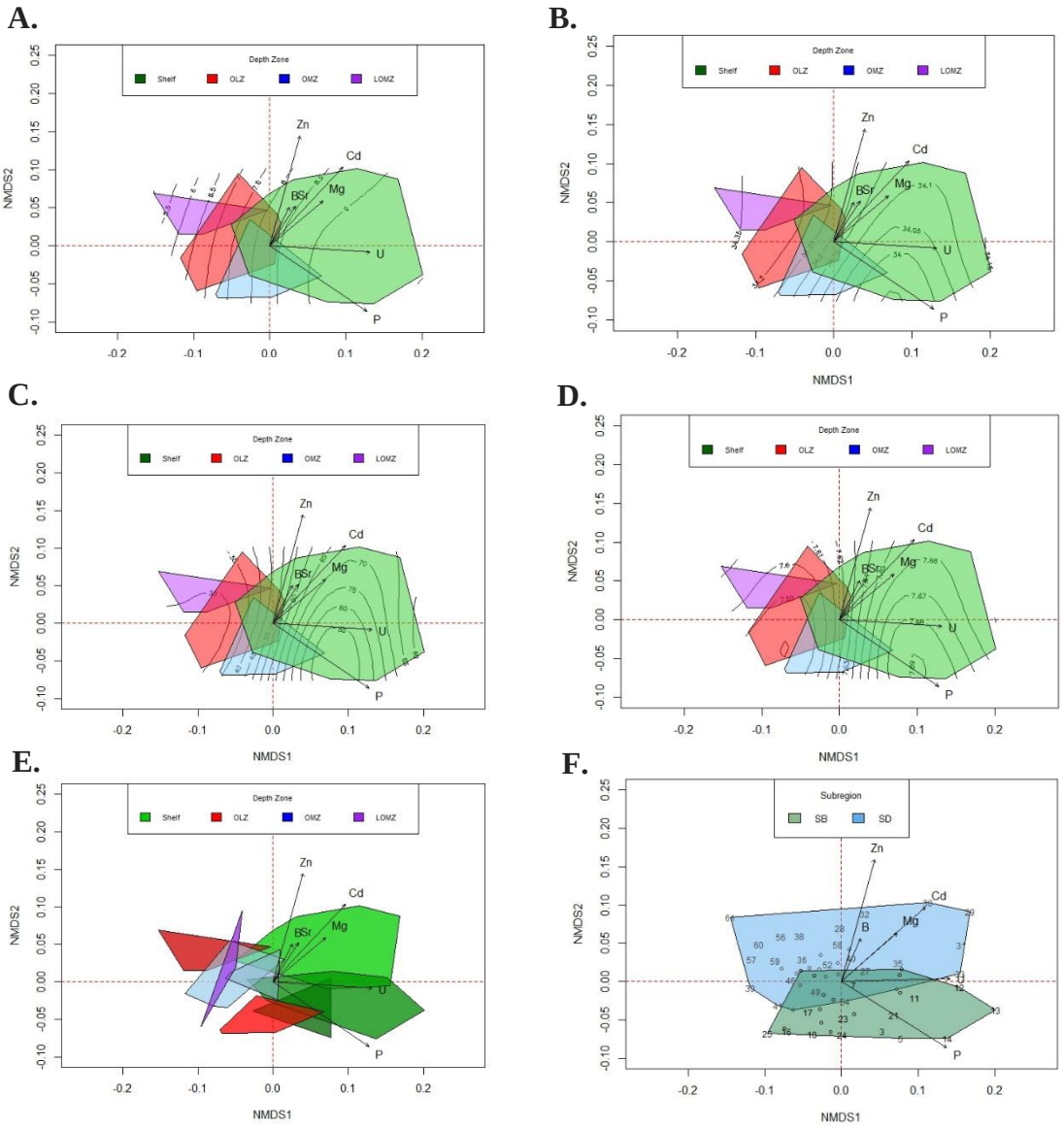

Figure 4.7. Nonmetric multidimensional scaling plot depicting elemental compositional dissimilarity among *Strongylocentrotus fragilis* urchin plates identified by all sites pooled into 4 depth zones with respect to gradients in **A)** temperature (°C), **B)** salinity (PSU), **C)** dissolved oxygen (µmol oxygen kg^{-1} seawater), and **D)** *in situ* pH_{Total}. Green: Shelf = <200 m; Red: OLZ = Oxygen Limited Zone (22-60 µmol oxygen kg^{-1}); Blue: OMZ = Oxygen Minimum Zone core (< 22 µmol oxygen kg^{-1} or 0.5 mL L^{-1}); Purple: LOMZ = Lower Oxygen Minimum Zone (<750 m where dissolved oxygen begins to increase). **E)** Convex hulls represent trawl sites and hull color represent zone. **F)** Sites are grouped into two subregion in the Southern California Bight (San Diego – Blue; Santa Barbara – Green). Element-loading vector lengths are proportional to the correlation between ordination axis and the element. Vector direction indicates the direction of the gradient. Convex hulls are shown in each plot to indicate differences in relative variability among class designations, but note sample size discrepancies.

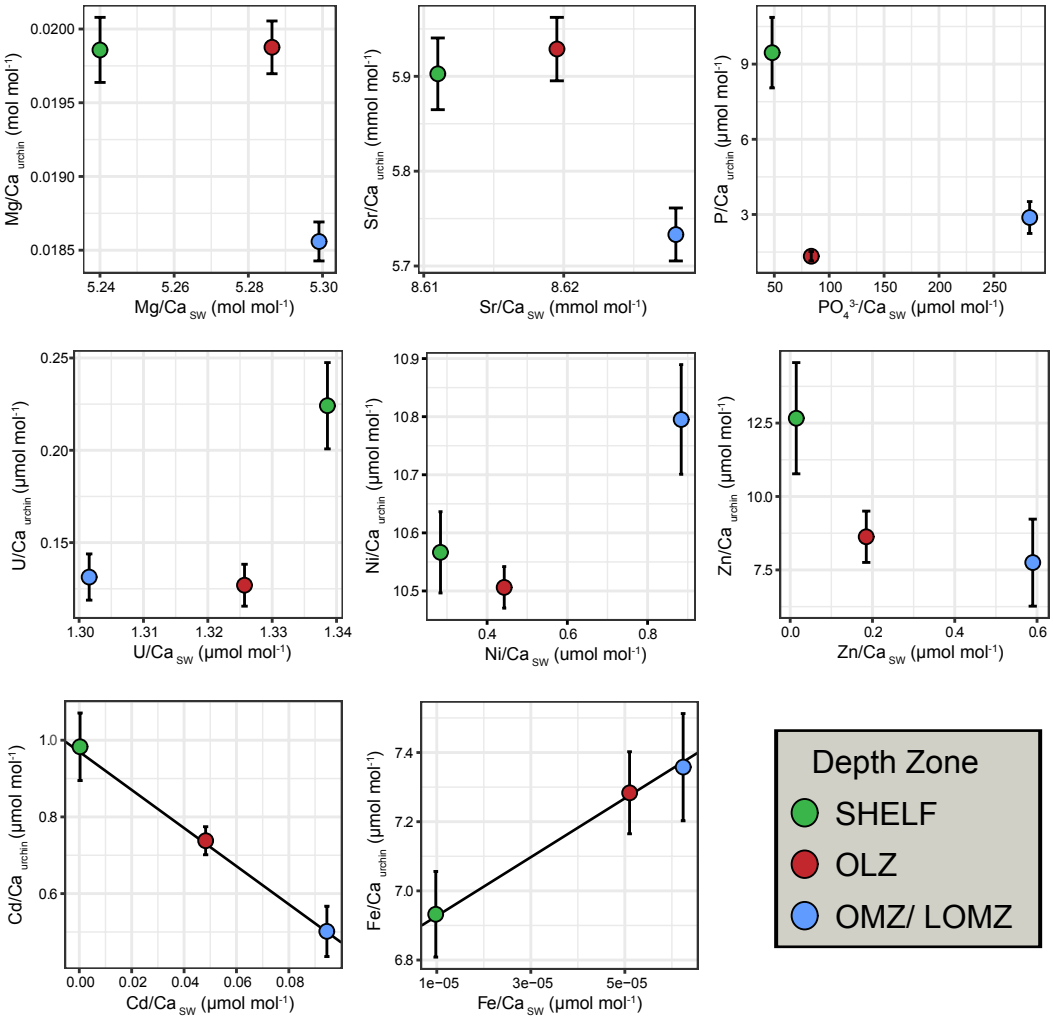

Figure 4.8. Relationships between element to calcium ratios in *Strongylocentrotus fragilis* test plates (E/Ca_{urchin}) and element to calcium ratios in seawater (E/Ca_{SW}) within different depth zones. E/Ca_{urchin} were averaged across depth bins: Shelf (green), Oxygen Limited Zone (red), and Oxygen Minimum Zone (blue). Black lines indicate significant linear regression relationships which yielded empirical partition coefficients (D_{metal}) for Cd and Fe only. Elemental concentrations of various elements in seawater (Mg, Sr, P, U, Ni, Zn, Cd, Fe, and Ca) in the upper 1,000 m of the water column were extracted from Biller and Bruland (2013) and Dr. Kenneth Johnson's *Periodic Table of Elements in the Ocean*. Available online at: http:// www.mbari.org/science/ upper-ocean-systems/chemical-sensor-group. Error bars indicate ± 1 standard error.

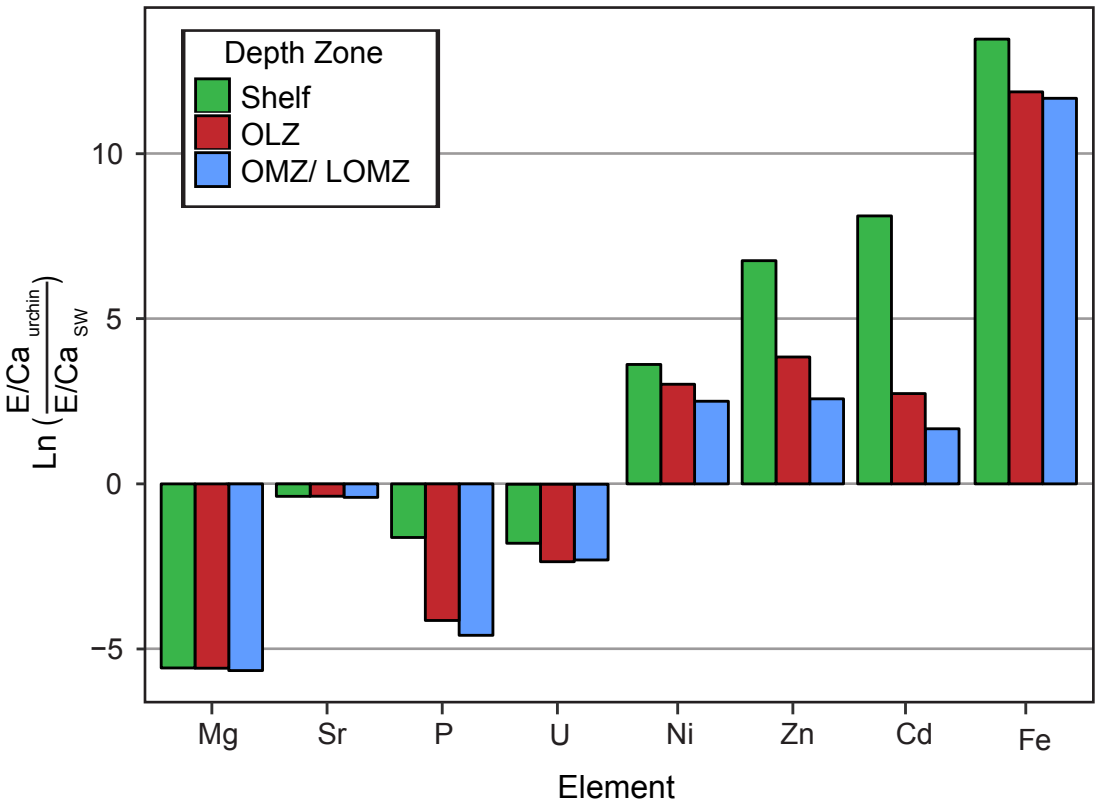

Figure 4.9. Natural log-transformed ratios of elemental incorporation in *Strongylocentrotus fragilis* [E/Ca_{Urchin}] versus element concentration ratios in seawater [E/Ca_{SW}]. Values > 0 indicate [E/Ca_{Urchin}] > [E/Ca_{SW}]. Values < 0 indicate [E/Ca_{Urchin}] < [E/Ca_{SW}]. Elemental concentrations of various elements in seawater (Mg, Sr, P, U, Ni, Zn, Cd, Fe, and Ca) in the upper 1,000 m of the water column were extracted from Biller and Bruland (2013) and Dr. Kenneth Johnson's *Periodic Table of Elements in the Ocean*. Available online at: http://www.mbari.org/science/upper-ocean-systems/chemical-sensor-group. Mean concentration values of [E/Ca_{Urchin}] and [E/Ca_{SW}] in Shelf (green), OLZ (red), and OMZ/LOMZ (blue) bins are reported in Table 4.1.

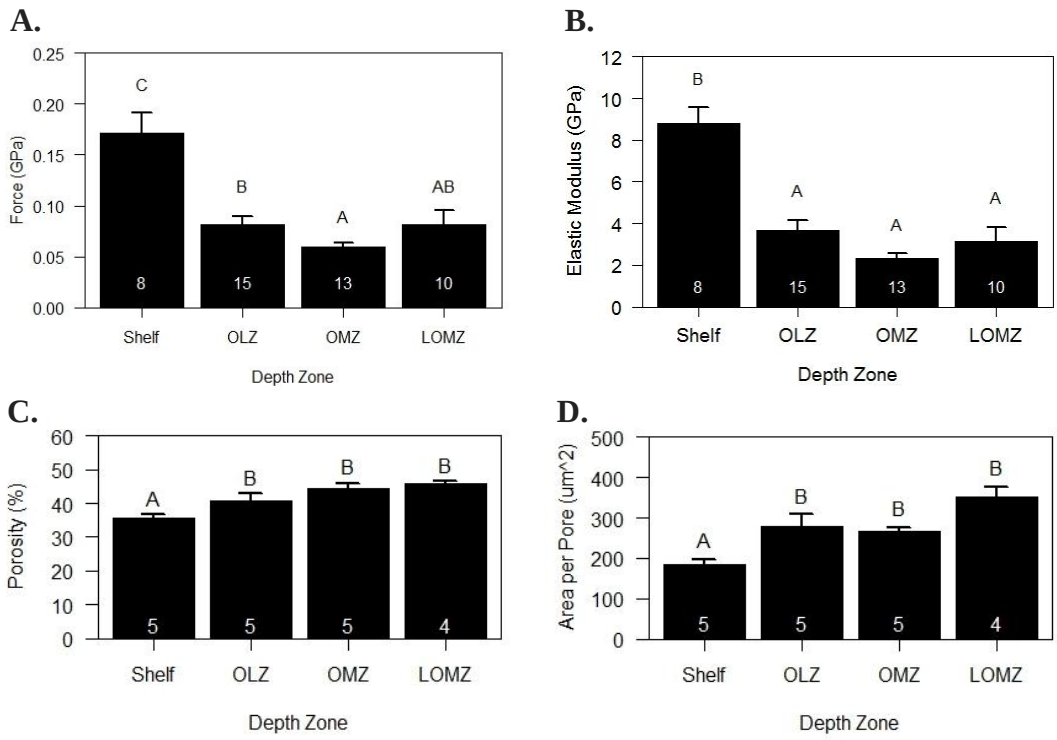

Figure 4.10. Mean biomechanical and microstructural properties of *Strongylocentrotus fragilis* across depth zones. **A)** Hardness (GPa). **B)** Stiffness (*i.e.*, Elastic Modulus). **C)** % Porosity. **D)** Area per pore (μm^2). White numbers inside bars indicate number of individual urchin replicates. Errors bars indicate +1 standard error. Shelf = <200 m; OLZ = Oxygen Limited Zone (22-60 µmol oxygen kg^{-1}); OMZ = Oxygen Minimum Zone core (< 22 µmol oxygen kg^{-1}); LOMZ = Lower Oxygen Minimum Zone (>750 m where dissolved oxygen begins to increase).

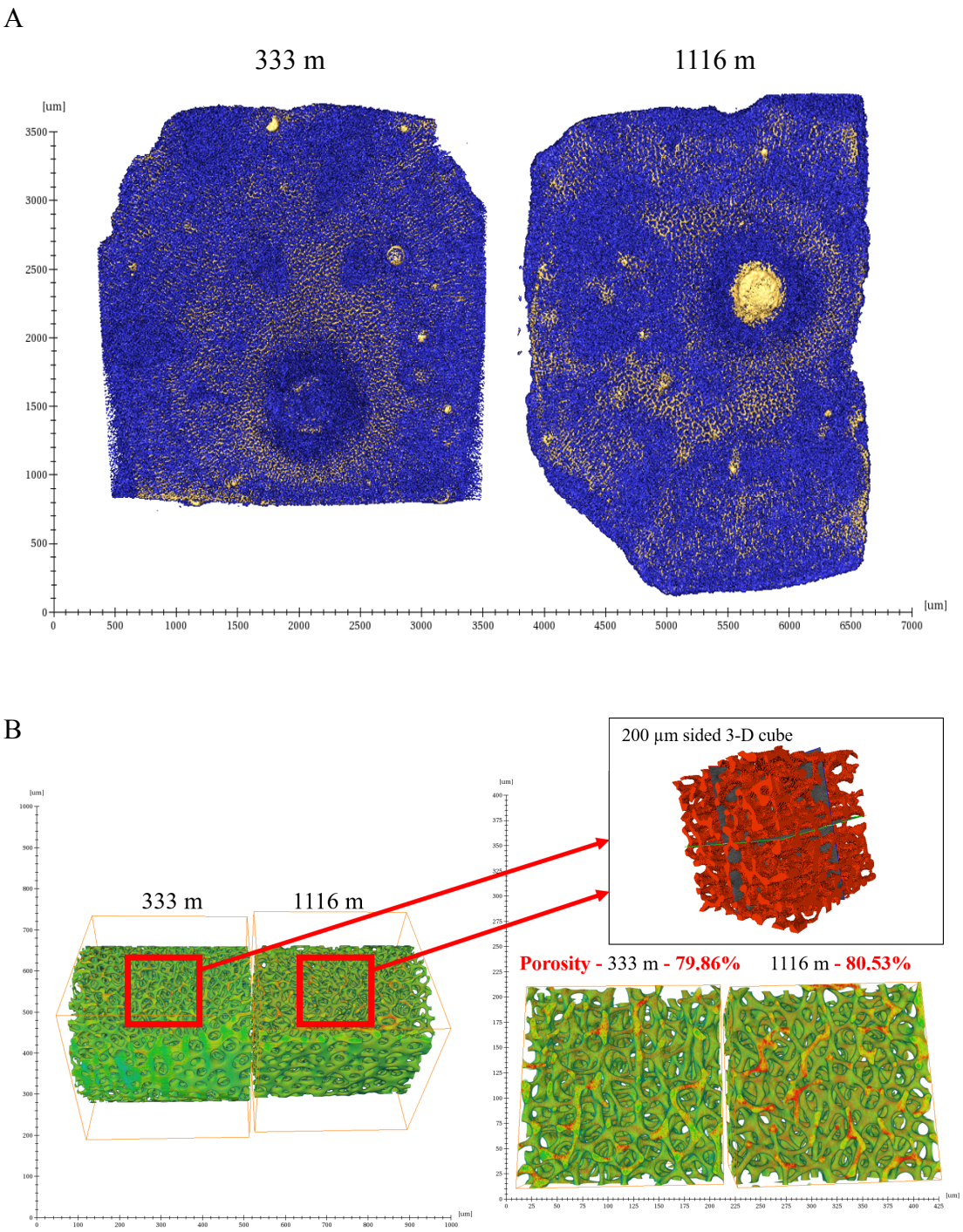

Figure 4.11. High-resolution micro-computed tomography (HR-µCT) images of Strongylocentrotus fragilis test plates from 333 m and 1116 m. A. Distribution of surface porosity was visualized by adjusting the threshold range limits (i.e., average range threshold limits (Purple) and upper range (low porosity) threshold limits (Gold)). B. 3-D porosity for each sample was measured in a 200-µm sided box calculated from Material Statistics outputs (Amira software, FEI Visualization).

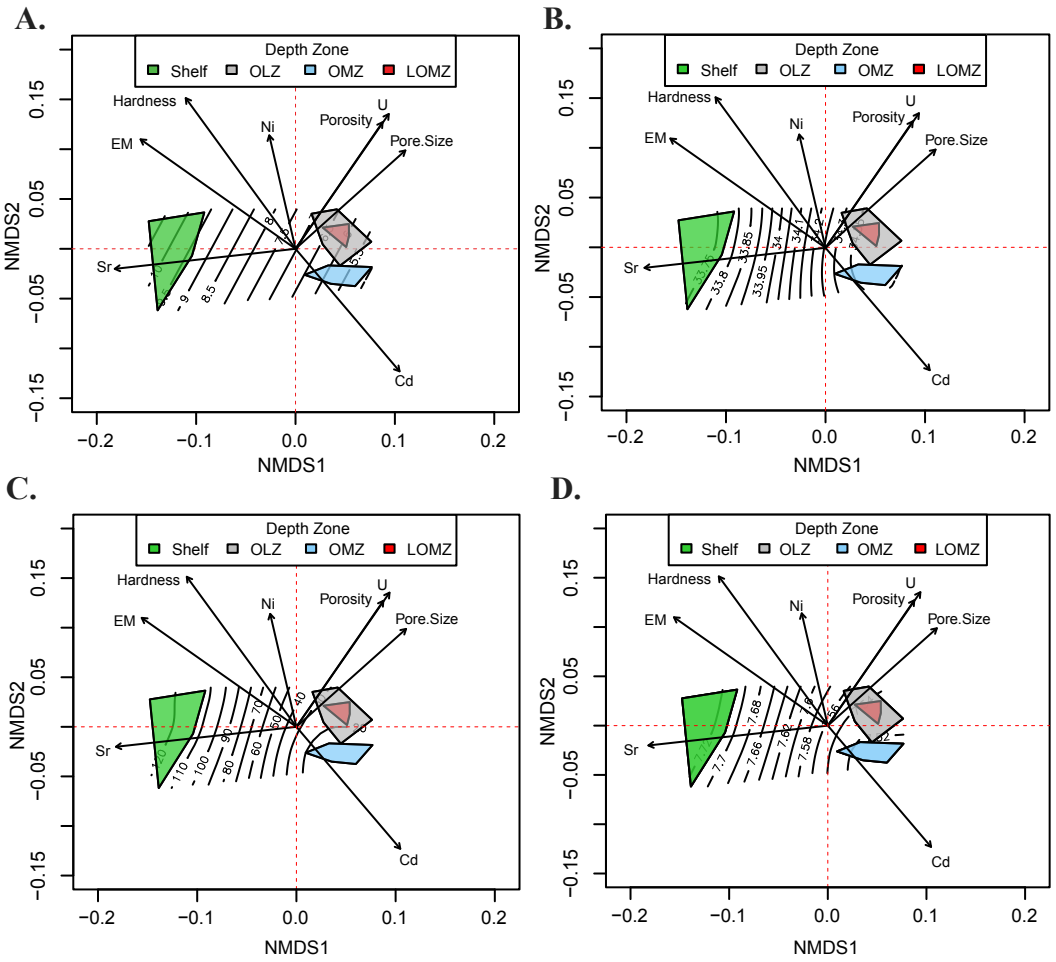

Figure 4.12. Nonmetric multidimensional scaling plot showing dissimilarity among *Strongylocentrotus fragilis* sites pooled into 4 depth zones overlaying environmental variables: **A)** temperature (°C), **B)** salinity (PSU), **C)** dissolved oxygen (µmol oxygen kg^{-1} seawater), and **D)** *in situ* pH_{Total}. Green: Shelf = <200 m; Red: OLZ = Oxygen Limited Zone (22-60 µmol oxygen kg^{-1}); Blue: OMZ = Oxygen Minimum Zone core (< 22 µmol oxygen kg^{-1} or 0.5 mL L^{-1}); Purple: LOMZ = Lower Oxygen Minimum Zone (>750 m where dissolved oxygen begins to increase). Vector length is proportional to the correlation between ordination axis and the environmental, elemental, or biomechanical variable. Vector direction indicates the direction of the gradient.

Appendix 4.1. Collection sites by depth zone. Agency Key: NOAA = National Oceanic and Atmospheric Administration; LACSD = Los Angeles County Sanitation District; CSD = City of San Diego; VRG = Vantuna Research Group; CLAEMD = City of Los Angeles Environmental Monitoring Division. Scripps Institution of Oceanography Student Cruise Key: MV = R/V *Melville* ; NH = R/V *New Horizon*; SP & RGS = R/V *Robert Gordon Sproul.*

* = *Strongylocentrotus fragilis* test plates measured for elemental composition only. † = Measured for elemental composition and mechanical hardness and stiffness. § = Measured for elemental composition, mechanical hardness and stiffness, and porosity.

Depth Zone	Agency/ SIO Cruise ID	Trawl Site ID	Date Collected	Latitude (˚N)	Longitude (˚W)	Depth (m)
Shelf	NOAA*	17372	7/16/2014	34.0069	-118.9009	84
	NOAA§	17262	7/15/2014	33.9044	-119.5017	93
	MV1217	T2	12/9/2012	32.9641	-117.3136	100
	LACSD	9251	8/14/2013	33.7668	-118.4605	130
	CSD	9014	8/6/2013	32.5954	-117.3286	136
	CSD	9019	8/1/2013	32.6434	-117.4277	150
	VRG	9403	8/22/2013	34.2064	-119.6327	154
	VRG	9385	8/23/2013	34.1327	-119.3699	172
	CSD	9053	8/8/2013	32.8254	-117.3660	182
	CSD	9051	8/7/2013	32.9092	-117.2951	184
	VRG*	9414	8/21/2013	34.2251	-119.7320	196
	CLAEMD	9287	9/4/2013	33.9340	-118.5905	200
	NH1414†	T4	7/27/2014	32.8075	-117.3676	200
	VRG	9432	8/21/2013	34.2778	-119.7183	200
OLZ	MV1215	T1	11/3/2012	32.6736	-117.3602	215
	VRG	9394	8/22/2016	34.1687	-119.5417	237
	LACSD	9228	8/14/2013	33.6941	-118.3465	253
	VRG	9379	8/21/2013	34.1182	-119.6289	260
	LACSD	9237	8/16/2013	33.7214	-118.4179	293
	MV1209	T5	7/8/2012	32.8786	-117.3436	300
	MV1217	T10	12/15/2012	32.6916	-117.3758	300
	MV1217	T4	12/9/2012	32.9523	-117.3184	300
	MV1217	T7	12/12/2012	32.8100	-117.4004	300
	NH1318	T1	7/27/2013	32.6694	-117.3975	300
	NH1407	T1	4/20/2014	32.6986	-117.3765	300
	LACSD	T4	2/13/2014	33.6787	-118.3276	305
	LACSD	T5	2/13/2014	33.6787	-118.3276	305
	SP1510	T6	6/13/2015	32.7209	-117.3737	325
	NOAA	17462	7/16/2014	33.9551	-118.6931	333
	SP1408	T1	11/1/2014	32.7070	-117.3760	340
	SP1504	T1	4/11/2015	32.7244	-117.3660	340
	SP1524	T1	10/18/2015	32.7244	-117.3660	340
	SP1603	T1	3/13/2016	32.7035	-117.3776	340
	SP1612§	T1	7/9/2016	32.7013	-117.3796	340
	NH1414†	T1	7/26/2014	32.7010	-117.3852	360
	CSD	9107	8/13/2013	33.0938	-117.4172	400
	MV1217	T3	12/9/2012	32.9471	-117.3416	400
	MV1217	T6	12/12/2012	32.8100	-117.4004	400
	RGS131019A	T1	10/19/2013	32.7502	-117.4127	427
	CSD	9023	8/1/2013	32.6701	-117.4209	435
	NOAA	19514	7/14/2014	33.1547	-117.5011	443
OMZ	NOAA	17547	7/20/2014	33.9203	-118.6997	459
	NOAA*	18528	7/21/2014	33.5548	-118.1257	465
	LACSD	9223	8/16/2013	33.6759	-118.3325	470
	NOAA*	20605	7/16/2014	32.8990	-118.6182	475
	VRG*	9309	8/20/2013	33.9774	-118.8764	493
	NOAA	20758	7/17/2014	32.7824	-117.4419	555
	NH1414*	T5	7/29/2014	32.8908	-117.4745	698
	NH1414	T7	7/29/2014	32.8128	-117.4670	700
	SP1506§	T1	4/18/2015	32.8109	-117.4710	715
	NOAA†	20738	10/14/2014	32.8279	-118.0311	768
LOMZ	SP1612§	T2	7/9/2016	32.8242	-117.5394	900
	NOAA	19490	7/1/2014	33.2165	-118.2318	1116

CHAPTER 5

Conclusions

Implications of multiple changing climate variables on the continental shelf and slope were described for sea urchins across a spectrum of biological organization ranging from the urchin guild scale (Chapter 2), to the individual life history attributes (Chapter 3), to the geochemistry, biomechanics and porosity of sea urchin calcium carbonate skeletal tests (Chapter 4). Understanding past and future changes in marine ecosystems is critical to informing management and climate policy decisions, and to future research on climate change, characterized by multiple interacting environmental stressors. Special consideration was made to describe various management-relevant traits in considering a potential hypoxia- and hypercapnia-tolerant sea urchin fishery for the deep-sea pink urchin, *Strongylocentrotus fragilis* (Chapter 3).

Quantification of biological and environmental patterns in nature across multiple spatial and temporal scales provides the ecological context necessary to elucidate the difference between acclimation and stress effects caused at least in part by anthropogenic changes in climatic drivers on life in the ocean. This ecological principle was employed throughout the chapters of this dissertation using sea urchins on the southern California upwelling margin as a model system.

At the regional scale, population sizes and depth distributions for multiple cohabiting urchin species evaluated from 1994 to 2013 revealed how climatological drivers (*e.g.*, El Niño Southern Oscillation (ENSO), ocean dissolved oxygen, and pH) are linked to habitat suitability (Chapter 2). Spatiotemporal changes in depth distributions and

densities of multiple, deep-margin urchin species in the Southern California Bight were shown to be strongly related to both varying degrees of ENSO strength and longer-term trends in dissolved oxygen and pH. Observed patterns of shoaling and density decreases of a subtidal benthic urchin (*Lytechinus pictus*) in the upper 200 m since 1994 suggest that trends in decreased oxygen and lower pH in southern California are closely linked to habitat compression. In contrast, patterns of shoaling and increased density of a deeper urchin species, *S. fragilis*, within the upper 500 m, are consistent with a shoaling of the hypoxic (and reduced pH) boundary and low oxygen and low pH during La Nina years, suggest that *S. fragilis* has expanded its habitat from 2003 to 2013.

Chapter 2, published as Sato *et al.* (2017) is significant because it builds on the dearth of evidence within the marine scientific literature demonstrating habitat compression and expansion for benthic species on a regional scale. Both vulnerable and tolerant urchin species in southern California may be affected by long-term trends predicted to occur in the future due to anthropogenic climate change, but changes in habitat are also linked to natural interannual climate oscillations. These conclusions were made possible by integrating two distinct datasets, one hydrographic and one benthic, collected by long-term monitoring programs (CalCOFI and SCCWRP), thereby highlighting the importance of their utility and maintenance and the need for more integrative analyses.

The remaining chapters focus on the comparison of various trait-based characteristics of the deep-sea pink fragile urchin, *S. fragilis*, along vertical gradients of multiple climate change variables. The tight relationship between dissolved oxygen and pH covariables (Reum *et al.* 2016) through the Oxygen Minimum Zone in southern CA provided the opportunity to substitute space for time to investigate the realistic implications

of ocean deoxygenation and ocean acidification. If *S. fragilis* populations continue to increase in the future because they are tolerant of harsh oxygen and pH conditions, to what extent might *S. fragilis* be affected by the predicted loss of oxygen and acidification of OMZ waters? This question was first considered by describing various life history attributes necessary to consider the development of a climate change-tolerant future *S. fragilis* urchin fishery (Chapter 3), and further investigated by elucidating the environmental influence on geochemical, microstructural and mechanical properties of the urchin calcium carbonate structures (Chapter 4). *S. fragilis* data were collected over a broad spatial extent using multiple methods *via* ship-based bottom trawls and video surveys by remotely operated vehicle (ROV). Each cruise and trawl provided the unique opportunity to both explore and test hypotheses about changes in community composition and relative abundance of *S. fragilis*.

In Chapter 3, relative growth rates and reproductive potential were both found to be positive in the low oxygen, low pH OMZ core, but optimal conditions for growth and gonad production were found to occur at the shallowest depths where *S. fragilis* occurs. Spatial, seasonal, and interannual patterns of reproduction were documented for *S. fragilis*, which relies on kelp drift as a primary food source. While the gonad production of *S. fragilis* is highest in the Fall/Winter months, a year-round low of gonad index in 2015 was presumed to result from the abnormally warm conditions and reduced kelp abundance during that year (Reed *et al.* 2016). Various food quality properties of the gonads, upon which the current red urchin (*Mesocentrotus franciscanus*) fishery depends, were compared between *S. fragilis* and *M. franciscanus*. Despite large, well-fed *S. fragilis* individuals having significantly smaller and softer gonads than *M. franciscanus*

(Boolootian *et al.* 1959), the similarities in color and advantageous tolerance to low oxygen and low pH make these results relevant to sea urchin stakeholders.

Extensive sampling, sorting, and counting of deep-sea megafauna throughout southern CA also revealed the depth bin at which *S. fragilis* density peaked. In addition, a potential threshold of *S. fragilis* abundance around 500 m water depth was verified by two independent visual surveys using ROVs (Chapter 3). While only two ROV surveys confirmed the hypothesis that *S. fragilis* primarily occurs in the upper 500 m of the continental slope in southern CA, their occasional presence in deeper trawls (*i.e.*, the core of the OMZ) suggest a high tolerance of this species to seemingly unfavorable conditions.

In Chapter 4, patterns of elemental composition, material properties, and microstructural porosity of *S. fragilis* skeletal tests were evaluated throughout its full depth distribution to better understand the extent of potential warming, deoxygenation and acidification impacts on a tolerant species. Although *S. fragilis* may be tolerant of future climatic changes than other species, observed increases in porosity and mean pore size coupled with decreases in mechanical hardness and stiffness of the calcitic skeletal structure in individuals collected from deeper, more corrosive and oxygen-deprived environments suggest *S. fragilis* may be more vulnerable to crushing predators in the future. Data generated in this study suggest that *S. fragilis* may also respond to unfavorable future conditions by attaining smaller sizes, as seen in other animals, including *S. purpuratus*, by limiting gonad production, or by growing slower (Ebert 2007).

The relatively low solubility of low-magnesium calcite compared to other mineral phases of calcium carbonate (*e.g.*, aragonite, high-Mg calcite, amorphous calcium carbonate) suggests a potential evolutionary strategy employed by *S. fragilis* to tolerate

unfavorable conditions (Lebrato *et al.* 2016). These results shed light on my initial observations of abundant calcifying urchin populations in oxygen-limited and corrosive waters on board the San Diego Coastal Expedition in June 2012 (Cruise ID MV1209). Mg/Ca and Sr/Ca ratios in *S. fragilis* calcite collected throughout southern CA were correlated with various environmental parameters. Higher concentrations of trace metals (Fe, Cd, Ni, Zn) in urchin calcite relative to the surrounding seawater suggest *S. fragilis* may actively control the incorporation of these trace metals into the test, but passive kinetic effects on trace metal incorporation are also possible and may be element-specific. Further study is required to better understand the influence of trace metals in the *S. fragilis* calcification processes, on solubility of calcite and on other fitness features within the benthic boundary layer.

The studies presented here are based on study of adult sea urchin fitness attributes. Previous research has shown that larval responses to climate stressors in the form of reduced growth, calcification or survival can have direct population-level effects as well as carry over effects on adult fitness (Hettinger *et al.* 2012, Kurihara *et al.* 2012, 2013). Expanding the research approach presented here to larval and juvenile stages could enhance understanding of climate impacts on SCB margin sea urchins.

In summary, this dissertation highlights the tolerance and vulnerabilities of deep-sea calcifying sea urchins in an upwelling region. One of the most significant results of this study was the finding that *S. fragilis* growth rate, size, gonad index, test hardness and stiffness (and possibly elemental incorporation) all exhibit a parabolic trend with water depth (Figures 3.6, 4.4, 4.5, 4.10) with lowest values in the OMZ (500-900 m). These patterns are consistent with strong influence of low pH (*in situ* $pH_{Total} < 7.57$) and low O_2

(< 22 µmol kg^{-1}) on fitness, independent of pressure or temperature changes. The trait-based fitness properties described within Chapters 3 and 4 provide a framework from which hypothesis-driven laboratory experiments might inform the knowledge gaps that inhibit the interpretation of results within this dissertation. Although Chapter 1 suggests that *S. fragilis* may do better than other calcifying urchins in the future ocean, Chapters 3 and 4 demonstrate how *S. fragilis* may still be vulnerable *via* sublethal effects on skeletal structure and material properties.

References

Booloottian, R. A., A. C. Giese, J. S. Tucker, and A. Farmanfarmaian. 1959. A contribution to the biology of a deep sea echinoid, *Allocentrotus fragilis* (Jackson). The Biological Bulletin 116: 362–372.

Ebert, T. A. 2007. Growth and Survival of Post Settlement Sea Urchins. *In* Edible Sea Urchins: Biology and Ecology, 2nd edn, pp. 95–134. Ed. by J. M. Lawrence. Elsevier, Amsterdam.

Hettinger, A., E. Sanford, T. M. Hill, A. D. Russell, K. N. S. Sato, J. Hoey, M. Forsch, H. Page, and B. Gaylord. 2012. Persistent carry-over effects of planktonic exposure to ocean acidification in the Olympia oyster. Ecology 93: 2758–2768.

Kurihara, H., Y. Takano, D. Kurokawa, and K. Akasaka. 2012. Ocean acidification reduces biomineralization-related gene expression in the sea urchin, *Hemicentrotus pulcherrimus*. Marine Biology 159: 2819–2826.

Kurihara, H., R. Yin, G. N. Nishihara, K. Soyano, and A. Ishimatsu. 2013. Effect of ocean acidification on growth, gonad development and physiology of the sea urchin *Hemicentrotus pulcherrimus*. Aquatic Biology 18: 281–292.

Lebrato, M., A. J. Andersson, J. B. Ries, R. B. Aronson, M. D. Lamare, W. Koeve, A. Oschlies, M. D. Iglesias-Rodriguez, S. Thatje, M. Amsler, S. C. Vos, D. O. B. Jones, H. A. Ruhl, A. R. Gates, and J. B. McClintock. 2016. Benthic marine calcifiers coexist with $CaCO_3$ -undersaturated seawater worldwide. Global Biogeochemical Cycles 30: 1038–1053.

Reed, D., L. Washburn, A. Rassweiler, R. Miller, T. Bell, and S. Harrer. 2016. Extreme warming challenges sentinel status of kelp forests as indicators of climate change. Nature Communications 7: 13757.

Reum, J. C. P., S. R. Alin, C. J. Harvey, N. Bednaršek, W. Evans, R. A. Feely, B. Hales, N. Lucey, J. T. Mathis, P. McElhany, J. Newton, and C. L. Sabine. 2016. Interpretation and design of ocean acidification experiments in upwelling systems in the context of carbonate chemistry co-variation with temperature and oxygen. ICES Journal of Marine Science 73: 582–595.